

https://dspace.org/

Development, optimisation and application of diffusive gradients based passive sampler monitoring of arsenic, selenium and mercury in waters

Maputsoe, Xolisiwe

2019

https://hdl.handle.net/10539/28832

Downloaded from a DSpace repository. https://dspace.org/

Development, optimisation and application of diffusive gradients based passive sampler for monitoring of arsenic, selenium and mercury in waters



Xolisiwe Maputsoe

A Thesis submitted to the Faculty of Science, University of the Witwatersrand, Johannesburg, in fulfilment of the requirements for the Degree of Doctor of Philosophy

March 2019

DECLARATION

I declare that this thesis is my own, unaided work. It is being submitted for the Degree of Doctor of Philosophy at the University of the Witwatersrand, Johannesburg. It has not been submitted before for any degree or examination at any other University

_____

Xolisiwe M. Maputsoe

_____ day of _____ 20_____ in _____

ABSTRACT

The diminishing levels of untainted fresh water sources suggest the need for more stringent monitoring approaches. Traditionally, grab sampling is the commonly used technique; however, the large number of associated limitations has led to the development and advancement of alternative and complimentary techniques such as passive sampling. One of the most widely used passive samplers is diffusive gradients in thin-films (DGT). DGT was designed for the *in situ* measurement of labile trace metal species in natural water. It operates on the fundamentals of an integrative passive sampler whereby analytes accumulate linearly with time, against a concentration gradient. Since the accumulation of analytes occurs at a definable rate DGT is able to provide time integrated concentrations of pollutants. Additionally, because analytes enter the passive sampler exclusively via diffusion, it provides information on the bioavailable fraction. DGT is made up of two functional layers: a diffusive layer and a binding layer. The binding layer can be modified to suit the target analytes.

In recent years polyethylenimine (PEI) has attracted a lot of attention as an adsorbent for metals. Cross-linked polyethylenimine (CPEI), the insoluble version of PEI showed great potential as a remediation and analytical sorbent. In particular, phosphonated and sulphonated CPEI showed high efficiency in the removal of arsenic, selenium and mercury. Therefore, sulphonated and phosphonated CPEI polymers were considered as a DGT binding layer resins. In addition, DGT sample holders used in this study were manufactured from a 3.0 cm diameter polytetrafluoroethylene (PTFE) rod. The sample holder design and dimensions were similar to commercial DGT. Modifications were only made on the DGT cap, which would allow the same performance as commercial DGT but with the added advantage of being re-usable.

CPEI was modified using two methods; in the first method, CPEI underwent a sulphonation reaction using 3-chloropropanesulfonyl chloride to form sulfonated cross-linked polyethyenimine (SCPEI). In the second, phosphonation proceeded by reacting CPEI with phosphoric acid and formaldehyde to form phosphonated cross-linked polyethyenimine (PCPEI).

Due to the polymeric nature of the sulphonated and phosphonated CPEI resins, they had to be optimised as DGT binding layers, and two considerations had to be made: firstly, the optimum ratio of SCPEI and PCPEI in the resin mixture had to be determined. Secondly, how the polymeric resin mixture would be assembled into a binding layer. Binding layer assembly was carried out using two methods. In the first method the resin mixture was embedded in an agarose gel solution. In the second, 0.4 and 0.8 g of SCPEI-PCPEI resin mixtures in their loose polymer form were used. This resin mixture consisted of 80% SCPEI and 20% PCPEI of total resin mass used. The DGT sampler was also calibrated under laboratory conditions to determine the influence of the following parameters: pH, sample concentration and turbulence. The passive sampler was further calibrated using environmental samples in laboratory based experiments: the passive samplers were deployed in spiked and un-spiked dam water, dissolved efflorescent crust as well as spiked acid mine drainage water. The optimised DGT passive samplers were then deployed in Fleurhof Dam for 12 days.

Results from binding layer optimisation show that mixing 80% of sulphonated CPEI and 20% phosphonated CPEI per total mass showed better adsorption of arsenic, selenium and mercury. In addition, unlike commercial DGT, the passive sampler with the resin mixture incorporated in agarose showed grossly reduced capacity, especially for deployments longer than 9 days. The maximum capacity was achieved using 0.8 g of SCPEI-PCPEI in the loose polymer form. Calibration results of the DGT sampler show that it can operate in the pH range of natural water under stagnant conditions. The passive sampler also showed better performance in dilute solutions, preferably less than 0.5 mg L^{-1}.

Results from the spiked and un-spiked dam water samples show that arsenic and selenium were accumulated linearly with time by DGT. Mercury accumulation was linear only in the spiked sample; it did not follow a specific trend in the un-spiked dam water solution. In dissolved efflorescent crust, only arsenic showed linear mass accumulation with time. Conversely, no selenium and mercury were detected in the passive samplers. The same trend was observed for samplers deployed in spiked AMD water. All deployments in environmental samples

revealed that the SCPEI-PCPEI resin mixture can also accumulate other metal ions. In both the dissolved crust and AMD water deployments iron concentrations were elevated. This resulted in the formation of colloid particles within the passive sampler binding layer. These particles behaved as secondary adsorption sites, leading to the non-specific accumulation of analytes. During field deployments in dam water, the DGT passive sampler was able to accumulate arsenic linearly but showed reduced capacity for selenium and mercury since there was no increase in mass over time. Field deployments were able to highlight that SCPEI-PCPEI resin mixture is highly subjected to reduced selectivity and capacity for the target analytes in the presence of competing ions. This could be due to the high uptake of metal ions found in the dam water. Despite these challenges, SCPEI-PCPEI based DGT could be used for successful *in situ* measurement of labile arsenic in environmental waters. Measurement of selenium and mercury were however, unsuccessful.

ACKNOWLEDGMENTS

I would like to thank my supervisor Professor Ewa Cukrowska for giving me the opportunity to work with her. I am grateful for her continuous support throughout my PhD study, for her patience, immense knowledge and attention to detail as well as instilling a sense of ownership for my work.

I would equally like to thank my co-supervisor Professor Luke Chimuka for his contribution towards my work. I am thankful for his guidance, encouragement and support throughout my studies. Thank you for always having a few minutes to spare despite your busy schedule.

The Environmental Analytical Chemistry group Research group has been a source of support and inspiration during my studies. Special thanks goes to Professor Hlanganani Tutu for imparting valuable knowledge during group presentations. I would also like to thank past and present group members, namely Dr Nikita Tavengwa, Dr Somandla Ncube, Dr Bongani Yalala, Dr Charlene Makita, Dr Bronwyn Grover, Dr Joy Mokone, Mr Kitondo, Mr Yannick Nuapia, Mr Alseno Mosai, Ms Odwa Mbanga, Ms Andelina Monyai, Ms Mathabo Ramaqele and the rest of the group members for their willingness to help at all times. I am particularly appreciative of Ms Nthabiseng Motsoane and Mr Pfano Nekhunguni and for their friendship and always going the extra mile to assist.

I had the pleasure of supervising Ms Mulweli Nethathe, Ms Ashla Mothiba, Ms Tebogo Peega and Ms Nthabiseng Makaota during their Honours projects. It was a pleasure working with them and I could not have asked for better students

A special mention goes to Don McKenna from the Physics workshop for working tirelessly to design and manufacture the DGT sample holders from a PTFE rod.

My family and friends have been so patient, kind and understanding throughout my studies. I would like to thank my mother, Khohlisa Maputsoe, without her sacrifices and immeasurable love, I could not have dreamt of making it this far. To my brothers Moponya and Bongani Maputsoe thank you for always seeing the best in me. Special thanks go to the Sebutsoe family. To my friends Mpho

Mosotho, Likonelo Buasi, my cousin Tumi Lephatswane thank you for the love and the countless phone calls during the difficult times.

I would like express profound gratitude to my husband Tshele Sebutsoe for his endless encouragement, love and support throughout my studies. Thank you for always pushing me towards greatness. To my son Lekota, you inspire hope.

A special mention goes to my late grandparents James and Julia Dingizwyo for paving the way towards my education. To my late father Thabo W. Maputsoe and my late father in law Mosioua Sebutsoe thank you for everything.

Above all else I would like to thank God the almighty for the gift of life, family and for sustaining me during this period.

TABLE OF CONTENTS

DECLARATION i

ABSTRACT ii

ACKNOWLEDGMENTS v

TABLE OF CONTENTS vii

LIST OF FIGURES xiv

LIST OF TABLES xvii

LIST OF ABBREVIATIONS AND ACRONYMS xviii

Chapter 1: Introduction 1

1.1 Monitoring of aquatic environments 2

Chapter 2: Literature review 6

2.1 Trace elements in the environment 7

2.1.1 Arsenic in the environment: sources and distribution 7

2.1.1.1 Arsenic toxicity 8

2.1.1.2 Arsenic speciation and bioavailability 9

2.1.1.3 Ion interactions with arsenic 12

2.1.1.4 Adsorption in the biogeochemical cycle of arsenic 13

2.1.2 Selenium in the environment: sources and distribution 15

2.1.2.1 Selenium toxicity 17

2.1.2.2 Selenium speciation and bioavailability 18

2.1.2.3 Ion interactions with selenium 20

2.1.2.4 Selenium biogeochemical cycle 21

2.1.3 Mercury in the environment: sources and distribution 22

2.1.3.1 Mercury speciation 24

2.1.3.2 Mercury toxicity 25

2.1.3.3 Ion interactions with mercury 28

2.1.3.4 Mercury biogeochemical cycle 28

2.1.4 Interactions between arsenic, selenium and mercury 30

2.1.5 Characteristics of acid mine drainage (AMD) 31

2.2 Conventional sampling methods 35

2.2.1 Problems associated with conventional sampling methods 35

2.3 The theory of passive sampling 37

2.3.1 Passive sampling 37

2.3.2 Advantages of passive sampling 40

2.3.3 Examples of passive samplers for inorganic analytes 41

2.3.3.1 Chemcatcher® 41

2.3.3.2 Passive integrative mercury sampler (PIMS) 42

2.3.3.3 Polymer inclusion membrane (PIM) - based passive samplers 43

2.4 Diffusive gradients in thin-films (DGT) 44

2.4.1 Principles of the DGT passive sampler 47

2.4.1.1 Accumulation of mass and C_{DGT} 47

2.4.1.2 Diffusion coefficient and the diffusive boundary layer 48

2.4.2 Factors affecting DGT measurements 50

2.4.2.1 Turbulence and the DBL 51

2.4.2.2 Fouling 52

2.5 Application of DGT: fate, transport and risk assessment 53

2.5.1 Trends DGT passive sampler 54

2.5.1.1 Hydrogels as diffusion barriers 55

2.5.1.2 DGT with single adsorbent resin 57

2.5.1.3 Multi-layer and mixed DGT resins 60

2.5.1.4 Phosphate and sulphonyl functional groups 61

2.5.1.5 Polyethylenimine 61

Chapter 3: Research aim and objectives 64

3.1 Aim 65

3.2 Specific objectives 65

3.3 Research statement and novelty 65

Chapter 4: Materials and methods 67

4.1 Materials 68

4.2 Instrumentation 68

4.2.1 Elemental analysis 68

4.2.2 Anion analysis 68

4.2.3 Fourier transform infrared (FT-IR) spectra 68

4.2.4 Solid state NMR 69

4.2.5 CHNS analysis 69

4.2.6 Physico-chemical properties of water 69

4.3 Experimental procedure 69

4.3.1 Synthesis of polyethylenimine as a sorbent for DGT 69

4.3.1.1 Cross-linked polyethylenimine (CPEI) 69

4.3.1.2 Sulphonated cross-linked polyethylenimine (SCPEI) 70

4.3.1.3 Phosphonated cross-linked polyethylenimine (PCPEI) 70

4.3.2 Batch studies 70

4.3.2.1 The uptake efficiency of SCPEI-PCPEI polymer mixture 70

4.3.2.2 The uptake factor 71

4.3.2.3 Elution efficiency of different eluents 71

4.3.2.4 The elution factor 72

4.3.3 Construction of passive sampler 72

4.3.3.1 Construction of sample holders 72

4.3.3.2 Preparation of resin embedded in agarose 73

4.3.3.3 Preparation of diffusive gel layer 73

4.3.4 Assembly and deployment of DGT passive sampler 73

4.3.5 Calibration of DGT passive sampler 75

4.3.5.1 Effect of SCPEI as DGT binding layer 75

4.3.5.2 Effect of SCPEI-PCPEI resin mixture dispersed in agarose gel 75

4.3.5.3 Effect of SCPEI-PCPEI resin mass on DGT capacity 76

4.3.5.4 Effect of the diffusive gel in SCPEI-PCPEI based DGT 77

4.3.5.5 The diffusive gel thickness and flux 77

4.3.5.6 The effect of turbulence on DGT uptake 78

4.3.5.7 The effect of sample concentration on DGT uptake 79

4.3.5.8 The effect of pH on DGT uptake 79

4.3.6 Determination of diffusion coefficients and diffusive boundary layer 79

4.3.6.1 The diffusion coefficient (*D*) in agarose gel 79

4.3.6.2 The diffusive boundary layer (DBL) 80

4.3.7 Determination of the blank and method detection limit (MDL) 80

4.3.8 Field deployment of optimised SCPEI-PCPEI based DGT 80

4.3.8.1 Construction of sampling cages 80

4.3.8.2 Description of sampling sites 81

4.3.8.3 DGT deployment in Fleurhof Dam water 83

4.3.8.4 Deployment in dissolved efflorescent crusts 83

4.3.8.5 Passive sampler deployment in AMD 84

4.3.9 PHREEQC modelling software 85

Chapter 5: Results and discussion 86

5.1 Characterisation of functionalised CPEI 87

5.1.1 FT-IR analysis 87

5.1.2 Solid state NMR 89

5.1.3 CHNS analysis 90

5.2 Batch studies 91

5.2.1 Uptake factors of different SCPEI and PCPEI resin mixtures 91

5.2.2 Elution factor (f_e) 94

5.3 Design and manufacture of DGT sample holders 97

5.4 Calibration of DGT passive sampler 99

5.4.1 Effect of SCPEI as DGT binding layer 99

5.4.2 Effect of SCPEI - PCPEI resin mixture dispersed in agarose gel 101

5.4.3 Effect of SCPEI-PCPEI resin mass on DGT capacity 103

5.4.4 Effect of the diffusive gel in SCPEI-PCPEI based DGT 104

5.4.5 The diffusive gel thickness 105

5.4.6 The effect of turbulence on DGT uptake 106

5.4.7 The effect of sample concentration on DGT uptake 108

5.4.8 The effect of pH on DGT uptake 110

5.5 Determination of diffusion coefficients and DBL thickness 112

5.5.1 The diffusion coefficient in agarose gel 112

5.5.2 The DBL (δ) 115

5.6 Determination of resin blanks and method detection limits 116

5.7 Comparison of DGT resin sorbents and maximum deployment time 116

5.8 Deployment of optimised SCPEI-PCPEI based DGT in field samples 118

5.8.1 DGT uptake in laboratory-based experiments using dam water 118

5.8.1.1 Composition of dam water 118

5.8.1.2 Deployment of DGT in dam water under laboratory conditions 119

5.8.1.3 Uptake of other cations from Fleurhof dam water 121

5.8.1.4 Changes in the physico-chemical properties of dam water 122

5.8.2 Deployment in the dam 123

5.8.2.1 Uptake of target analytes during field deployment 123

5.8.2.2 Accumulation of other metals during field deployments 124

5.8.3 Deployment of DGT in dissolved efflorescent crust 125

5.8.3.1 Composition of dissolved efflorescent crust 125

5.8.3.2 DGT deployment in dissolved efflorescent crust 128

5.8.3.3 Uptake of other cations by DGT 130

5.8.4 Uptake in laboratory-based experiments using AMD drainage water 131

5.8.4.1 Composition of AMD 131

5.8.4.2 Accumulation in AMD drainage water 132

5.8.4.3 Simultaneous uptake of other cations 134

Chapter 6: Conclusions and recommendations 136

6.1 Conclusions 137

6.2 Recommendations 138

References 140

Appendix 190

LIST OF FIGURES

Figure 2.1: The Eh–pH diagram for arsenic at 25◦C and 101.3 kPa 11

Figure 2.2:The biogeochemical cycle of arsenic and interactions involved 14

Figure 2.3: pE-pH diagram of Se-O-H at 298 K 19

Figure 2.4: The biogeochemical cycle of selenium. 22

Figure 2.5: pE-pH diagram of mercury. 25

Figure 2.6: The biogeochemical cycle of mercury.....30

Figure 2.7: The geochemical pH-buffering regions associated with AMD 32

Figure 2.8: Analyte accumulation pattern followed by passive samplers.....37

Figure 2.9: Depiction of how equilibrium and integrative samplers operate.....38

Figure 2.10: Chemcatcher passive sampling device 42

Figure 2.11: PIMS passive sampler for air monitoring of mercury vapour 43

Figure 2.12: Example of a PIM based passive sampling device 44

Figure 2.13: Commercial DGT sampling device 45

Figure 2.14: Two methods of assembling modified DGT sample holders 46

Figure 2.15: DGT diffusion layers and their relationship with the DBL 49

Figure 2.16: The repeating units that make up agarose. 56

Figure 2.17: Structure of branched polyethylenimine 62

Figure 4.1: PTFE rod used in the construction of DGT sample holder units 72

Figure 4.2: The assembly of SCPEI-PCPEI based DGT. 74

Figure 4.3: Laboratory-based deployment of passive samplers. 75

Figure 4.4: Sample vials containing the SCPI-PCPEI resin mixture 77

Figure 4.5: Constructed sampling cages used for housing DGT in the field. 81

Figure 4.6: Arial view of the sampling area 82

Figure 4.7: The efflorescent crust used in this study. 84

Figure 4.8: Experimental set up of DGT sampling devices in AMD water. 84

Figure 4.9: PHREEQC input script 85

Figure 5.1: a) CPEI b) sulphonated and c) phosphonated CPEI derivatives 87

Figure 5.2: FT-IR spectra of CPEI, sulfonated CPEI, phosphonated CPEI. 88

Figure 5.3: ^{13}C solid state NMR spectra for SCPEI and PCPEI 90

Figure 5.4: The influence of mixing the sulphonated (S) and phosphonated (P) CPEI resins in different ratios.....92

Figure 5.5: The different modes of adsorption by the SCPEI and PCPEI. 94

Figure 5.6: The elution factors of arsenic, selenium and mercury 95

Figure 5.7: Extraction of arsenic, selenium and mercury using different eluents 96

Figure 5.8: Extraction of arsenic and selenium using different eluents.....97

Figure 5.9: Comparison of commercial and modified DGT sample holders 98

Figure 5.10: Preliminary study using SCPEI-based DGT 100

Figure 5.11: Effect of dispersing SCPEI-PCPEI resin mixture in agarose 101

Figure 5.12: The influence of SCPEI-PCPEI resin mass on the accumulation ..103

Figure 5.13: The effect of the agarose diffusive gel on uptake 105

Figure 5.14: The changes in flux due to increasing diffusive gel thickness 106

Figure 5.15: The effect of turbulence on mass uptake 108

Figure 5.16: The effect of bulk solution concentration on uptake 109

Figure 5.17: Influence of pH on the accumulation. 111

Figure 5.18: Time series experiment for the determination of diffusion coefficients 112

Figure 5.19: The reciprocal mass with varying diffusive layer thickness. 115

Figure 5.20: Uptake in spiked and un-spiked dam water. 120

Figure 5.21: Accumulation of metals from dam water in the laboratory-based experiments 121

Figure 5.22: Accumulation of target analytes in field deployments 124

Figure 5.23: Accumulation of metals during field deployments 125

Figure 5.24: Accumulation of target elements in dissolved efflorescent crust ...128

Figure 5. 25: Accumulation of metals from dissolved efflorescent crust. 130

Figure 5.26: Fouling of DGT after deployment in AMD water.....133

Figure 5.27: Uptake of arsenic from AMD water.....133

Figure 5.28: Accumulation of metals from AMD water 134

LIST OF TABLES

Table 2.1 Important sulphides involved in the production of acid mine drainage (Skousen et al. 1998). 32

Table 2.2: Examples of validated DGT binding layers and their target analytes. .58

Table 2.3: Examples of mixed resin DGTs and their target analytes.....60

Table 2.4: Examples of PEI modification for enhanced selectivity 63

Table 5.1: Description of the absorption bands observed in figure 5.3. 88

Table 5.2: Elemental analysis of the polymers. 91

Table 5.3 Flux differences between stirred and stagnant solutions. 107

Table 5.4: Determination of the diffusion coefficient (*D*) 113

Table 5.5: Comparison of arsenic and selenium diffusion coefficients. 113

Table 5.6: Some examples of how some resin gels were prepared 117

Table 5.7: Anion and metal composition of water sampled at Fleurhof Dam. ...119

Table 5.8: Changes in the physico-chemical properties of Fleurhof Dam water.123

Table 5.9: Anion and metal analysis of the dissolved efflorescent crusts. 127

Table 5.10: Mole percentages of metals found in efflorescent crusts.....127

Table 5.11: Anion and metal composition in AMD water.....132

LIST OF ABBREVIATIONS AND ACRONYMS

AMD	Acid mine drainage
CPEI	Cross linked polyethylenimine
DGT	Diffusive gradients in thin-films
EC	Electrical conductivity
Eh	Redox potential
FT-IR	Fourier transforms infrared
HFO	Hydrated iron oxide
ICP-MS	Inductively Coupled Plasma - Mass Spectrometry
ICP-OES	Inductively Coupled Plasma Optical Emission Spectrometry
LOD	Limit of detection
LOQ	Limit of quantification
MDL	Method detection limit
PCPEI	Phosphonated cross linked polyethylenimine
PES	Polyethersulphone
PTFE	Polytetrafluoroethylene
RSD	Relative standard deviation
SCPEI	Sulphonated cross linked polyethylenimine
TWA	Time weighted average
USEPA	United States Environmental Protection Agency

WHO	World Health Organisation
C	Concentration of labile analyte in bulk solution
M	Mass of analyte
V_e	Volume of eluent
V_g	Volume of binding gel
F	Flux
f_e	Elution efficiency
DBL	Diffusive boundary layer
D	Diffusion coefficient
Δg	Diffusive gel thickness

Chapter 1: Introduction

This chapter addresses the importance of environmental monitoring and problems commonly associated with conventional sampling methods.

1.1 Monitoring of aquatic environments

Water is essential for life and the natural environment. However, in recent years sources of freshwater systems have become particularly vulnerable in both quantity and quality as a result of issues related to climate change, contamination from point and diffuse sources as well as over-utilisation amongst others (Russo, 2017). Consequently, attempts have been made globally to implement regulations that would help in preserving water quality (Brack et al. 2017; Malaj et al. 2014).

According to Brack et al. (2017), the current regulations are based on limited information of single chemicals. To address this issue, several research activities have been implemented with the aim of improving current information (Brack et al. 2017). Specific attention has been placed on the identification, assessment and prioritisation of emerging pollutants (Brack et al. 2017; Von der Ohe et al. 2011).

Periodic monitoring of aquatic systems is fundamental for the management of water quality. The information obtained could allow proper assessment of current policies and whether they are relevant and cost-effective (Brack et al. 2017; Gray and Shimshack 2011; Lovett et al. 2007; Russo 2017; Voulvoulis et al. 2017; Vrana et al. 2005). Water monitoring is based on the evaluation of the physico-chemical and hydromorphological characteristics of the water body, the distribution of biota as well as chemical pollutants, with particular attention on elements that are part of the critical elements' list (Todo and Sato 2002).

Various sampling techniques have been employed for the evaluation of water quality. Most commonly used are spot or grab sampling and biomonitoring methods. Spot or grab sampling is based on the collection of water samples, transport to the laboratory and their filtration prior to analysis (Allan et al. 2006a; Allan et al. 2006b; Montero et al. 2012). Spot sampling is a validated method and has been accepted for regulatory and legislative processes. Nonetheless, this technique provides an overview of the overall water quality at a particular sampling site (Madrid and Zayas 2007). Representative samples can only be obtained over time through the collection of large samples. This in turn makes quality control difficult; it also involves the physical difficulty of carrying the

samples from the sampling site to the laboratory. Sample extraction is labour intensive and analysis is also challenged by high costs (Madrid and Zayas 2007).

Biomonitoring is a monitoring technique based on the use of biological organisms to measure the accumulation of pollutants. The advantage of biomonitoring over spot sampling is that it is able to provide time weighted concentrations (TWA) due to both active and passive diffusion within the organism (Namieśnik et al. 2005).

In biomonitoring, the species of interest should be easy to identify, abundant, stationary, long-lived and unaffected by any changes in environmental conditions. Most importantly, biomonitors need to be able to concentrate the target pollutants in their tissues (Søndergaard et al. 2014). Generally, most biomonitors accumulate lipophilic compounds faster (Namieśnik et al. 2005). This could be a major drawback if the target analytes do not fall within this criterion.

The passive sampling technique uses the same approach as biomonitors. It consists of a biomembrane mimetic, as well as a sorption or receiving phase where the analytes of interest can be accumulated over time (Kot et al. 2000; Vrana et al. 2005). Unlike biomonitors, passive samplers can be deployed in any environment without considerations of whether they will survive or not. Secondly, passive samplers are not susceptible to the same issues faced by biomonitors such as diseases, predators, lack of food and oxygen, death resulting from pollution, requirement to reproduce, amongst others. Most importantly, passive samplers can be adapted to suit the analytes of interest (Kot et al. 2000; Vrana et al. 2005).

The South African Witwatersrand gold mining operations have played a huge role in the growth of the economy. However, one of the major repercussions has been the degradation of surface and ground water from the slow seepage of acid mine drainage (AMD). Due to the high acidity, AMD characteristically has a high concentration of dissolved metals and trace elements, putting a serious strain on fresh water systems (Cheng et al. 2009; Naicker et al. 2003; Tutu et al. 2008).

Arsenic, selenium and mercury are amongst the elements found in AMD and they can be distributed within various environmental compartments depending on pH, redox potential and other factors that favour mobilisation. The toxicity of mercury and arsenic is well documented; on the other hand, selenium becomes toxic above a certain threshold. Currently there is little information on bioavailable arsenic, selenium and mercury within wetlands affected by AMD. Most information is based on total concentrations. Monitoring approaches therefore need to focus on the acquisition of bioavailable data.

Passive sampling is a growing area of research with new passive samplers continuously being developed. Diffusive gradients in thin-films (DGT) is an *in situ* passive sampling device (DGT Research Ltd., UK). It comprises of a filter membrane that serves as a protective layer, a diffusive gel that controls the rate of mass transfer into the passive sampler and a resin layer, which acts as a sink for the target analytes. These components are layered on a Teflon piston base and sealed from the external environment with a cap that has a small exposure window. The cap in commercial DGT is disposable, which is not cost effective for extensive monitoring. Furthermore, the resin layer contains Chelex-100 resin which specifically targets divalent cations (Garmo et al. 2003; Hooda et al. 1999; Zhang et al. 1995a; 1995b; Zhou et al. 2018). Arsenic and selenium are oxyanions and will therefore not adsorb efficiently on the Chelex resin. Mercury has also shown poor adsorption (Dočekalová and Diviš 2005; Gao et al. 2011).

Previous studies have shown that DGT is an invaluable tool for obtaining information on bioavailable fractions, however, due to the lack of selectivity for arsenic, selenium and mercury a new resin needs to be explored. Polyethyleimine (PEI) has been used as an adsorbent for metals due to the large number of primary, secondary and tertiary amine groups (Ma et al. 2014; Li. et al. 2016; Setyono and Valiyaveettil 2016). Although PEI mostly targets metals, PEI was modified with phosphate and sulphonyl functional groups to target arsenic, selenium and mercury in mine waste waters (Saad et al. 2011; Saad et al. 2012; Saad et al. 2013a; 2013b). The phosphonated polymer showed 88% efficiency in the removal of arsenic, 81% and 87% efficiency removal for selenium and

mercury by the sulphonated polymer, respectively (Saad et al. 2012b; Saad et al. 2013a; Saad et al. 2013b).

In this study, a new DGT passive sampler comprising of a SCPEI-PCPEI resin mixture as a binding layer is described. The selectivity of this resin is shown in batch studies. The DGT sample holders used in this study were manufactured in our in-house workshop with the added advantage of being re-usable, making the passive sampler affordable. The performance of these devices was assessed in time series experiments under controlled laboratory conditions to test the influence of turbulence, sample concentration and pH. The calibration results show this DGT device can be considered a valid kinetic passive sampler. Field deployments demonstrate the influence of the sample matrix on the SPEI-PCPEI resin mixture.

Chapter 2: Literature review

This chapter provides a comprehensive literature review on trace elements in the environment, with particular attention placed on arsenic, selenium and mercury, their behaviour in the environment as well as interactions with AMD. Diffusive gradients in thin-films passive sampler are also the main focus of this work.

2.1 Trace elements in the environment

Living organisms can be exposed to non-essential trace elements such as arsenic, cadmium, mercury, lead to name a few. These elements are not required for either growth or function of the organism and they disrupt normal physiological processes at the cellular or even at the molecular level by inactivating enzymes, blocking functional groups and even disrupting the membrane's structural integrity (Rascio and Navari-Izzo 2011).

Sources of trace elements can either be natural or anthropogenic. Processes that release trace elements into the biosphere such as weathering and volcanic eruptions are natural sources. On the other hand, examples of anthropogenic activities are mining, smelting, electroplating, waste water discharge, deposition of industrial fumes, and use of sewage sludge. Anthropogenic activities are deemed the main contributors of trace elements in the environment, especially for areas in close proximity (Rinklebe et al. 2017).

2.1.1 Arsenic in the environment: sources and distribution

Arsenic is a metalloid widely distributed in the natural environment. It is the 20th abundant element in the Earth's crust, 14th in seawater and 12th in the human body (Mandal and Suzuki 2002). The ubiquity of arsenic does not necessarily mean it is profuse: the estimated concentration range in the Earth's crust is between 1.5 and 3 mg kg^{-1} (Cullen and Reimer 1989; Drewniak and Sklodowska 2013; Zhao et al. 2010), and an average concentration of 0.5 to 2.5 mg kg^{-1} is found in rocks, including igneous and sedimentary rocks (Kabata-Pendias and Pendias 1984). However, higher concentrations ranging between 0.4 and 188 mg kg^{-1} have been reported in sedimentary rocks such as phosphorites (Mandal and Suzuki 2002). The concentration range in fresh water is estimated to be between 0.15 and 0.45 µg L^{-1}, and is dependent on the source, availability, as well as the geochemistry of the catchments (Bissen and Frimmel 2003; Smedley and Kinniburgh, 2002). Concentrations in sea water are usually less than 2 µg L^{-1} (Ng 2005).

Arsenic is found in over 200 mineral forms (Onishi 1969; Mandal and Suzuki 2002). These minerals are ores with the most prevalent being arsenic sulphides such as realgar (As_4S_4), arsenopyrite (FeAsS) and orpiment (As_2S_3) (Mandal and Suzuki 2002; Smedley and Kinniburgh 2002; Farooq et al. 2016). Arsenic also has a strong association with iron oxide and hydroxide minerals, which are weathering products (Reeder et al. 2006).

Arsenic makes its way into the environment through natural processes or as a result of anthropogenic activities. Natural processes include weathering, biological activities, geochemical reactions, volcanic eruptions, with soil erosion and leaching contributing between 612×10^8 and 2380×10^8 g $year^{-1}$ (Mackenzie et al. 1979; Mohan et al. 2007). Anthropogenic activities such as mining have led to increased arsenic concentrations in water, soil, sediments and vegetation (Smedley and Kinniburgh 2002). Additionally, it can be distributed into the environment through the infiltration of arsenic contaminated groundwater (Smedley et al. 2003). Arsenic is also a component of pesticides and herbicides, crop desiccants and livestock feed (Mohan et al. 2007). These pollution trends are exacerbated by population growth and industrial development.

2.1.1.1 Arsenic toxicity

Although arsenic is found in trace concentrations, it has been classified as a class 1 carcinogen by the International Agency of Research on Cancer (IARC) (IARC, 2012). The primary mode of exposure to arsenic is through ingestion of contaminated water (Sharma and Sohn 2009). The U.S. Environmental Protection Agency (EPA) and World Health Organization (WHO) have declared the limit of arsenic levels in drinking water as 10 µg L^{-1}.

It is estimated that between 60 and 100 million people globally may be at risk of arsenic poisoning (Ng et al. 2003). High arsenic concentrations have been recorded in South and South-East Asia, and this is a serious toxicological concern (Brammer and Ravenscroft 2009). The first health issues resulting from arsenic toxicity were identified in West Bengal in the 1980s. Subsequent diagnosis in Bangladesh only occurred in 1993. One of the most common external symptoms

of arsenic poisoning is skin disorders including hyper or hypopigmentation and keratosis. In some cases even skin cancers have been reported. These symptoms were identified in as high as 200 000 patients (Smith et al. 2000). What makes the situation rife in these areas is that for drinking water they rely heavily on ground water sources (Smedley and Kinniburgh 2002).

Arsenic contamination is unfortunately not limited to fresh and ground water. Soil contamination is a growing area of concern in agricultural areas (Mishra et al. 2014). Arsenic is not a nutrient and it has toxic effects on plants (Farooq et al. 2016). Secondly, arsenic has the ability to bioaccumulate in plants which are later consumed by humans (Finnegan and Chen 2012). One example of arsenic contamination issues and vegetation is rice cultivation in the Hunan province in China. Rice grain from this region contained up to 723 µg g^{-1} of arsenic, far exceeding the allowed Chinese maximum of 150 µg g^{-1} (Okkenhaug et al. 2012; Williams et al. 2009).

Another example was a study conducted by Abad-Valle et al. (2018) where they evaluated the effects on the ecosystem after the closure of a mine 2 km from the south of the Barruecopardo Village, in the North-West of the Salamanca province, Spain. The mine is in close proximity to an agricultural farming area. They found that this area showed high levels of arsenic. Concentrations ranged between 138–854 mg kg^{-1} in soil. It was concluded that the use of such highly contaminated lands for grazing poses a serious risk of transferring and accumulating arsenic in higher food chain trophic levels (Abad-Valle et al. 2018).

2.1.1.2 Arsenic speciation and bioavailability

Exposure to non-essential elements is not enough to cause toxicity; instead speciation determines how much of the total element present will actually interact, and be absorbed across a physiological membrane (Reeder et al. 2006). Speciation also controls an element's solubility. Solubility consequently influences the mobility and exposure rate. Additionally, once a pollutant has entered an organism, transformation speciation may occur within biological fluids and organ

systems, affecting subsequent absorption, detoxification, excretion and storage (Reeder et al. 2006).

Arsenic exists in the −3, 0, +3 and +5 oxidation states; 0 (As), -3 (e.g. AsH_3), +3 (e.g. As_2O_3) or +5 (e.g. Na_3AsO_4) (Mohan and Pittman 2007; Smedley and Kinniburgh 2002; Zhang et al. 2017). The two inorganic arsenic species commonly found in natural waters are arsenic (III) and arsenic (V) simply referred to as arsenite and arsenate, respectively. The interconversion between the two species is strongly influenced by abiotic factors such as redox potential (Eh) and pH together with microorganisms (Nearing et al. 2014; Zhao et al. 2010; Farooq et al. 2016). Arsenic can also exist as methylated arsenite and arsenate derivatives, arsenobetaine, arsenocholine and arsenosugar (Ng 2005). Most organoarsenical compounds are found in aquatic and terrestrial environments (Francesconi and Edmonds 1997; Grotti et al. 2008).

The pH of surface and ground water is between 6.5 and 8.5, with most surface waters having a moderate Eh (200-600 mV) and a neutral pH (Smedley and Kinniburgh 2002; Zhang et al. 2017). Arsenic is susceptible to mobilisation at this pH range, under both aerobic and anaerobic conditions (Smedley and Kinniburgh 2002). In this pH range arsenite exists as an uncharged species whereas arsenate exists as an oxyanionic species (Smedley and Kinniburgh 2002).

Arsenite is a hard acid and favours complexation with oxides and nitrogen. On the other hand arsenate is a soft acid and forms complexes with sulphides (Bodek et al. 1988). Examples of arsenate species include AsO_4^{3-}, $HAsO_4^{2-}$, and H_2AsO^{4-}. Arsenate species predominate in oxidising conditions, the dominant species at pH values less than 6.9 is $H_2AsO_4^-$. At higher pH $HAsO_4^{2-}$ is the major species (Mohan and Pittman 2007). Alternatively, under extremely acidic and alkaline conditions $H_3AsO_4^0$ and AsO_4^{3-} may be present, respectively (Smedley and Kinniburgh 2002). In moderately reducing anaerobic environments arsenite species are found in higher concentrations. Examples of arsenite species include $As(OH)_3$, $As(OH)^{4-}$, AsO_2OH^{2-} and AsO_3^{3-}. The arsenite species H_3AsO_3 predominates at pH values less than 9.2 (Mohan and Pittman 2007). This information is summarised in Figure 2.1.

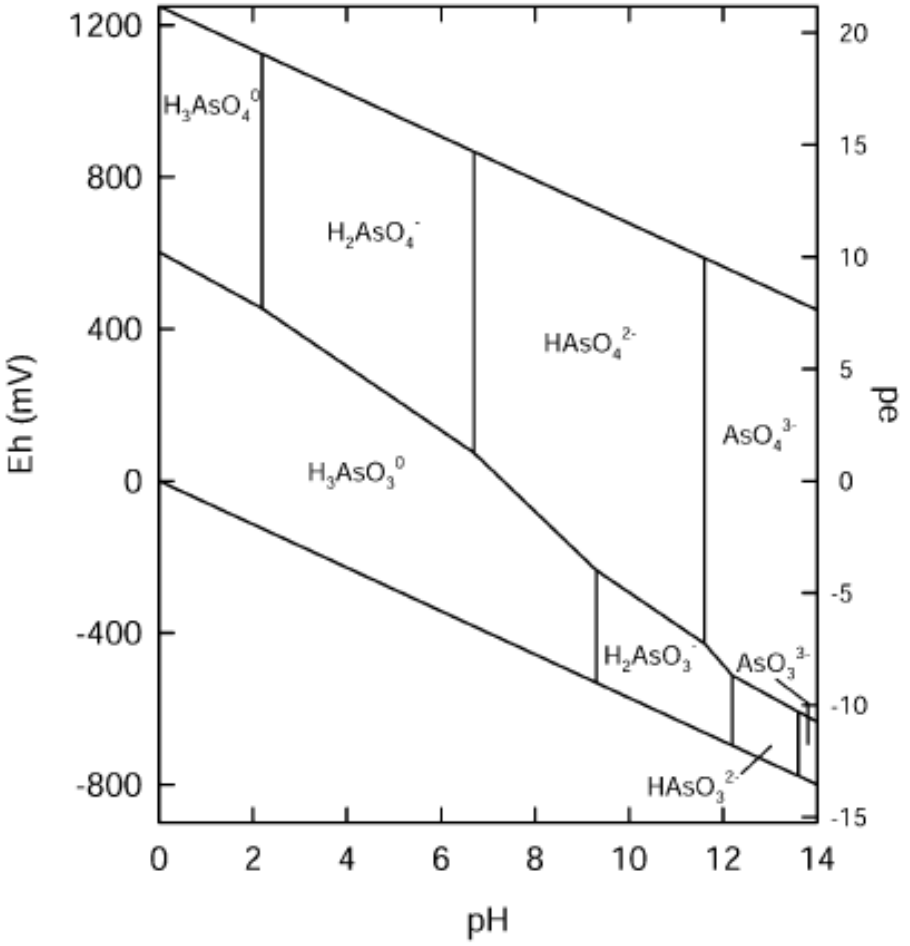


Figure 2.1: The Eh–pH diagram for arsenic at 25◦C and 101.3 kPa (Wang and Mulligan, 2006).

Inorganic arsenic is considered more toxic to humans and animals compared to the organic counterparts (Meharg and Hartley-Whitaker 2002; Ng 2005). Furthermore, it can undergo methylation through microbial activity to form less toxic organic arsenic such as monomethylarsenic (MMA) and dimethylarsinic acid (DMA) (Broka et al. 2016; Jin et al. 2010). Arsenobetaine, is the most prevalent organoarsenical in marine animals but it is not common in vertebrates and invertebrates found in freshwater systems (Schaeffer et al. 2006). Arsenolipids have also been identified in cod fish oil (Rumpler et al. 2008).

Mass et al. (2001) showed that arsenite, MMA and DMA derived from arsenite are more toxic than arsenate and its methylated derivatives. Additionally, some studies have even suggested higher toxicity in MMA and DMA derived from arsenite compared to their parent compound, arsenite (Mass et al. 2001; Petrick et al. 2000). Acute toxicity of trivalent arsenic could be due to higher affinity for sulfhydryl and cysteinyl groups of many enzymes including glutathione and lipoic acid (Aposhian and Aposhian 2006).

2.1.1.3 Ion interactions with arsenic

The presence of ions in water can either inhibit or promote the adsorption of arsenic. Oxyanions such as phosphate, sulphate, carbonate and silicate have a competitive and inhibitory effect. Inhibition is to varying degrees, with the effect intensifying as the anion concentration increases (Zhang et al. 2017). In particular, Cl^-, $H_2PO_4^-$, and SO_4^{2-} have a strong inhibitory effect on the adsorption of arsenite (Livesey and Huang 1981; Zhang et al. 2017). Some studies have reported carbonate and biocarbonate causing the solubilisation of arsenic from sediments and iron oxyhydroxides (Anawar et al. 2004; Appelo et al. 2002; Arai et al. 2004; Kim et al. 2000; Stachowicz et al. 2007). In contrast, the presence of Cl^-, F^-, and SO_4^{2-}, and their combination with sediments promote the adsorption of arsenate (Goh and Lim, 2005). Some of the highest arsenic concentrations have been found in groundwater with low SO_4^{2-}concentrations (Zhang et al. 2017). Alternatively, cations such as Ca^{2+}, Mg^{2+}, and Na^+ promote the adsorption of both arsenite and arsenate, and this becomes stronger with increasing cation concentration. Cations attach to the surface of the adsorbent, increasing electro-positivity. This increases the electrostatic force with arsenic anions, forcing them to attach to the adsorbent surface (Smith et al. 2002).

According to a study conducted by Smedley et al. (2003) in Huhhot Basin, inner Mongolia, arsenic concentrations in ground water are masked by the high concentrations of iron, manganese, phosphorus, ammonium, and hydrogen carbonate. Seddique et al. (2008) also looked at arsenic levels and the hydrological conditions of ground water in Sonargaon (mid-East Bangladesh). The study showed that the main hydrochemical types of high arsenic groundwater

are calcium, magnesium and hydrogen carbonate. A study by Deng et al. (2011) on high arsenic groundwater on Hetao Plain in Northern China, reveals the hydrochemical types to include carbonate bound to chloride; free chloride and hydrogen carbonate.

2.1.1.4 Adsorption in the biogeochemical cycle of arsenic

Adsorption is also important in determining the concentration and speciation of arsenic in natural water (Sharma and Sohn 2009). Arsenate adsorption is not only affected by competition for active sites but by the redox potential as well as co-precipitation (Han et al. 2007; Ciardelli et al. 2008).

Iron oxides and hydroxides together with microorganisms are involved in the geochemistry of arsenic (Figure 2.2a). In the absence of iron or in systems with low iron concentration, clays, calcium compounds, aluminium and manganese oxides and oxyhydroxides play a role in the sorption of arsenic (O'Day, 2006). Adsorption increases with decreasing $(CaO + MgO)/(Al_2O_3 + Fe_2O_3)$ ratio; (Onken and Adriano 1997). Arsenic fixation can also happen via manganese oxides; the cation provides a positive surface charge (Takematsu et al. 1985). A synergistic interplay happens between manganese and iron; manganese (IV) is reduced to manganese (II) before iron (III) reduction that way the concomitant release of arsenic from manganese is re-adsorbed by iron oxides or hydroxides (Moore et al. 1988).

MMA and DMA found in herbicides and pesticides are used by some microorganisms as a source of carbon. MMA and DMA are transformed into either arsenate or arsenite through microbial activity (Figure 2.2b). Arsenite can also be methylated into gaseous trimethylarsine, returning deposited arsenic back into the atmosphere. Inorganic arsenic deposited in aqueous systems is converted into water-, lipid organic compounds (Rensing and Rosen 2009).

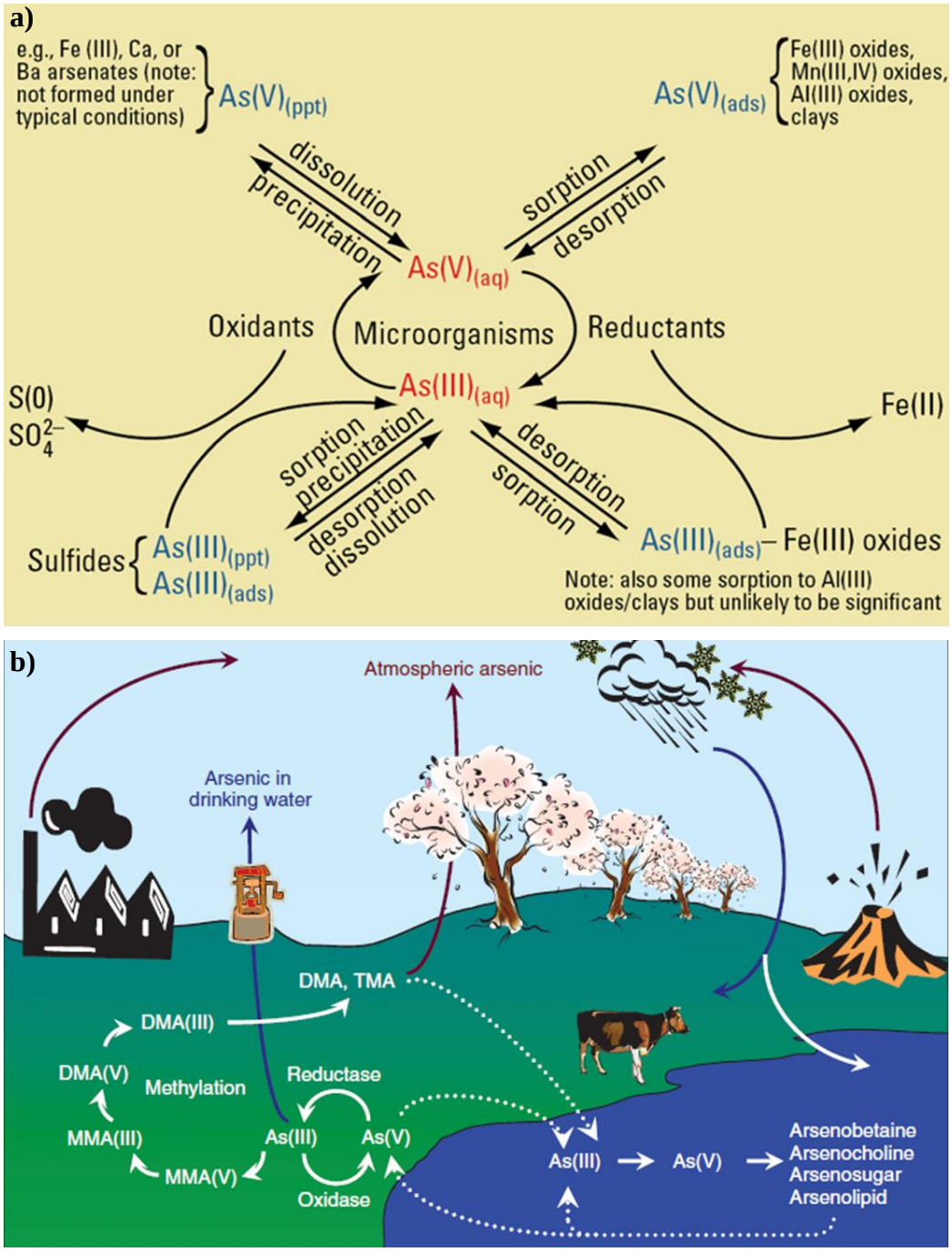


Figure 2.2: a) the geochemical cycle of arsenic in the environment (Adapted from Rensing and Rosen 2009). b) summary of the interactions involved in the arsenic geochemical cycle (Reisinger et al. 2005; Sharma and Sohn 2009).

2.1.2 Selenium in the environment: sources and distribution

Selenium is the 30th abundant non-metal trace element in the Earth's crust (Tan et al. 2016). Similar to arsenic, it is ubiquitous and it is spread out in different environmental compartments like ores, sedimentary rocks, soil, fossil fuels, water, air and vegetation (Fernández-Martínez and Charlet, 2009; Santos et al. 2015; Khoei et al. 2017). The concentration of selenium is estimated to be between 0.05 and 0.5 mg kg^{-1} in the Earth's crust (Lemly 2004) and between 0.01 to 2 mg kg^{-1} in soil (Floor and Roman-Ross 2012). Seleniferous soils which are defined as soils rich in selenium produce vegetation with more than 5 µg g^{-1} of selenium (Dhillon and Dhillon 2000). Concentrations in these soil types can reach as high as 1200 mg kg^{-1} of total selenium and 38 mg kg^{-1} of soluble selenium (Selim and Sparks 2001; Fordyce 2007; Wakim et al. 2010). Concentrations higher than 5 mg kg^{-1} have been recorded in Canada, France and Western USA (Sigrist et al. 2012).

The average concentration of selenium in freshwater is 0.02 µg L^{-1} (Fernández - Martínez and Charlet 2009) and less than 0.08 µg L^{-1} in sea water (Mitchell et al. 2012). On the other hand concentrations in groundwater are usually higher as a result of the close contact with rocks (Santos et al. 2015). In non-contaminated areas, away from volcanic activity, natural atmospheric levels are between 0.01 and 1 mg m^{-3} (Fordyce 2013). Selenium is also found in certain food types, especially protein rich food like eggs, meat, chicken, fish and cereals. Fruits and vegetable have lower concentrations ranging between 10 and 20 µg kg^{-1} (Klapec et al. 2004; Ventura et al. 2009).

Selenium is an essential micronutrient for both humans and animals; it is required for the synthesis of selenoproteins. Selenium is also involved in antioxidant functions, regulation of thyroid hormone metabolism and the immune system. It is also suggested to have a role in suppressing the progression of AIDS. Selenium has a role in cardiovascular diseases, mood disorders as well as reproduction (Combs and Gray 1998; Goldhaber 2003; Rayman 2000; Taylor et al. 2009). It was discovered that optimum concentrations of selenium can help reduce cancer (Combs and Gray 1998; Rayman 2000). Selenium may possibly have an

important detoxification function as a result of its antagonism with mercury. This role however, is reliant on the molar ratios of the two elements (Burger and Gochfeld 2012; Lemly 2014, Penglase et al. 2014).

Selenium is capable of being essential and toxic at the same time, with the margin of toxicity being very thin (Brozmanová et al. 2010; Thiry et al. 2012). Selenium toxicity arises when concentrations are well above those required by the body. This leads to carcinogenesis, cytotoxicity and genotoxicity (Zhang et al. 2014; Sun et al. 2014). The recommended amount of selenium will depend on factors such as gender, age, human condition as well as geographical location (Kieliszek and Błażejak 2013). The international standard for dietary intake has been set between 30 and 55 µg per day (Winkel et al. 2011).

In contrast, some diseases result from selenium deficiency, which may be corrected through supplementation (Combs 2000). It is assumed that globally, between 500-100 million people are selenium deficient, this accounts for 15% of the world population (White et al. 2012). Soils are considered selenium deficient if they have concentrations less than 0.5 mg kg^{-1} (Fordyce 2007; Mirlean et al. 2017). Geographical locations deficient in soil selenium have been associated with heart disease and bone disorder cases (Lemly 1999). One such example was seen in China. There were reports of widespread cases of Keshan and Kashin-Beck, which are heart and osteoarthropathy cases. These incidences took place in the North-West to the South-West regions of China, typically characterised by low selenium concentrations of approximately 0.125 mg kg^{-1} (Fordyce 2007).

Selenium environmental pollution can either be through natural or anthropogenic sources. Rock-water interactions, the actual weathering of rocks as well as biological activities are all involved in the natural distribution of selenium (Fernández-Martínez and Charlet 2009). In addition, volcanic activities also naturally release selenium into the atmosphere as high temperature gases, leaving volcanic rocks with very low selenium levels (Fleming 1980; Jacobs 1989; Neal 1995; Nriagu 1989).

Alternatively, anthropogenic sources of selenium include industrial coal combustion, mining activities and oil refineries. Selenium also has various industrial applications, approximately 40% of its application is in metallurgy, 25% in glass production, 10% in agriculture to name a few (Fernández-Martínez and Charlet 2009; Jewell and Kimball 2015; Hamilton 2004; Tuzen and Sari 2010; Santos et al. 2015; Tan et al. 2016). These applications also release selenium into the environment.

Large scale selenium is not mined; instead it is obtained as a by-product in copper and lead refinery as well as sulphuric acid processing plants (El-Ramady et al. 2014; Johnson et al. 2010; Nancharaiah and Lens 2015). It is suggested that more than 80% of commercially available selenium is obtained from anode slime, which is a by-product in copper refinery (Young et al. 2010, Anderson 2013). A potential problem is that production of selenium is dependent on parent material, this means that if for example, copper ores become depleted in the future, there is going to be an even higher demand for selenium and pressure to find alternative sources (USGS 2015; Tan et al. 2016). Selenium contamination in the environment has the potential to cause long term problems (Brown and Arthur 2007; Staicu et al. 2015).

2.1.2.1 Selenium toxicity

Risks associated with selenium are through direct exposure from contaminated water, soil or aquatic food sources. As previously mentioned, the dietary intake of selenium has to be well managed in order to avoid toxic effects. This is because selenium has the tendency to bioaccumulate, despite the generally low concentrations (Lemly 2004; Lemly 2014; Stewart et al. 2010). Inorganic selenium is able to accumulate between 100 to 400 times the original concentration, while organic selenium can bioaccumulate up to 350 000 times. Even in aquatic systems with concentrations as low as 0.1 µg of L^{-1}, selenium can still reach toxic levels within the food chain trophic levels (Lemly 2004).

Furthermore, there has also been evidence of selenium biomagnification in water organisms (Muscatello and Janz 2009). Muscatello et al. (2008) looked at the

accumulation pattern of selenium in the aquatic ecosystem surrounding the uranium mine in northern Saskatchewan, Canada. Aqueous selenium concentrations were relatively lower than concentrations found in biota at the reference sites, suggesting bioaccumulation. Biomagnification was evident amongst the different trophic levels, with selenium concentrations being 1.5 to 6 times high amongst plankton, invertebrates and small bodied fish.

Selenium contamination in fresh water places a lot of pressure on ecological wildlife (Luoma and Presser 2009). This is particularly true for vertebrates that are reliant on water to lay their eggs. This toxic effect was seen in the embryo mortality of waterfowls and the larva deformities of fish (Chapman et al. 2010). California's Kesterson Wildlife reservoir was one of the worst hit with selenium contamination. The aquatic life in this reservoir experienced physical deformities, reproductive failures, mutations and death (Ellis et al. 2003). In another incident, the fish from a lake that was contaminated with selenium from a coal fired power plant were reported to have teratogenic effects, spinal and craniofacial malformations (Lemly 2014).

2.1.2.2 Selenium speciation and bioavailability

The bioavailability and mobility of selenium, together with the concentration in the surrounding soil, sediment or water, is a function of the geochemical reactions and speciation (Persico and Brookins 1988). Speciation in water is in turn determined by redox conditions, pH, available sites on sorbing surfaces as well as biological activities (Santos et al. 2015; Sharma et al. 2015).

Selenium exists in five oxidation states: -2, -1, 0, +4 and +6; 0 (Se), selenide (-2), selenite (+4), selenate (+6) and organic selenium. Each species presents different chemical properties and toxicity (Santos et al. 2015). Under environmentally relevant conditions, the predominating inorganic selenium species are selenide (Se^{2-}), selenite (SeO_3^{2-}), selenate (SeO_4^{2-}) and elemental selenium (Se^0). Selenate is the completely oxidised form of selenium and the SeO_4^{2-}oxyanion predominates in oxidising conditions whereas selenite oxyanion SeO_3^{2-} is found at between pH 3 and 8 in moderately to lower redox potential (Fernández-Martínez and Charlet

2009; Goh and Lim 2004; Latorre et al. 2013). Selenate can exist as either biselenate ($HSeO_4^-$) or selenate (SeO_4^{2-}). Selenite is also present as a weak acid named selenious acid (H_2SeO_3), biselenite ($HSeO_3^-$) or selenite (SeO_3^{2-}) (Séby et al. 2001). Se^0 is insoluble in water and is usually found in soil and sediments (Vesper et al. 2008). This information is summarised in Figure 2.3.

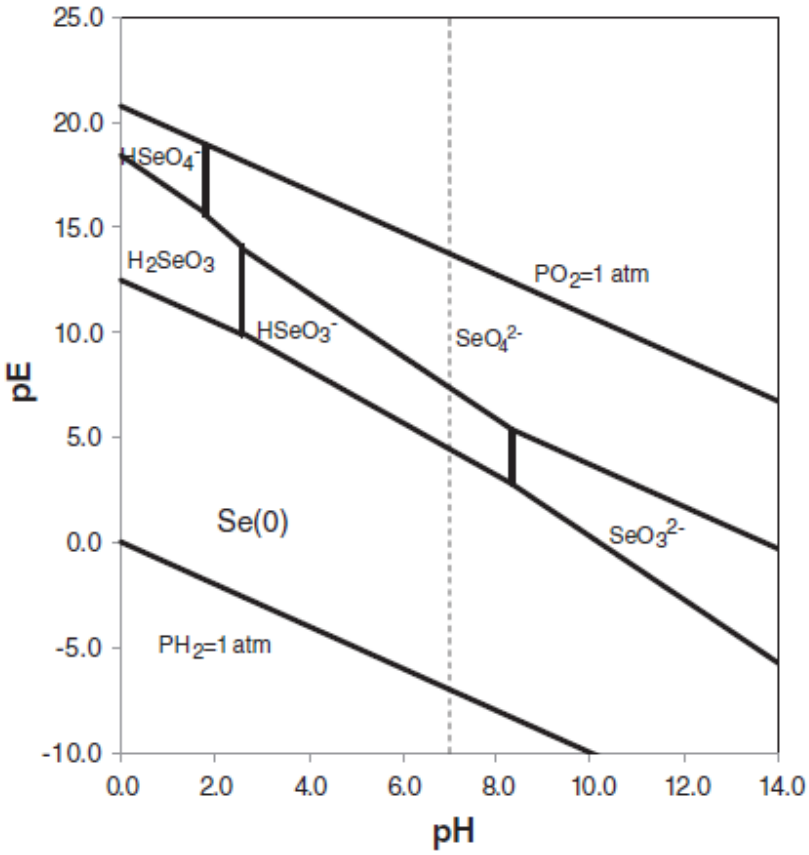


Figure 2.3: pE-pH diagram of Se-O-H at 298 K (Santos et al. 2015)

Selenite (SeO_3^{2-}) and selenate (SeO_4^{2-}) oxyanions are also found in industrial wastewaters. These two oxyanions are toxic to living organisms, with selenite oxyanion being more toxic compared to selenite (Vesper et al. 2008). On the other hand organic selenium compounds are usually found in air, soil and plants as methylselenides, dimethylselenide, dimethyldiselenide, trimethylselenonium ions or seleno amino-acids (Fernández-Martínez and Charlet 2009; Lenz et al. 2006;

Pyrzynska 2002). These methylated derivatives are mainly by-products from bacterial methylation (Fernández-Martínez and Charlet 2009). Organic selenium derived from selenide is the most bioavailable form and readily absorbed by algae compared to the inorganic species (Lemly 1993; Maier et al. 1993).

2.1.2.3 Ion interactions with selenium

Selenium also has a strong relationship with iron, aluminium and manganese oxides and hydroxides, as well as carbonates and organic matter (Selim and Sparks 2001). Iron and aluminium oxides in particular, have variable charged surfaces depending on pH. At lower pH values, the mineral surface takes on a positively charged surface increasing the sorption capacity towards selenite and selenate (Yu 1997). The likelihood of selenite being adsorbed onto solid inorganic surfaces such as ferric hydroxide or organic matter is higher compared to selenate. Alternatively, selenate oxyanion SeO_4^{2-} is highly soluble with low adsorption and precipitation propensities (Fernández -Martínez and Charlet 2009; Goh and Lim 2004; Vesper et al. 2008).

Selenium speciation in water and wastewater can also be influenced by other metal ions (Torres et al. 2011; Vesper et al. 2008). Torres et al. (2011) looked at the interaction of selenite and selenate with predominant metal species found in natural waters. They found that depending on the pH and redox potential of the surrounding environment, the interaction with metal ions can either be negligible or considerable. For example, in the presence of alkaline earth metal ions, selenite; $HSeO_3^-$ is present as a free anion, especially at low pH. Torres et al. (2011) further stated the contribution of the transition metals copper, zinc and cadmium in keeping selenium in solution, depending on the pH. In some cases certain cations can mask the presence of selenium, reducing its bioavailability. Additionally, the predominant selenium species in water are anionic and will therefore compete for protons with other anions, especially those originating from other trace elements (Torres et al. 2011; Zhang et al. 2005).

The adsorption of selenium is also influenced by competition between anions such as sulphate and phosphate (Balistrieri and Chao 1990). Chan et al. (2018) studied

the competition of the selenite and selenate anions with phosphate and sulphate anions and their adsorption on Fe/Si and Al/Si co-precipitates. The study revealed that phosphate effectively inhibited both selenite and selenate adsorption on both the Al/Si and Fe/Si co-precipitates. Similarly, Dhillon and Dhillon (2000) showed that phosphate anions directly compete with selenite for sorption sites found in soil. They claim that as the amount of selenite adsorbed increased, adsorption of phosphate decreased, implying competition for the same adsorption sites. Alternatively, sulphate only affected the adsorption of selenate at greater degree compared to selenite (Chan et al. 2018). Wijnja and Schulthess (2000) also support this notion by suggesting that competition between selenium and sulphate is only specific for the selenate species.

Although there are some chemical similarities between selenium and sulphur since they are both in group 16 of the periodic table, their behaviour and fate in natural water is markedly different: The differences reside in the magnitude of redox as well as acid-base reactions (Bodek et al. 1988; Torres et al. 2011). For example under similar conditions, the interaction of divalent cations with SO_4^{2-} will be stronger than their interaction with SeO_4^{2-}. Moreover, in freshwater, the concentration ratio between sulphur and selenium is 20 000. (Torres et al. 2011).

2.1.2.4 Selenium biogeochemical cycle

The biogeochemical cycle of selenium (Figure 2.4) begins with the release into the atmosphere from natural and anthropogenic processes. Atmospheric selenium undergoes transformations and it is released back on land and water through wet or dry deposition. On land, selenium is up taken by plants and soil microorganisms. In addition, selenium can undergo various redox reactions as well as methylation and de-methylation reactions by microorganisms. Some of it is adsorbed onto organic matter and soil minerals. In water, selenium still undergoes methylation and de-methylation reactions through microbial action in addition to redox reactions. Selenium makes its way into the food chain through uptake by bacterial algae and it is biomagnified with each trophic level of the food chain (Winkel et al. 2015).

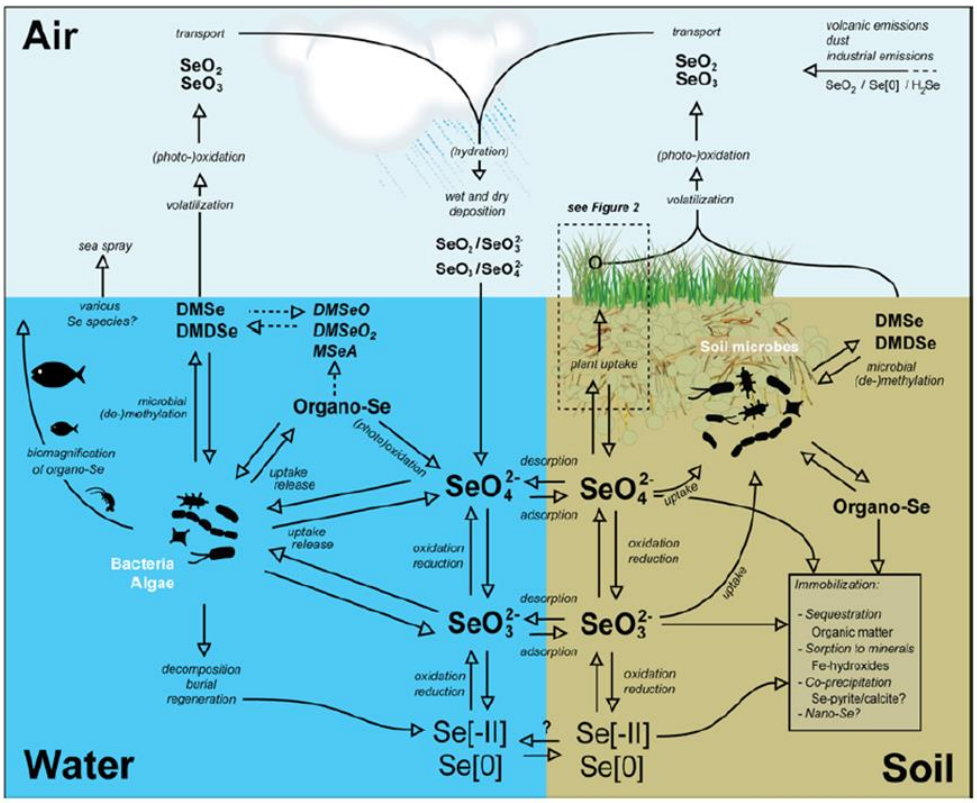


Figure 2.4: The biogeochemical cycle of selenium, including abiotic and biotic influences on transformation and speciation (Winkel et al. 2015).

2.1.3 Mercury in the environment: sources and distribution

Mercury is a naturally occurring metal in the environment. The amount in different types of soils can range between 0.58 and 1.8 mg kg^{-1}, and the global average is estimated at 1.1 mg kg^{-1}, with higher concentrations observed in Histosol and Cambisol soil (Kabata-Pendias 2010). Concentrations of mercury in water are generally low. Total mercury concentrations obtained from Antarctic surface water are considered global baselines due to their pristine nature. Concentrations in Antarctic lakes and glacial streams range between 2.2 and 9.5 pM; dissolved mercury is between 0.5 and 2.2 pM and methylmercury concentrations range from < 0.4 and 2.1 pM (Vandal et al. 1998; Lyons et al. 1999).

In contaminated water, concentrations can be in the μg L^{-1} range (Ullrich et al. 2001). The percentage of methyl mercury is higher in fresh water compared to estuarines whereby methyl mercury is usually less than 5% of the total mercury (Coquery et al. 1997; Mason and Sullivan 1999) whereas the proportion in freshwater and lakes can be as high as 30% (Kudo et al. 1982; Meili 1997; Leermakers et al. 1996). Mercury in the environment can be acquired from both natural and anthropogenic sources and it is widely distributed on the Earth's surface (Frohne et al. 2012).

Natural processes such as weathering of mercury containing rocks in the Earth's crust, geothermal activity or volcanic eruptions all lead to the release of mercury into different environmental compartments (AMAP/UNEP, 2013). It is estimated that emissions into the atmosphere from natural sources are approximately 80 to 600 tons $year^{-1}$ (Mason et al. 2012). Pirrone et al. (2010) suggest that oceans are accountable for approximately 50% of mercury emissions from natural sources. They release 2.68×10^6 kg $year^{-1}$. Emissions from oceans are in turn affected by three factors: mercury concentration gradient at the ocean-air interface; the temperatures at the water air interface as well as solar irradiation (Li and Tse 2015). Contributions of mercury emissions from natural sources vary depending on factors such as volcanic activity, the rate of geothermal activity, geological formations, as well as the frequency of natural fires (Ferrara 1998; Ferrara 2000; Pirrone et al. 2001).

Conversely, anthropogenic sources release approximately 1960 tons $year^{-1}$ of mercury (AMAP/UNEP 2013) with Asia and Africa being the major contributors of the global total. The main sectors that contribute to mercury pollution are artisanal and small scale gold mining (ASGM), coal combustion, metal refineries, cement production as well as the disposal of mercury containing waste (AMAP/UNEP 2013; Feng et al. 2004; Mason et al. 2012; Wu et al. 2006). In North America, 40% of total mercury emissions can be attributed to discarded thermometers, batteries and florescent lamps. Additional contributors are barometers, wind tunnels and engine manufacturing. In agriculture, mercury emission stems from the use of fertilizers and pesticides, sewage sludge and

irrigation water (Hseu et al. 2010). Furthermore, mining activities directly deposit mercury into the environment through the release of mine waste without prior treatment, leading to seepage in the adjacent soil (Qiu et al. 2005).

The global mercury emissions into the atmosphere were reported to reach as high as 3000 tons in 2005 (Branch 2008). Issues related to the initial release of mercury are compounded by re-emissions. Re-emissions are described as emissions that arise from previous natural and anthropogenic deposits. For example, mercury deposited in the Earth's surface including soil, rocks, snow, ice and surface water can re-emerge through conductive conditions (AMAP/UNEP 2013; Mason et al. 2012). Additionally, mercury within the atmosphere returns to the Earth's surface through either wet or dry deposition, which accounts for approximately 90% of emitted mercury (Lindqvist et al. 1991). It is estimated that mercury re-emissions can be as high as 4000 to 6300 tons $year^{-1}$ (AMAP/UNEP 2013; Mason et al. 2012).

After undergoing either dry or wet deposition, mercury can become trapped by organic matter over time, enriching the top layers of soil. This process is governed by the amount and quality of organic matter, as well as the partitioning of the organic matter between the aqueous and solid phases (Semu et al. 1987). Similarly, mercury that enters the aquatic system may be adsorbed by inorganic particles, biological particles or organic matter (Ullrich et al. 2001).

2.1.3.1 Mercury speciation

Mercury exists in 3 valence states; 0, +1 and +2 across its biogeochemical cycle. The dissolved primary species in water are elemental mercury (Hg^0), inorganic mercury (Hg^{2+}) complexed with inorganic and organic ligands, as well as organic mercury, particularly methyl- and dimethyl-mercury (Leemakers et al. 2005; Ullrich et al. 2001). The characteristics of these species as well as their reactions will determine solubility, mobility, toxicity and potential for methylation in the aquatic environment (Li et al. 2011; Ullrich et al. 2001).

Anoxic conditions increase the activity of sulphate-reducing bacteria, which in turn facilitate the methylation of mercury, in addition to forming sulphides and polysulphides. The presence of sulphides and polysulphides cause mercury to precipitate. At the same time, highly reducing conditions can also increase mercury solubility by converting HgS^0 to Hg^0 (Benoit et al. 1999) or HgS_2^{2-} which is highly soluble and stable (Wollast et al. 1975). Significant solubility is observed in highly oxygenated environments with redox potentials between 350 and 400 mV (Barrow and Cox 1992). The major mercury species in the presence of sulphur and chloride ions are shown in Figure 2.5.

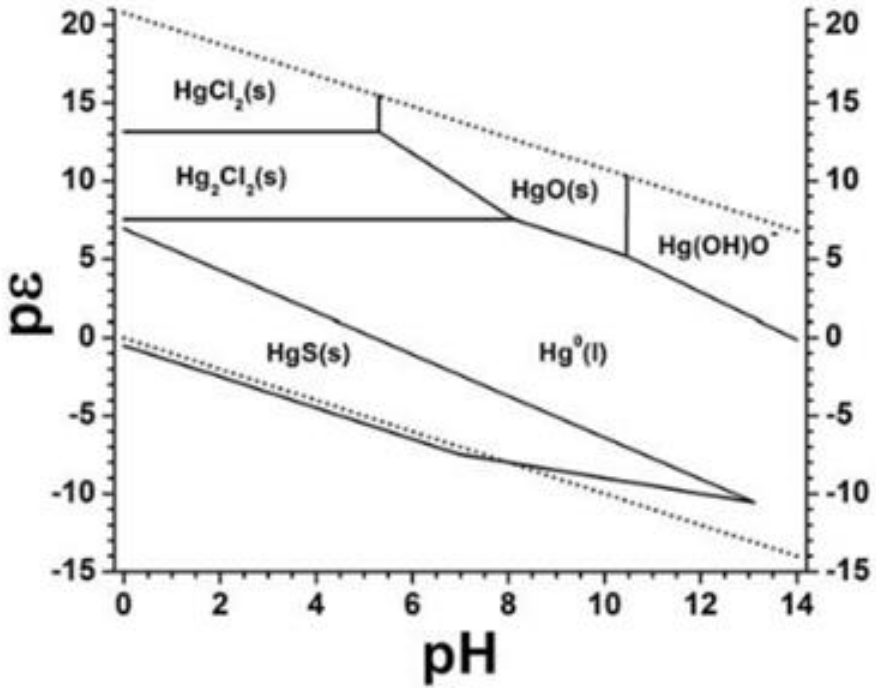


Figure 2.5: pE-pH diagram of mercury (Spyropoulou et al. 2018)

2.1.3.2 Mercury toxicity

Proper function of living organisms requires free thiol groups. At the same time methyl mercury (CH_3Hg^+) and inorganic mercury both display high affinity for thiol (-SH) groups. Mercury executes its toxicity by attacking thiol groups in proteins and membranes (Bjørklund et al. 2017; Risherand Tucker 2017a).

The two major sources of mercury vapour are ambient air and amalgam dental fillings. Clarkson (2002) suggests that dental amalgam poses no significant health risks. The US Environmental Protection Agency (USEPA) found that the lowest concentration of elemental mercury that could have adverse effects is 0.3 µg m^{-3} (Hassett-Sipple et al. 1997). It is estimated that exposure to ambient mercury is 0.032 µg per day in rural areas and 0.16 µg in urban areas (UNEPA 2002).

Conversely, occupational exposure has potentially more dire effects. Professions in dental clinics, mercury, gold and silver mining can expose workers to a significant amount of mercury (Li et al. 2011). Approximately 80% of inhaled mercury remains in the body a week after exposure and only 7 to 14% is exhaled (Clarkson 2002). Once inhaled, elemental mercury accumulates in red blood cells where it is transported to various tissues in the body such the blood-brain and placental barriers (Magos and Clarkson 2006). Prolonged exposure can affect the nervous system leading to tremors and psychological disorders.

Mathiesen et al. (1999) showed that the performance in neuropsychological tests of 70 workers, previously exposed to mercury ranging between 8 and 584 µg m^{-3}, was inferior compared to those in the control group. Besides neurological disorders, elemental mercury exposure can also cause cardiovascular, respiratory, renal, immune and reproductive disorders (UNEPA 2002).

Inorganic mercury prevails in soil and surface water; exposure is therefore through consumption of food that has come into contact with the contaminated water and soil. WHO (1991) found that the average daily intake of inorganic mercury could approximate 4.2 µg day^{-1}; 0.6 µg from fish and 6.3 µg from other foods. Some personal products containing mercury also increase the likelihood of inorganic mercury adsorption.

Mercury (II) salts are soluble and highly toxic, with as little as 1 g causing fatality (Magos and Clarkson 2006). In contrast to elemental mercury, mercury (II) is less likely to cross the blood - brain barrier; however, it is able to accumulate in the liver and kidneys. Once the kidneys have been affected, it can lead to renal failure

and the development of other complications such as immune system disorders (Magos and Clarkson 2006).

Mercury is readily taken up by plants. Studies have shown that crops grown in soil with mercury contaminations have raised total mercury concentrations (Wang et al. 2012). Qian et al. (2009) showed that vegetables grown in soil that had 0.09 to 0.54 mg kg^{-1} of mercury contained between 0.05 to 0.13 mg kg^{-1} of total mercury. Another example is a study on rice grown in mercury contaminated soil in China, rice from the Wanshan mining area contained 4.9 to 215 µg kg^{-1} of mercury. Methylmercury concentrations were as high as 147 µg kg^{-1} (Feng et al. 2007). Approximately 95% of methylmercury is absorbed in the gastrointerstinal tract whereas inorganic mercury is between 10 and 30% (Morcillo and Santamaria 1995; Piotrowski et al. 1992).

Methylmecury is of primary concern because it can accumulate in fish and marine mammals to concentrations a few orders of magnitude higher than concentrations of the surrounding water (Horvat et al. 2011). Predatory fish higher in the food chain such as lake trout generally have higher mercury concentrations because they consume a wide variety of prey lower in the food chain and they have a longer life span (Swanson and Kidd 2010). This means populations with a diet high in fish consumption are most susceptible to methyl mercury poisoning (Harada 1995; Harada et al. 2001). Zhang et al. (2010) reported that in China, populations that are further inland and have lower fish consumption, rice becomes the main source of methyl mercury exposure.

Plants grown in contaminated soil can undergo mercury toxicity which presents itself in the host through following ways: by affecting the anti-oxidative system (Israr and Sahi 2006); affecting the photosynthetic processes (Patra et al. 2004); by impeding plant growth, yield, nutrient uptake and homeostasis (Patra and Sharma 2000). Mercury toxicity can also induce genotoxicity (Sharma 1990).

2.1.3.3 Ion interactions with mercury

Chloride ions play an important role in the mobilisation of mercury so much that they are capable of outcompeting hydroxide ions (Kabata-Pendias 2010; Gabriel 2004; Yin et al. 1996; Yin et al. 1997). In the presence of high chloride ion concentration, there is reduced binding of mercury with organic matter. Reddy and Aiken (2001) showed that high chloride ion concentration increased mercury-chloride complexes and reduced mercury-fulvic acid complexes. Modelling and simulation studies have reported similar findings (Xu et al. 2014), even though these simulations suggest that a pH-dependent mercury dissolution exist even in the presence of chloride ions.

Hydrogen sulphide, a by-product of bacterial sulphate reduction is normally found in anoxic, organic-rich sediments. It can also be found in surface water contaminated with industrial or wastewater. In the presence of sulphide, mercury forms mercury sulphide, which is insoluble. This in turn decreases the availability of mercury for methylation (Ullrich et al. 2001).

2.1.3.4 Mercury biogeochemical cycle

Elemental mercury is liquid at room temperature but readily evaporates into mercury vapour, which is colourless and odourless (UNEPA 2002). It is particularly stable, and it can remain in the atmosphere for 6 months to 2 years. The long range transport in the atmosphere means it can be conveyed away from a point source to even the most remote areas not experiencing mercury pollution (Fitzgerald et al. 1998; Pirrone and Mahaffey 2005; Fu et al. 2010). Emitted elemental mercury can undergo gaseous and aqueous reactions that ultimately affect transportation and deposition. For example, it can be oxidised to inorganic mercury in the presence of ozone and hydrogen or by atomic bromine (Holmes et al. 2006). The resulting inorganic mercury is deposited back to the Earth's surface and aquatic environment via wet and dry deposition, in a 60 and 40% ratio, respectively (Li and Tse 2015).

Inorganic mercury in the environment exists as divalent cationic salts such as mercuric sulphide (HgS) and mercuric chloride ($HgCl_2$) (UNEPA, 2002). It is also 10^5 times more soluble in water compared to elemental mercury. Inorganic mercury can therefore not travel long distances in the atmosphere and has a higher chance of being deposited back to Earth (Li and Tse 2015; Bullock 2000).

Inorganic mercury that has been deposited back to Earth can undergo biochemical transformations in soil which are affected by organic matter and soil temperature: The degradation of organic matter may cause anoxic conditions which may facilitate the mobilisation and methylation of inorganic mercury (Cossa and Gobeil 2000). Alternatively, any changes that arise due to seasonality may affect the rate of methylation, with higher temperatures promoting microbial activities, which in turn enhance methylation and inhibit the de-methylation processes. Consequently, higher methylation takes place in summer (Korthals and Winfrey 1987; Ullrich et al. 2001; Li and Tse 2015).

Inorganic mercury can subsequently be transformed back into elemental mercury under specific conditions such as photolytic reduction and HO_2 radicals (Lin et al. 2006). Higher concentrations of inorganic mercury in aquatic systems are due to chloride ions, which facilitate the oxidation of elemental mercury into inorganic mercury (Magalhães and Tubino 1995; Yamamoto 1996). Conversely, organic mercury specie is found in very little to no concentration in surface water. This is because any methyl-mercury present is immediately degraded by solar ultraviolet rays (Suda et al. 1993). Additionally, high salinity can slow down the methylation of mercury, which is why the process is slower in oceans and seas compared to fresh water systems (Barkay et al. 1997). Furthermore, high sulphide concentration inhibits mercury methylation due to the formation of mercury sulphide (Ullrich et al. 2001). The biogeochemical cycle (Figure 2.6) as explained above highlights the persistence of mercury in the environment

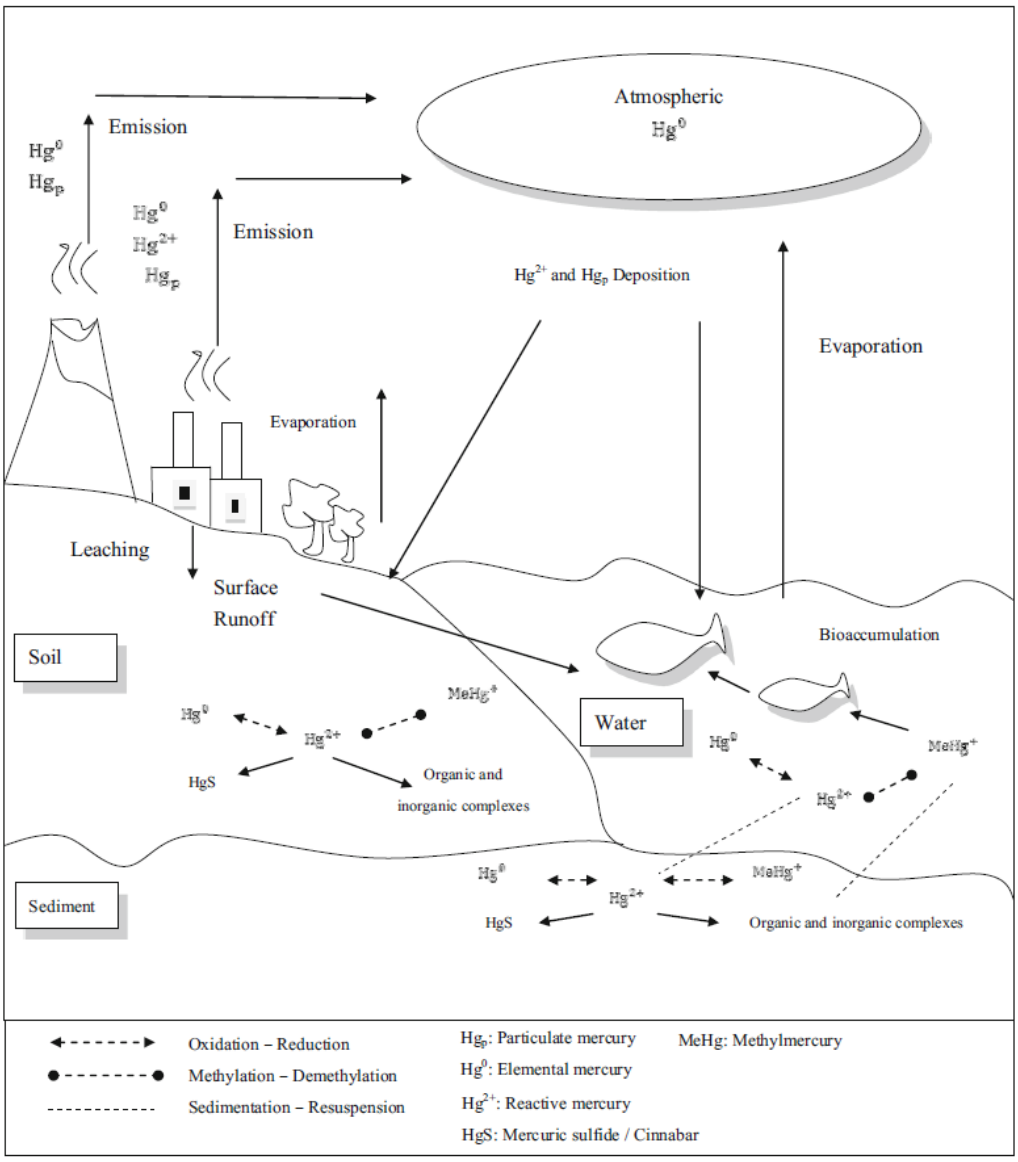


Figure 2.6: The biogeochemical cycle of mercury (Lin and Tse 2015)

2.1.4 Interactions between arsenic, selenium and mercury

A synergistic relationship exists between arsenic, selenium and mercury. After arsenic exposure, arsenate is immediately reduced to arsenite. Arsenite is then methylated through the action of arsenite methyltransferase and excreted. Selenium reduces arsenic toxicity through the formation and excretion of the arsenic-selenium compound $[(GS_3)_2AsSe]^-$ (Kojima et al. 2009; Sun et al. 2014). When selenium concentrations are low, Sun et al. (2014) describes an antagonistic

relationship with arsenic and a synergistic one at higher selenium concentrations. For instance at lower selenium concentrations the association between selenium and arsenite methyltransferase becomes limited. Any remaining arsenic is excreted as MMA and DMA. Alternatively, at higher concentrations, selenium inhibits arsenite methylatransferase and the subsequent arsenic methylation and $[(GS_3)_2AsSe]^-$ formation. Arsenic and MMA are consequently retained, enhancing toxicity in the body.

Mercury reportedly binds selenium with extremely high affinity, with log K values as high as 10^{45} compared to sulphur (log $K=10^{39}$) (Berry and Ralston, 2008; Dyrssen and Wedborg 1991). Selenium has been known to reduce mercury toxicity; the replacement of sulphur with selenium in cysteine amino acid of selenoproteins leads to higher nucleophilicity compared to sulphur based proteins Bjørklund et al. 2017a; 2017b). Some studies even report that increased selenomethionine in adult fish and their eggs are able to decrease mercury toxicity (Penglase et al. 2014).

Simultaneous exposure to arsenic and mercury results in the formation of arsenic-selenium and mercury-selenium compounds, suggesting that both elements target selenium metabolism (Gailer 2007). Exposure to arsenic and mercury will therefore, cause some of the dietary selenium to become unavailable for proper organism functioning. Considering that selenium deficiency is linked to cancer in humans, arsenite and mercury induced selenium deficiency will elevate cancer risk (Gailer 2002).

2.1.5 Characteristics of acid mine drainage (AMD)

Acid mine drainage is a global environmental problem. It is caused by the oxidation and hydrolysis of metal sulphides such as pyrite (Gray 1998). Examples of sulphide minerals that can lead to AMD are listed in Table 2.1.

Table 2.1 Important sulphides involved in the production of acid mine drainage (Skousen et al. 1998).

Metal sulphide	Chemical formula
Pyrite	FeS_2
Marcasite	FeS_2
Pyrrhotite	Fe_1-S_x
Chalcocite	Cu_2S
Covelite	CuS
Chalcopyrite	$CuFeS_2$
Molybdenite	MoS_2
Millerite	NiS
Galena	PbS
Sphalerite	ZnS
Arsenopyrite	FeAsS

Natural weathering results in the oxidation of mineral deposits to produce acid, however, this process is slow enough for natural neutralisation processes to have adequate time to remove the acid (McCarthy, 2011). Moreover, ground water has little turbulence allowing acid-neutralisation reactions to occur as AMD comes into contact with carbonate, hydroxide and other basic solids. These solids have different neutralisation capabilities, therefore, along the AMD flow path different regions will have distinct pH (Figure 2.7) (Cheng et al. 2009).

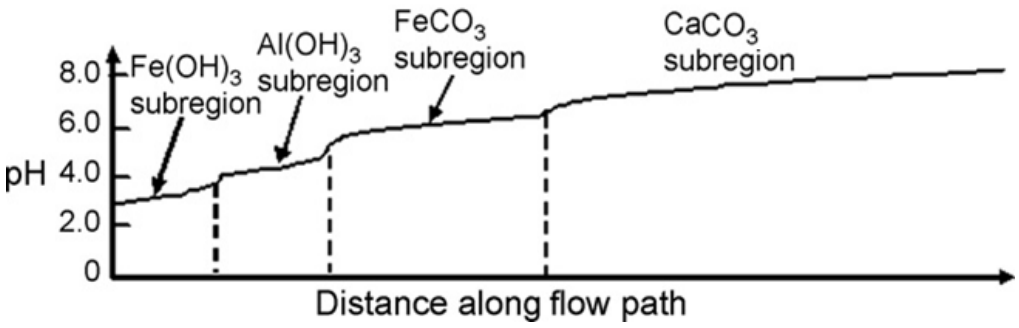


Figure 2.7: The geochemical pH-buffering regions associated with AMD (adapted from Blowes et al. 2003).

The excavation of minerals leads to the exposure of the sulphide minerals to oxygen, water (Johnson 2003; Johnson and Hallberg 2005) as well as microorganisms (Ali 2011; Akcil and Koldas 2006). During the mining process, the surrounding rock mass becomes significantly fragmented and this increases the surface area, effectively increasing the rate of AMD production (McCarthy 2011).

The Witwatersrand gold mining operations have been in existence for more than 100 years (Werdmüller 1986). Currently, majority of these mines have undergone closure, due to the lack of resources and profit, as well as impacts on the ecosystem (McCarthy 2011; Mengistu et al. 2012). AMD is found in both operating and dormant mining sites. The situation is particularly dire in abandoned mines because water pumps are switched off leading to the recovery of water tables (Blowes et al. 2003; Johnson and Hallberg 2005).

Gold in the Witwatersrand is associated with pyrite (FeS_2). The oxidation of pyrite happens in two stages: the first stage results in the production of sulphuric acid and ferrous sulphate. Ferric hydroxide, which is orange-red in colour, is produced in the second stage, along with more sulphuric acid. The first reaction proceeds as follows:

$$2FeS_2 + 7O_2 + 2H_2O \rightarrow 2Fe^{2+} + 4SO_4^{2-} + 4H^+ \quad (2.1)$$

The first indicator of sulphide mineral oxidation is sulphate. The rate of pryrite oxidation is dependent on different factors such as microbial activity and the availability of oxygen and water. Under an adequately oxidising environment, with pH greater than 3.5, as well as sufficient bacterial activity, the resulting ferrous ion from Equation (2.1) is oxidised to ferric iron (Akcil and Koldas 2006; Blowes et al. 2003; Lapakko 2002):

$$4Fe^{2+} + O_2 + 4H^+ \leftrightarrow 4\,Fe^{3+} + H_2O \quad (2.2)$$

The reaction according to Equation (2.2) is the rate limiting step (Singer and Stumm 1970). Additionally, the conversion of ferrous iron to ferric iron is slow at pH values lower than 5 (Skousen et al. 1998). Alternatively, between pH 2.3 and

3.5 the resulting ferric iron from reaction (2.2) may precipitate as $Fe(OH)_3$ in the following reaction:

$$Fe^{3+} + 3H_2O \leftrightarrow Fe(OH)_3 + 3H^+ \quad (2.3)$$

leaving very low concentrations of Fe^{3+} in solution, while concomitantly lowering the pH (Akcil and Koldas 2006; Blowes et al. 2003;).

At pH values less than 2, ferric hydrolysis products such as $Fe(OH)_3$ are unstable allowing Fe^{3+} to remain in solution (Dold 2010). Any Fe^{3+} from Equation (2.2) that does not precipitate into $Fe(OH)_3$ according to reaction (2.3) further oxidises any additional pyrite as follows (Akcil and Koldas 2006):

$$2FeS_2 + 14Fe^{3+} + 8H_2O \rightarrow 15Fe^{2+} + 2SO_4^{2-} + 16H^+ \quad (2.4)$$

Reaction (2.4) causes a further decrease in pH (Singer and Stumm, 1970). Initially, oxygen is the main oxidant of pyrite; however, the resulting ferric iron (Equation 2.1) becomes the dominant oxidant: below pH 3, the oxidation of pyrite by Fe^{3+} is 10 to 100 times faster compared to oxygen (Dold 2010; Ritchie 1994). This is because Fe^{3+} is better at transferring electrons compared to oxygen (Luther 1987; McKibben and Barnes 1986; Moses et al. 1987).

The production of ferrous iron via reaction (2.4), in the presence of oxygen, allows reactions (2.2) and (2.3) to proceed until either the ferric iron or pyrite are depleted. Even in the absence of oxygen, reaction (2.4) can proceed, increasing the concentration of ferrous iron in the water (Younger et al. 2002).

In naturally acidic water systems, reactions (2.2 and 2.4) may be accelerated by acidophilic bacteria such *Thiobacillus ferroxidans* (Jennings et al. 2008; Singer and Stumm 1970). It is suggested that these bacteria, along with other similar species are responsible for the widespread weathering of pyrite in the environment (Blowes et al. 2003; Singer and Stumm 1970).

The acidity of AMD is of great concern because most organisms have a specific pH range in which they can exist. A change in acidity affects both the organisms and their food sources (Brown and Sadler 1989; Turnpenny 1989; Rosemond et

al. 1992; Sutcliffe and Hildrew 1989). Additionally, pyrite contains toxic metals in high concentration, as the acidic water dissolves the pyrite; it increases the solubility of aluminium and metals found in the affected area making the water toxic to different degrees. Consequently, the rate of acidity as well as the concentration of toxic metals are dependent on the pyrite being weathered by the drainage water (Cheng et al. 2009). Although the water is eventually neutralised via dilutions and reactions with various soil and sediment minerals, some components such as sulphate have high solubility and remain in solution despite neutralisation efforts (McCarthy 2011).

Water from AMD is initially clear but becomes a characteristic orange colour with time: The neutralisation of drainage water results in the precipitation of iron oxides and hydroxides causing the water to become orange in colour (Cotter and Brigden 2006). This precipitate is very fine and can deposit on the river, stream or ocean bed. This iron deposit obstructs the benthic organisms' food source (Fripp et al. 2000). The ultimate depletion of benthic organisms as a food source will affect organism further up in the food chain.

Furthermore, mine tailings generally have elevated water tables, especially in abandoned mines. During the recovery of water tables ground water continues to rise above the water table until it intersects with the soil surface, causing a capillary rise of contaminated ground water on the soil surface. Exposure to the atmosphere causes these ion-rich solutions to evaporate; the dissolved minerals precipitate, leaving behind what is known as efflorescent crusts. Efflorescent crusts are therefore a common feature in AMD (Tutu et al. 2011; Naicker et al. 2003).

2.2 Conventional sampling methods

2.2.1 Problems associated with conventional sampling methods

In aquatic monitoring, it is common practice to collect grab or spot water samples at specific sites and at a given time. There are a few concerns regarding this

monitoring approach. Firstly, in situations where pollutants are found in trace amounts, large samples have to be collected in order to obtain representative data. Large sample volumes in turn make quality control difficult. Additionally, large samples are also met with physical challenges during collection. Increased sampling frequency is also expensive (Madrid and Zayas 2007; Vrana et al. 2005). Secondly, there is an increased possibility of contamination and changes in metal speciation during storage and transport of these samples. This is further complicated by adsorption of analytes to glass bottles or filtration equipment (Horowitz 1997; Vrana et al. 2005; Allan et al. 2006a; 2006b).

Laboratory analysis of these samples only provides snapshot information on the concentration of pollutants, based on sampling location and time. This means, episodic events could be unintentionally omitted, leading to the possible over-estimation or under-estimation of concentrations depending on the sampling conditions at that time (Dworak et al. 2005; Vrana et al. 2005; Allan et al. 2006a; 2006b, Montero et al. 2012). Also, analysis of data obtained through spot sampling produces different results, depending on the pre-treatment method used (Vrana et al. 2005). In addition, spot sampling provides information on the total amount of pollutant present and not the dissolved, bioavailable fraction. Over and above, the spatial distribution of the sampling sites is based on convenience, experience, instinct, which leads to sampling bias (Dixon and Chiswell 1999; Madrid and Zayas 2007; Khalil and Ouarda 2009, Wang et al. 2015).

Biomonitoring, another sampling technique commonly used, is met with a few challenges: Firstly, the species of choice will be restricted to a particular aqueous environment and temperature. Secondly, due to differences in metabolism and excretion rates, some analytes of interest may not be accumulated. Thirdly, within the same species bioaccumulation rates may vary according to age, sex and the general condition of the organism. Also, lipophilic compounds are most likely to be accumulated at a faster rate compared to lipophobic ones, implying that the use of biomonitors will be limited for polar organic compounds (Namieśnik et al. 2005). Some of the challenges faced for both spot sampling and biomonitoring are overcome through passive sampling.

2.3 The theory of passive sampling

2.3.1 Passive sampling

Passive sampling can be described as any technique that is based on the free flow of analytes against a concentration gradient, according to Fick's first law of diffusion. They move from the bulk solution through a well-defined diffusion barrier or membrane onto a receiving phase within the sampling device. Analytes are adsorbed and retained on a receiving or reference phase which can be a solvent, a chemical reagent or an adsorbent. The net flow from the bulk solution to the receiving phase continues until equilibrium is established or sampling is stopped (Górecki and Namieśnik 2002; Namieśnik et al. 2005).

The uptake of analytes by passive samplers follows the general pattern depicted in Figure 2.8; after the deployment of a clean passive sampler, the uptake of analytes continues pseudo-linearly over time; this mode is termed the kinetic regime (Roll and Halden 2016; Vrana et al. 2005). Eventually the rate begins to slow down until the passive sampler reaches thermodynamic equilibrium with the environment; this is referred to as the equilibrium regime (Roll and Halden 2016; Vrana et al. 2005).

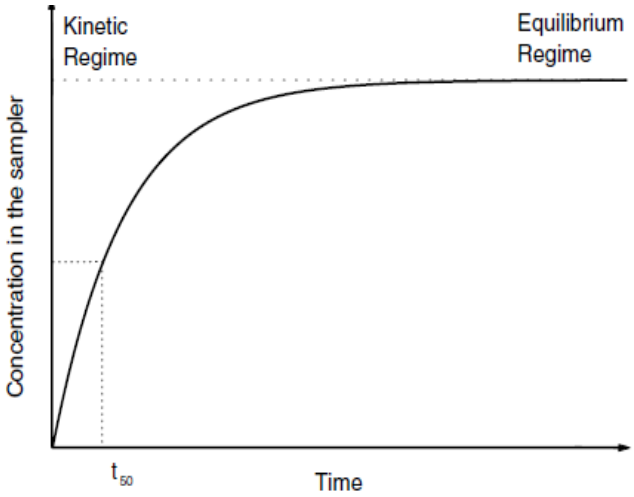


Figure 2.8: Analyte accumulation pattern followed by passive samplers over a specific time period (Vrana et al. 2005).

Passive samplers can be designed such that they operate exclusively in the kinetic or equilibrium mode (Figure 2.10) (Roll and Halden 2016). Both kinetic and equilibrium based passive samplers sequester and pre-concentrate analytes of interest onto their respective receiving phases. Differences lie in the mode of operation: equilibrium samplers are dependent on establishing equilibrium with their environment; this means that any fluctuations experienced in the bulk solution will also affect the amount accumulated within the passive sampler. Equilibrium passive samplers are therefore biased towards the concentration at the specific sampling period. Alternatively, kinetic or integrative samplers provide an average concentration for the sampling duration (Roll and Halden 2016).

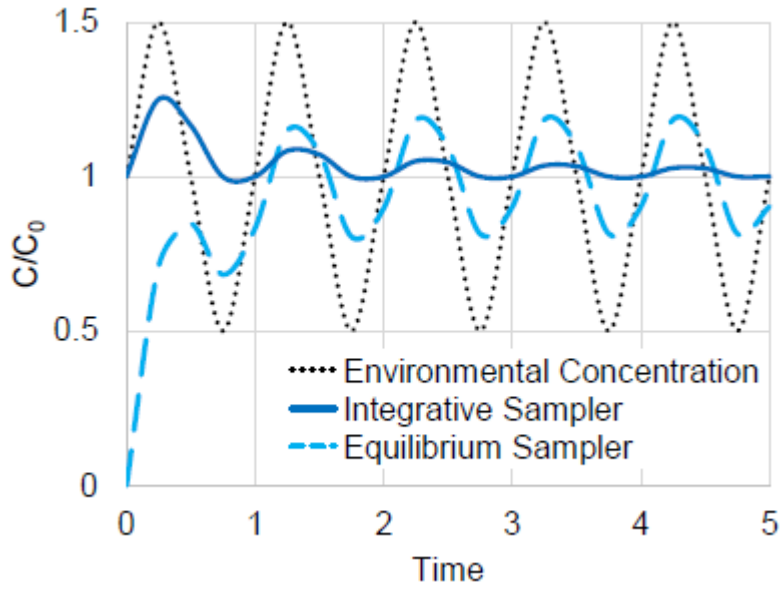


Figure 2.9: Depiction of how equilibrium and integrative samplers provide time-weighted average concentrations relative to fluctuations of analyte concentrations in the environment (Roll and Halden 2016).

The design of equilibrium passive samplers ensures rapid equilibration between water and the receiving phase (Mayer et al. 2003; Vrana et al. 2005). The sampler response time has to be shorter than any fluctuations that may be experienced

during deployment. Equilibrium samplers that attain equilibrium within a very short space of time are considered to be comparable to grab sampling techniques (Mayer et al. 2003). Additionally, the capacity of an equilibrium-based passive sampler needs to be below that of the sample in order to avoid sample depletion during deployment (Mayer et al. 2003; Vrana et al. 2005). One major drawback of using equilibrium based passive samplers is that once equilibrium between the sampler and sampled medium has been established; any decrease in aqueous concentration could lead to analytes diffusing back into the surrounding medium (Kot-Wasik et al. 2007).

Kinetic passive samplers, also known as integrative passive samplers provide the time weighted average (TWA) concentrations for the entire duration of sampling. This makes integrative samplers less sensitive towards fluctuations in analyte concentration (Kot et al. 2000), compared to equilibrium based samplers. This ensures that analyte concentrations are not over- or under-estimated (Coes et al. 2014; Roll and Halden 2016; Seethapathy et al. 2008; Vrana et al. 2005).

Exchange kinetics between the bulk solution and a passive sampler are described by the following first order Equation:

$$C_s(t) = C_w \frac{k_1}{k_2} (1 - e^{-k_2 t}) \qquad 2.5$$

where *Cs(t)* is the analyte concentration at exposure time t, *Cw* is the analyte concentration in the bulk solution and k_1 and k_2 are the uptake and offload rate constants, respectively. Equation (2.5) then becomes:

$$C_s = C_w \frac{\boldsymbol{k_1}}{\boldsymbol{k_2}} = C_w K, \qquad 2.6$$

where K is the partition coefficient.

Equation 2.5 is applicable for equilibrium sampling. Conversely, in kinetic sampling, the rate of mass transfer to the receiving phase is linear. During the initial stages of deployment, the rate of desorption is negligible, which is why Equation (2.6) becomes:

$$C_s(t) = C_w k_1 t \quad (2.7)$$

By rearranging Equation (2.7):

$$M_s(t) = C_w R_s t \quad (2.8)$$

where $M_s(t)$ is the mass of analyte accumulated in the receiving phase after deployment time (t). R_s is the sampling rate. The R_s value makes it possible to determine C_w, the TWA of analyte in the bulk solution. For samplers operating in the kinetic regime, the value of R_s does not vary with C_w. It is however, affected by water turbulence, temperature and biofouling.

The partitioning properties of the analytes being sampled will determine whether a passive sampler will operate in the equilibrium or non-equilibrium mode. This means that a given sampler may be in equilibrium for one analyte while sampling in the non-equilibrium phase for another during field deployments (Vrana et al. 2005).

2.3.2 Advantages of passive sampling

One of the main advantages of passive sampling over spot sampling and biomonitoring is that only a few sampling devices are required for a given sampling location. This inherently reduces the number of samples required for analysis, ultimately reducing sampling and analytical costs significantly. Secondly, because sampling devices are relatively small, transportation between the lab and sampling sites becomes more convenient (Kot-Wasik et al. 2007; Namieśnik et al. 2005). Passive samplers can operate without an external power source, which is another means of costs reduction. Furthermore, passive sampling ensures that decomposition of analytes usually associated with grab sampling is significantly reduced since analytes are separated from matrix components (Kot-Wasik et al. 2007). This is particularly important for analytes that exist in complex matrices (Namieśnik et al. 2005). In addition, the sampling as well as the sample preparation procedure is simplified because sampling and analyte pre-concentration are combined in a single step (Górecki and Namieśnik 2002; Namieśnik et al. 2005; Kot-Wasik et al. 2007). For analytes that exist in low

concentrations, the passive sampler will have a low sampling rate, and therefore require longer deployment periods. This can also be viewed as an advantage because longer sampling periods allow for TWA concentrations to be determined (Namieśnik et al. 2005).

Prior to field measurements; passive samplers need to be calibrated and sampling rates determined under laboratory settings. This will provide a better understanding on how different field conditions influence the sampling rates (Aguilar-Martínez et al. 2008; Castle et al. 2018; Petersen et al. 2015; Vrana et al. 2006).

2.3.3 Examples of passive samplers for inorganic analytes

2.3.3.1 Chemcatcher®

Chemcatcher passive samplers were designed for either organic or inorganic analytes. The inorganic version was designed for monitoring of cadmium, copper, nickel, lead and zinc in aquatic environments (Allan et al. 2008). The basic structure of Chemcatcher (Figure 2.10) for the determination of inorganic analytes consists of a circular watertight device made from Teflon. The device is 47 mm in diameter; this disc is overlaid with a 3 M Empore™ chelating disk that acts as the receiving phase. A cellulose acetate diffusion limiting membrane of 0.45 µm pore size that is 0.135 mm thick is placed on top of the receiving phase (Allan et al. 2008). Both the chelating disc and cellulose acetate membrane are the same diameter as the Chemcatcher disc (Allan et al. 2008). In order to reduce biofouling, the cellulose acetate membrane can be treated with a low surface energy coating such as polyfluorinated sulphonic acid polymer (Nafion) (Blom et al. 2002).

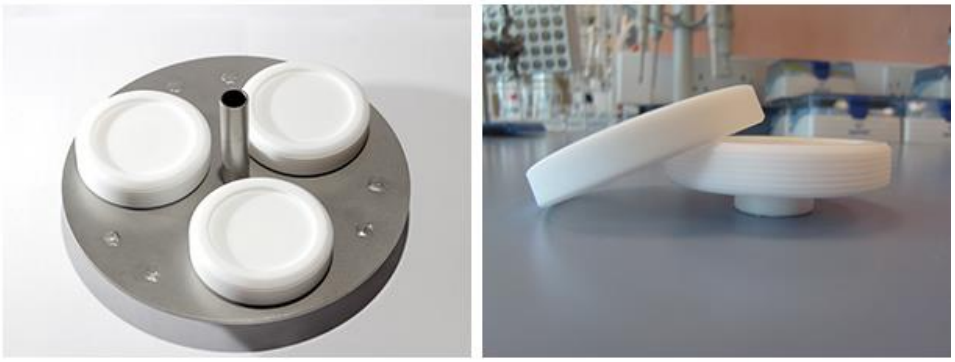


Figure 2.10: Chemcatcher passive sampling device (Kingston et al. 2000; Persson et al. 2001)

During field application, the Chemcatcher devices were deployed in the River Meuse, in the Netherlands. This was to assess if they are robust enough for routine monitoring. The sampling devices were deployed between 7 and 28 days. Results were compared to those obtained using conventional monitoring procedures. They found that concentrations obtained from the passive samplers were consistently lower than total and filtered concentrations. In some instances frequent spot sampling was more useful in providing information that could not be obtained with certainty from the passive samplers. Allan et al. (2008) concluded that both spot and passive sampling were complimentary and provided sound results.

2.3.3.2 Passive integrative mercury sampler (PIMS)

The PIMS passive sampler is used to monitor mercury vapour in air and neutral mercury in water, especially Hg^0. The device is made up of a lay-flat low density polyethylene (LDPE) tubing (Figure 2.11) that contains a mixture of nitric acid and gold stock solution. Gold was used because it is a good preservative of mercury in aqueous environments. On the other hand, nitric acid is compatible with the reagents required for mercury analysis (Brumbaugh et al. 2000).

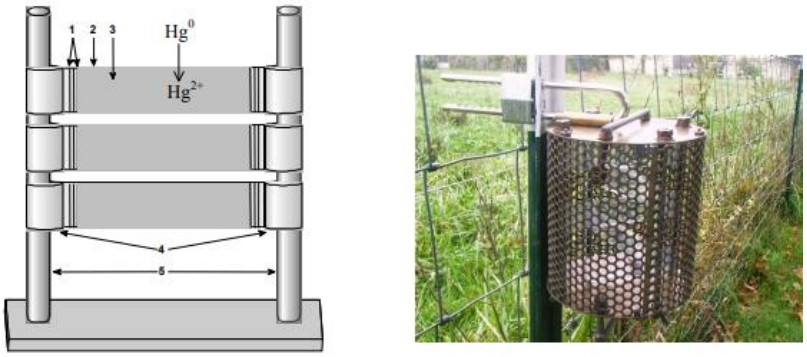


Figure 2.11: a) PIMS passive sampler for air monitoring of mercury vapour b) PIMS in stainless steel cage prior to deployment in an aqueous environment (Brumbaugh et al. 2000).

With the PIMS passive sampler, sampling can proceed for extended periods because the sampled mercury is oxidised and stabilised within the passive sampler. Ambient air was sampled for 12 weeks with 4 week cycles and water samples for two weeks. The results indicate that PIMS was effective at pre-concentring elemental mercury. (Brumbaugh et al. 2000).

2.3.3.3 Polymer inclusion membrane (PIM) - based passive samplers

PIMs are functionalised thin flexible membranes that generally comprise of an extractant or carrier, a polymer base such as poly vinyl chloride (PVC) or cellulose triacetate (CTA) and a plasticizer (Almeida et al. 2012; Turull et al. 2016). In PIM based passive samplers, one side of the membrane is in contact with a receiving solution. This allows the passive sampler to extract and desorb in a single step (Almeida et al. 2017). The carrier plays a central role in PIM extraction by complexing with the analyte of interest. It behaves as the phase-transfer agent, extracting the analyte from the aqueous phase to the membrane phase (Figure 2.12). The carrier does this by forming a complex or a hydrophobic ion-pair (Turull et al. 2016).The base polymer is selected based on the extraction solvent and specific application (Almeida et al. 2017).

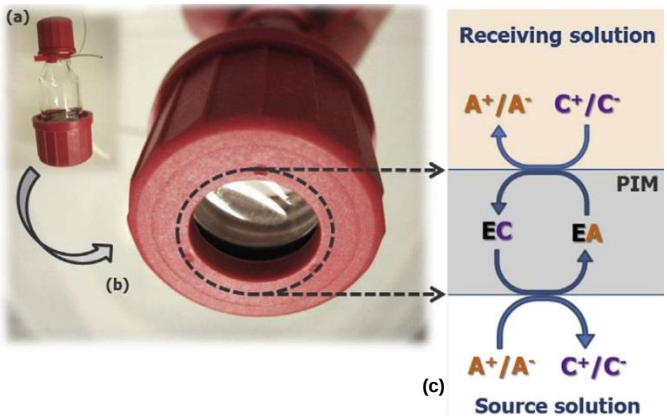


Figure 2.12 a) An example of a PIM based passive sampling device b) sampler cap with a small window exposing the PIM membrane c) schematic representation of PIM-based facilitated transport (A^+/A^-, charged target analyte; E, extractant; C, counter ion) (adapted from Almeida et al. 2017).

PIMs are simple and cheap to prepare. They have good mechanical properties and can target an array of compounds (Almeida et al. 2012; Turull et al. 2016). PIMs have been used in different applications but recently they have been used as used as a binding phase in a diffusive gradients in thin-films (DGT) passive sampler to target mercury (Turull et al. 2016). The PIM was functionalised with trioctylmethylammonium thiosalicylate (TOMATS). The study shows that for shorter deployment periods, a higher percentage of TOMATS is required but for longer deployments, the TOMATS percentage needs to be reduced. With regards to the actual sampling device, non-linear accumulation pattern was obtained, suggesting that PIM-based DGT was not operating as a kinetic passive sampler.

2.4 Diffusive gradients in thin-films (DGT)

DGT is a passive sampling technique that was first reported by Davison and Zhang (1994) for *in situ* measurements of labile trace metal species in natural water. *In situ* measurements mean that contamination problems normally

encountered during spot sampling and transport to the laboratory are reduced (Davison and Zhang 1994; Zhang and Davison 1995).

DGT is small piston shaped device that is 2.5 cm in diameter with a 2.0 cm window (DGT Research Ltd., UK). The functional part of DGT is made up of three layers: a cellulose acetate (CN) or polyethersulphone (PES) filter membrane with a pore size of 0.45 µm, a polyacrylamide hydrogel of known thickness (Δg) and a resin layer comprising of Chelex 100 cation-exchange resin impregnated in a hydrogel made up of acrylamide and agarose derived cross- linker (DGT Research Ltd). The resin gel is placed directly on the DGT piston followed by the diffusive gel. The layers are placed such that only the filter membrane has direct contact with the external environment, thus protecting the hydrogel from damage. Both the filter membrane and the hydrogel make up the diffusive layer (Zhang and Davison 1995; Li et al. 2002). A fully assembled DGT passive sampler, together with the structural and functional components are shown in Figure 2.13.

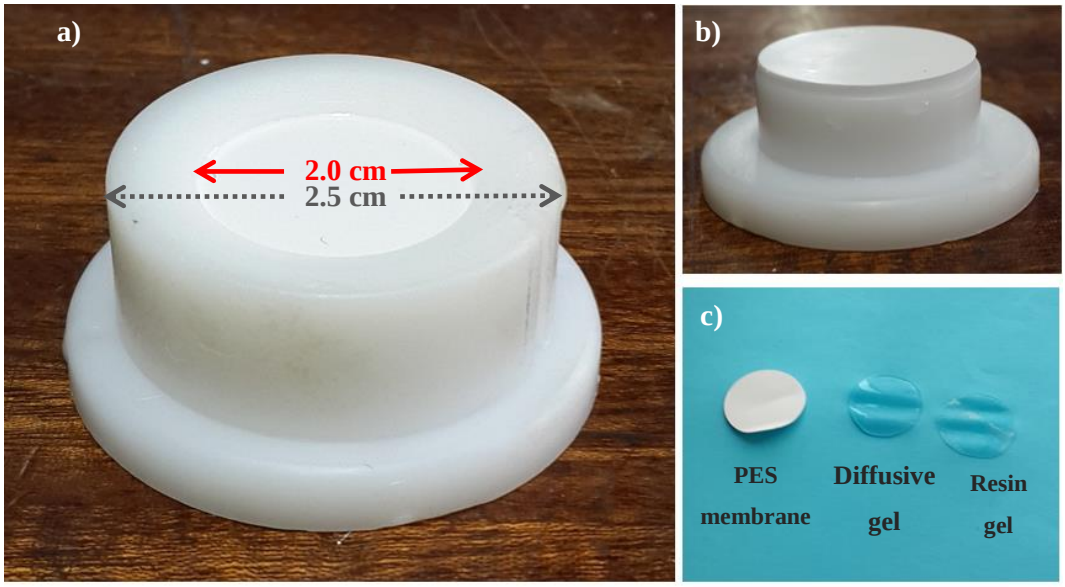


Figure 2.13: a) commercial DGT sampling device b) DGT without the cap c) the components that make up commercial DGT.

Ding et al. (2016) modified the design of the DGT sample holder (Figure 2.14). This new holder has two important components, the first is a DGT core comprising of an "O-shaped" ring and recessed base; the second is a hollow base that accommodates the DGT core. These components can be assembled in two different ways depending on the application: Firstly, the resin, diffusive gel and filter membrane are placed on the recessed base with a boundary wall 0.13 cm in height (which corresponds with the total thickness of the resin, diffusive gel and filter membrane, combined). The ring is then placed on top of this base leaving an exposure window 2.0 cm in diameter. For application in aqueous solutions, the DGT core is placed directly on top of the hollow base to give a piston-shaped sample holder that is similar in to commercial DGT holder.

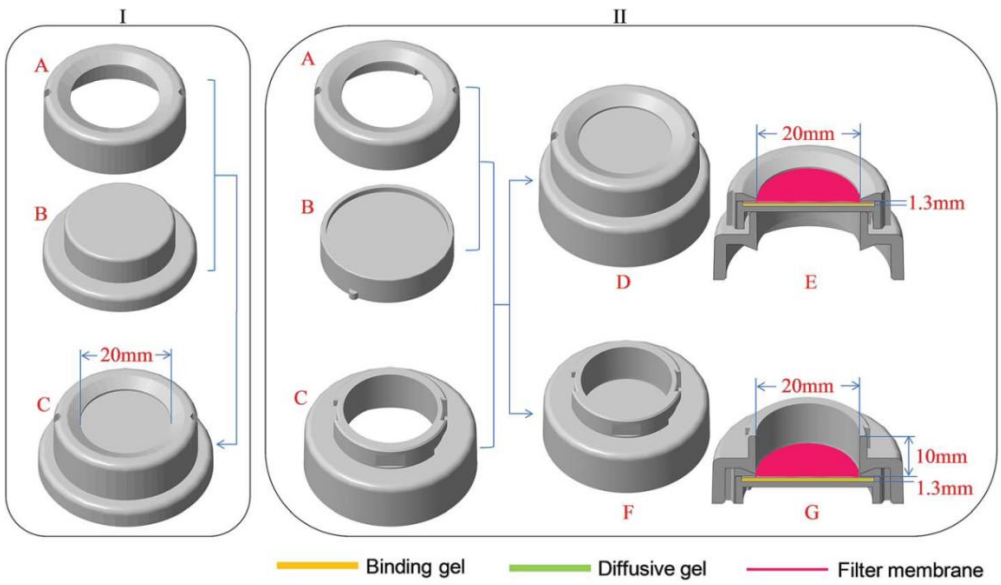


Figure 2.14: (I) Conventional DGT sample holder where A, B and C are the cap, piston base and the assembled unit, respectively. (II) New sample holder where A, and B are the “O-shaped” ring and the recessed base, respectively, which make up the DGT core. C is the hollow base used to lodge the DGT core. D and E are the two different ways of assembling the components (Ding et al. 2016).

In the second configuration, for deployment in soil/ sediment, the DGT core is placed below the hollow base, resulting with a unit that has a 1.0 cm deep open cavity. Prior to deployment, a soil paste is placed in this open cavity Ding et al. (2016). Ding et al. (2016) only assessed the performance of this new sampler housing for the configuration deployed in sediments since the piston shaped configuration was comparable to commercial DGT and they did not expect any notable changes in performance.

2.4.1 Principles of the DGT passive sampler

During the deployment of DGT, metal ions are gradually accumulated by the passive sampler against a concentration gradient. The fact that DGT operates on the fundamentals of a concentration gradient means that it is kinetically controlled. This is advantageous because it can be deployed for extended periods unlike equilibrium based techniques (Li et al. 2002). Kinetic / integrative passive samplers accumulate analytes at a definable rate and consequently provide time integrated concentrations. Results obtained are considered representative of the sampling area (Allan et al. 2006; Dunn et al. 2007; Bennett et al. 2010).

2.4.1.1 Accumulation of mass and C_{DGT}

The mass accumulated (M) in the DGT binding gels is calculated according to the following Equation when the elements are eluted with a known volume of eluent (V_e) and C_e is the concentration in the eluent: The volume of the gel (V_g) is usually 0.15 mL for commercial DGT and the elution factor (f_e) value commonly used is 0.80 (Zhang and Davison 1995).

$$\boldsymbol{M = \frac{C_e(V_g+V_e)}{f_e}} \tag{2.9}$$

Once the value of M has been determined, the concentration in bulk solution can be calculated as follows:

$$\boldsymbol{C_{DGT} = \frac{M\,\Delta g}{DAt}} \tag{2.10}$$

C_{DGT} is the DGT measured concentrations (ng mL^{-1} / µg L^{-1}); M is the mass adsorbed by resin (ng) during the deployment period and corrected with the

appropriate elution volume; Δg is the diffusive layer thickness (filter paper and diffusive gel); D is the diffusion coefficient through the diffusive layer ($cm^2\ s^{-1}$); A is the area of the device that is exposed to solution (3.14 cm^2 for 2.0 cm diameter exposure window) and t is the deployment time (s).

In order for Equation 2.10 to provide valid information, the deployment time must be sufficiently long enough for attainment of a steady state : when metals enter the diffusive gel, they are retained until the gel's capacity has been reached (this process does not take long considering how thin the diffusive gel is). The time taken to reach steady state can therefore be affected by two factors; slow diffusion of complexes and the binding of metal complexes to the diffusive gel functional groups, which is why the concept of lability is important. Therefore, binding of analytes on the diffusive gel or filter membrane can increase the time required to reach steady state (Davison and Zhang 2012).

Application of Equation 2.10 requires the concentration of the measured specie at the interface of the diffusion and binding gel to be negligible as this would imply fast binding. As the resin approaches full capacity, the concentration at the interface between the diffusion and binding gel becomes high, thereby reducing the uptake rate (Davison and Zhang 2012). Competition for binding sites with other elements in solution can also lower the capacity for a specific analyte, leading to a steady decrease in sensitivity as the capacity is reached (Davison and Zhang 2012).

Once C_{DGT} is known it can be used to calculate the pre-concentration factor:

$$\mathbf{C_e/C_{DGT}} \qquad (2.11)$$

2.4.1.2 Diffusion coefficient and the diffusive boundary layer

The diffusion coefficient (D) is determined by using either a diffusion cell or time series experiments where it is calculated from the slope of a linear plot of measured mass against time using Equation 2.12:

$$\boldsymbol{D = \frac{slope \Delta g}{CA}} \qquad (2.12)$$

where *A* is the area of DGT exposed to bulk solution (3.14 cm^2), *Δg* combined thickness of diffusive gel and membrane filter. *C* is the concentration in the glass container.

The interface between an immersed solid body and water is a thin area known as the diffusive boundary layer (DBL). In this region, mass transport is controlled exclusively by diffusion. This means diffusion of molecules into DGT depend on the diffusive gel thickness and the thickness of the DBL (Zhang and Davison 1995). The DBL could be considered an extension of Δg onto bulk solution (Warnken et al. 2006). Figure 2.15 shows how the DBL relates to the resin, diffusive gel layers as well as the concentration gradient.

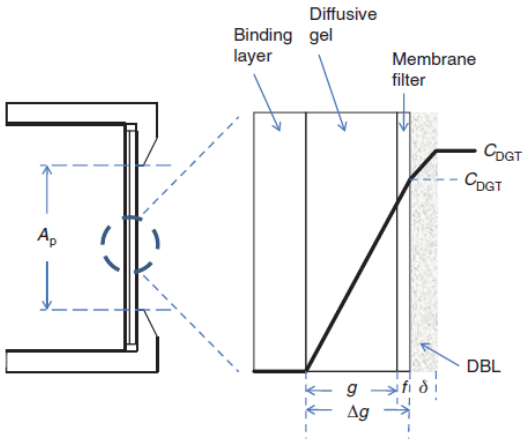


Figure 2.15: Representation of DGT with an expanded view of the resin layer and the diffusion layers and their relationship with the diffusive boundary layer. (Adapted from Davison and Zhang 2012).

The DBL can be affected by fluid mechanics; the thickness decreases with increasing fluid turbulence. In well-stirred solutions, the DBL thickness is presumed considerably thinner in comparison to the diffusive gel thickness and filter membrane (Warnken et al. 2006), in such situations the DBL is often neglected in calculations. If a thick DBL exists and it is ignored, the error may be

as high as 10%. By ensuring that the diffusive gel layer thickness is optimal, it is the DGT device rather than solution properties that control mass transfer (Zhang and Davison 1995). The DBL can also be affected by the deployment geometry (Warnken et al. 2006).

The DBL is calculated from a plot of 1/M versus Δg with slope (*m*) 1 / $DC_{DGT}At$ and intercept (*b*) δ/ $DC_{DGT}At$

$$\frac{\mathbf{1}}{\boldsymbol{M}} = \frac{\Delta \boldsymbol{g}}{\boldsymbol{DC_{DGT}At}} + \frac{\boldsymbol{\delta}}{\boldsymbol{DC_{DGT}At}} \quad (2.13)$$

Therefore the DBL (δ) is:

$$\delta = \frac{\boldsymbol{b}}{\boldsymbol{m}} \quad (2.14)$$

Inclusion of the DBL thickness in the calculation of C_{DGT} takes into account the 25 mm piston diameter since analytes will diffuse laterally within the diffusive gel (Huang et al. 2016).

C_{DGT} with DBL inclusion is:

$$C_{DGT} = \left(\frac{\mathbf{1}}{\boldsymbol{mDAt}}\right) \quad (2.15)$$

2.4.2 Factors affecting DGT measurements

Theoretically, it can be assumed that Fick's law of diffusion that governs passive sampling exists under steady-state conditions. In practice however, the uptake of analytes is controlled by environmental parameters such as temperature and concentration. This in turn influences the diffusion coefficient. Furthermore, the concentration could affect the boundary layer, which could then affect the flow of fluid across the sampling device (Seethapathy et al. 2008). Uncertainties during DGT measurements can be introduced in the following ways (Warnken et al. 2006):

- The elution factor used to calculate the mass

- Temperature variations during deployment which could affect the diffusion coefficient
- Errors when determining C_{TWA}
- Variations in diffusive gel thickness
- Different values of resin gel blank
- Measurements of diffusion coefficient
- DBL of unknown thickness

Some of these errors can be eliminated through extra measures; for example, prior to a 4 hour deployment, solutions could be stirred overnight to make sure that the temperature is stable. Secondly, use of higher spiking concentrations could ensure that the blank values are negligible. Additionally, plastic spacers could aid in having consistent diffusive gel thickness (Warnken et al. 2006). Measurements can also be affected by environmental factors such as turbulence, biofouling and ionic strength. Turbulence and biofouling are discussed in more detail.

2.4.2.1 Turbulence and the DBL

The DBL can be affected by the turbulence of the fluid as well as the deployment geometry. This means the DBL can extend the diffusional path length from DGT device into the bulk solution (Warnken et. 2006). In the instance where the DBL is significant, a plot of $1/\Delta g$ would be non-linear, also, there would be an error in the concentrations obtained from each Δg. Linearisation of such data is achieved by plotting 1/mass against Δg so that the DBL and C_{TWA} can be estimated (Zhang et al. 1998).

It is not advisable to make DGT measurements using one gel thickness during the determination of the DBL because the value of Δg is extended by an unknown distance, thus introducing errors of unknown measure. This is particularly true for devices that have very thin diffusive gels or ones that have filters without a diffusive gel. This is also a consideration for solutions with low stirring rates such as quiescent waters at the bottom of a lake (Warnken et al. 2006; Zhang et al. 1998).

In situations where the DBL is so thick that it cannot be ignored, then the following Equation must be used:

$$C_{DGT} = \frac{M\left(\frac{\Delta gel}{D_{gel}} + \frac{\Delta f}{D_f} + \frac{\delta}{D_w}\right)}{At} \quad (2.16)$$

where Δgel and Δf represent the gel and pre-filter, respectively; δ is the DBL thickness with D_f and D_w as the diffusion coefficients in the filter and DBL, respectively.

In the study by Warnken et al. (2006) it was concluded that in well stirred solutions it was unnecessary to consider the DBL since the value was negligible. However, in solutions stirred below 100 rpm, the thickness of the DBL was large enough to be considered. Therefore Equation 2.16 must be used.

2.4.2.2 Fouling

Biofouling occurs when surfaces immersed in water are exposed and become colonised by bacteria and form a biofilm. Biofilm thickness and type depends on exposure duration and sampling location respectively. Biofouling affects sampler uptake by blocking water-filled pores in a diffusion membrane as well as increasing the barrier thickness. Additionally, if the membrane is made of biodegradable material, it may become damaged by the bacteria (Huckins et al. 2006). Biofouling places major restrictions on water flux and membrane selectivity, shelf-life of the membrane as well as increasing the energy requirements of the system (Matin et al. 2011). The term fouling will be used in this study to represent the deposition of both biological and particulate matter on the surface of DGT.

The general assumption is that fouling physically restricts the diffusion pathway due to the additional layer that is formed (Feng et al. 2016; Turner at al. 2014; Webb and Keough 2002). Alternatively it has also been suggested that fouling clogs the filter membrane pores (Fernández-Gómez et al. 2012; Pichette et al. 2009). Uher et al. (2012) even suggested a mechanism for the sorption of trace metals as well as the interaction of organic matter with the diffusive gel. Devillers

et al. (2017) studied the effects of fouling on the uptake of cations and oxyanions including arsenic and selenium. They found that the accumulation of oxyanions and nickel was unaffected by fouling. The only elements affected by fouling were cadmium, copper and lead below pH 5.4 as they adsorbed on the fouling constituents.

2.5 Application of DGT: fate, transport and risk assessment

Understanding how pollutants evolve through time and space is an important aspect of monitoring. Fate and transport helps predict potential contamination into aquatic systems (Bennett et al. 2012). DGT has been applied in several studies to elucidate fate and transport as well as the risk assessment of environmental compartments. In these studies, commercial DGT was used, with Chelex-100 resin as the receiving phase.

Ruello et al. (2008) studied the fate of metals in contaminated soil as part of an environmental pollution assessment. Samples were collected from an industrial sludge treatment area. DGT and sequential extraction procedure (SEP) were used to determine labile concentrations of copper, iron, manganese and nickel. Results obtained from these two techniques were compared to those in soil and groundwater. DGT was able to accumulate the metal species that could desorb from the soil particles and not those that were kinetically inert or ones that formed part of colloidal particles (Harper et al. 1998; Zhang et al. 1995; Zhang et al. 1998). Some metal species could be soluble, however, if they are neutral or in their anionic forms, they cannot be accumulated by Chelex-100 in DGT (Ruello et al. 2008).

Uher et al. (2018) compared three techniques for monitoring metal concentrations in water: DGT, biomonitoring using caged gammarids and grab sampling. This study was conducted throughout France. Both DGT and gammarids were deployed at the same time. The aim was to establish whether these three analytical methods are complementary to each other and whether they could be effective

monitoring tools. The metals of interest were cadmium, chromium, cobalt, copper, manganese, nickel, lead and zinc. For cobalt and nickel there were no observable differences for the three monitoring methods. The gammarid biomonitors provided additional information as they could distinguish between lead and cadmium contamination. Overall, both gammarids and DGT provided the most information due to their integrative sampling behaviour. Uher et al. (2018) concluded that each method provides partial information but when combined the information obtained from each method is complementary and can be used as effective tools depending on the metal and fraction being studied.

Another risk assessment study was performed on soils in China that had previously undergone agricultural fertilization treatment (Guan et al. 2018). The assessment was on total and bioavailable metal concentrations in soil. From this study it could be deduced that after years of fertilization, total metal concentration had increased and consequently the bioavailable fraction as well. The information obtained after application of DGT samplers showed that the administration of organic fertilizers on these sites could possibly reduce metal uptake by crops. Information from DGT provided a different outlook to the problem.

DGT can also be used to determine speciation: Buzier et al. (2006) used DGT and Daphnia magna bioassays to investigate copper and cadmium speciation in diluted and spiked, filtered waste water. The two methods allowed the differentiation of metals between inorganic, organic and inert organic metal. DGT devices were prepared with both open-pore and restricted gels. The restricted gels, with smaller pore sizes could differentiate labile organic cadmium from labile organic copper. In this study, copper existed mainly as an inert organic complex, while cadmium was part of a labile organic complex. Buzier et al. (2006) concluded that DGT was a valid tool for differentiating labile from inert metal species.

2.5.1 Trends DGT passive sampler

DGT can be modified according to target analytes. Modifications range from the diffusive gel, to the resin gel / binding layer. The choice of DGT receiving phase controls the selectivity.

2.5.1.1 Hydrogels as diffusion barriers

Hydrogels are defined as polymers that have hydrophilic properties. The hydrophilicity stems from its polar monomers (Ahmed 2015). Hydrogels are important for controlling mass transport in DGT. During the initial stages of DGT deployment, solutes equilibrate with water within the hydrogels; the minimum time required for this to happen is determined by the diffusion coefficient of the solute in the gel. Zhang and Davison (1993) studied hydrogels used in DGT. The hydrogels were agarose; cross-linked polyacrylamide gel; Bis cross-linked polyacrylamide gel and pure agarose gel. The diffusion coefficients were measured using a diaphragm cell in the pseudo steady state mode. The second method involved exposing one side of the gel to a metal solution at different measured times.

Results showed that gels made from less than 2% agarose gels have an open structure and a large pore size, which is why the diffusion coefficient of simple ions are similar to those in water (Chramback 1985; Attwood et al. 1981). The agarose cross-linked polyacrylamide also had open-pores, however these were described as more robust compared to agarose. By using an agarose cross-linker, lower polymer concentrations were required. The diffusion coefficients obtained were also similar to water. Alternatively, Bis cross-linked gels hindered metal diffusion compared to water (Zhang and Davison 1999).

Hydrogels have two types of water: water that is bound to the hydrogel structure and free water that has similar behaviour to bulk water. Solutes diffuse via the free water more readily. Therefore, gels with a high propensity to swell will have a high proportion of free water (Khare and Peppas 1993; Quinn et al. 1988; Qu et al. 2000; Zhang and Davison 1993).

One issue that did arise from the use of polyacrylamide as a component of the diffusive gel was the ability of the amide nitrogen to bind mercury. This means possible retardation of mercury molecules in the diffusive gel (Bicak and Sherrington 1995; Docekalová and Divis 2005). Polyacrylamide also affects the uptake of nitrate by DGT (Huang et al. 2016; Cai et al. 2017). It is for this reason

agarose became an alternative component of the diffusive gel in some DGT devices (Cai et al. 2017; Docekalová and Divis 2005; Huang et al. 2016; Wang et al. 2016).

Agarose is defined as a purified linear polysaccharide originating from agar or marine algae containing agar. It is a linear polymer with alternating ^{D}D-galactose and 3,6-anhydro-^{L}L-galactose units linked by α-(1/3) and β-(1/4) glycosidic bonds (Figure 2.16). Polymerisation of agarose in water leads to the formation of double helices (Arnott et al. 1974).

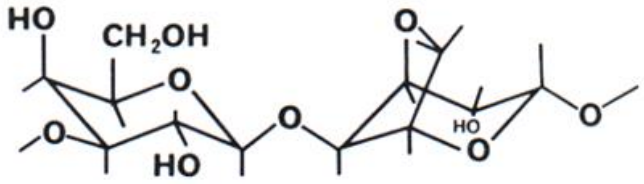


Figure 2.16 : The repeating units that make up agarose

Agarose binding sites are similar to those found in pyruvic and sulphonic functional groups (Fatin-Rouge et al. 2003). It is assumed that trace metals bind to agarose via the sulphonic functional groups .The binding sites largely constitute of negatively charged pyruvate groups, which attract and repel cations and anions, respectively. The strength of the interactions is dependent on ionic strength (Fatin-Rouge et al. 2003; Golmohamadi et al. 2012).

Agarose gel has open pores less than 5 μm which allow the diffusion of molecules less than 10^6 in molecular weight (Panther et al. 2014). The main advantage is that it is able to remain consistent in thickness in the pH range between 2 and 9, after initial swelling resulting from hydration (Panther et al. 2014).

2.5.1.2 DGT with single adsorbent resin

The resin layer in DGT can be altered or adjusted to suit the needs of the targeted analyte(s). This makes it a very important component in the pre-concentration of analytes and the choice should be carefully considered. It is important to select functional groups that will adsorb one or more of the target groups.

Gao et al. (2011) used 3-mercaptopropyl functionalized SBA-15 (SH-SBA) and 3-mercaptopropyl functionalized PMO (SH-PMO) as DGT resins. These resins were compared with commercially available resins that also contain thiol groups, together with the Chelex-100 resin used in commercial DGT. The thiol based resins showed high selectivity towards mercury due to the thiol and dithiocarbamate based groups. Conversely, Chelex-100 showed poor binding for mercury because of the low discriminatory properties of the iminodiacetate groups.

Bennett et al. (2012) aimed at understanding the mobilisation of arsenic under the influence of iron. Diffusive equilibration in thin films (DET) and DGT were used as the sampling methods of choice. DET is made up of similar components as DGT and it is used for the measurement of pore waters (Davison et al. 1991; Davison et al.1994). DET measured the concentration of iron (II) and arsenic in pore water through the mercapto-silica resin and DGT was for the measurement of inorganic arsenic via the Metsorb resin. The two elements were measured at the same time because arsenic mobility is closely linked to the biogeochemistry of iron. In the context of this study, *in situ* measurements using DGT and DET were important since sampling took place directly within the sediments, avoiding any speciation changes (Bennett et al. 2012). Research into different DGT binding layers is still a growing area of research. More examples of DGT binding layers and their target analytes are shown in Table 2.2.

Table 2.2: Examples of validated DGT binding layers and their target analytes.

Composition of resin / binding gel	Target analyte (s)	References
Chelex-100	Ni, Cu, Fe, Mn, Zn, Cd	Zhang et al. 1995
	Ni, Cu, Zn, Cd, Pb, Al, Mn, Ga, V, Cr, Fe, U, Mo, Ti, Ba, Sr, La, Ce, Pr, Nd, Sm, Eu, Gd, Tb, Dy, Ho, Er, Tm, Tb, Yb, Lu, Y, Li, Na, K, Rb, Mg, Ca, B, Tl, P, S, **As**, Bi, **Se**, Si, Sn, Sb, Te, Zr, Nb, Hf, Ta, W, Th, and Ag	Garmo et al. 2003
	Cr, Fe, Ni, Cu, Zn, **As**, Ag, Cd, **Hg**, Pb	Søndergaard et al. 2014
	Cd, Cu	Warnken et al. 2005
	Cd, Cu , Ni	Ernstberger et al. 2005
	Al, Cr, Fe, Mn, Co, Ni, Cu, Zn, Ga, Sr, Cd, Ba and U	Mengistu et al. 2012
	Cd, Cu, Ni, Pb, **As**,Cr, Sb, **Se**	Devillers et al. 2017
	Cd, Cu and Ni	Buzier et al. 2014
Ferrihydrite	V, As, Sb and Mo	Zhang et al. 2017
	As	Buzier et al. 2014
	As	Fitz et al. 2003
	As	Garnier et al. 2015
	As(III), As(V),	Panther et al. 2008
	As(V), Se(VI), Sb(V), V(V)	Luo et al. 2010
	Se	Sogn et al. 2008
	Se	Peng et al. 2017

Table 2.2 (*cont.)*

Composition of resin / binding gel	Target analyte (s)	References
Ferrihydrite	As(III), As(V), Se(IV), Se(VI), V(V), PO_4^{3-}	Price et al. 2013
Metsorb™ (titanium oxide)	As(III), As(V), Se(IV)	Bennett et al. 2010
	As	Garnier et al. 2015
	PO_4^{3-}	Panther et al. 2011
	U	Hutchins et al. 2012
Zirconium	PO_4^{3-}	Qin et al. 2018
	As	Sun et al. 2014
Duolite GT73 and Ambersep GT74	Hg	Pelcová et al. 2014
Spheron-Thiol	Hg	Docekalová and Divis 2005

2.5.1.3 Multi-layer and mixed DGT resins

Selectivity for a wider variety of analytes may be enhanced through multi-layer DGT, whereby different binding layers are stacked (Huang et al. 2017). Alternatively, mixed binding layers may be used, where different resins are mixed together into a single layer (Zhang et al. 2014, Motelica-Heino et al. 2003, Stockdale et al. 2008, Mason et al. 2005). Multiple and mixed binding layers are more favourable because they reduce the materials used, preparation time, deployment and analysis of many samples. The main disadvantage is that these layers could potentially reduce the intrinsic binding capacity for the individual analytes, consequently increasing competition between analytes and major ions (Huang et al. 2017). Some examples of mixed binding layers are listed in Table 2.3.

Table 2.3: Examples of mixed resin DGTs and their target analytes.

Composition of resin / binding gel	Target analyte (s)	References
AgI and Chelex-100	Sulphide and metals	Motelica-Heino et al. 2003
Chelex-100 and ferrihydrite	PO_4-P, Mn, Cu, Mo, Zn, and Cd	Mason et al. 2005
AgI and ferrihydrite	PO_4-P, V, As and sulfide	Stockdale et al. 2008; Huynh et al. 2012
Chelex- 100 and Zr-oxide	PO_4-P and Fe (II)	Xu et al. 2013
Chelex-100 and Metsorb	Cations (Mn, Co, Ni, Cu, Cd and Pb) and oxyanions (V, As, Mo, Sb,W and PO_4-P)	Panther et al. 2014
Chelex-Metsorb	Select cations and anions	Shiva et al. 2015
PrCH and A520E; Metsorb	Nitrogen and phosphorus	Huang et al. 2017
ZrO-Chelex	Sulphide, Fe and P	Ma et al. 2017
End-capped Bondesil® C8 and C18	Organotins	Cole et al. 2018
ZrO-Chelex and ZrO-AgI	Sulphur	Wang et al. 2017

2.5.1.4 Phosphate and sulphonyl functional groups

Arsenic and phosphorus share important chemical properties such as oxidation states. Arsenate ($HAsO_4^{2-}$) has very similar pKa values to phosphate (HPO_4^{2-}). The overall sizes are also very similar: the thermodynamic radius for phosphate is 2.38 Å and 2.48 Å for arsenate (da Silva and Williams 2001, Tawfik and Viola 2011). Proteins and enzymes have displayed very low phosphate-arsenate binding selectivity. It has been suggested that the lack of selectiveness could be a result of physico-chemical hindrances which have restricted the ability of these enzymes to distinguish between the two (Tawfik and Viola 2011). Secondly, the lack of evolutionary pressure means that there is no competition between arsenate and phosphate for certain binding sites when arsenate is introduced. The discriminatory challenge is due to the small size differences between arsenate and phosphate, as well as the partial negative charges of their oxygens (Tawfik and Viola 2011).

In a similar fashion, the radii of sulphur is similar to selenium, this means sulphur can replace selenium in metal sulphides (Huston et al. 1995; White et al. 2004). The uptake of selenium and sulphur by plants has shown antagonistic behaviour. It is suggested that selenate, being a sulphur analogue, is able to enter plants through sulphate transporters (Hawkesford and Zhao 2007; Terry et al. 2000), even though the extent of interaction will differ with each sulphate transporter (Parker et al. 1992; White et al. 2004). Additionally, a study by Saad et al. (2013) suggested an anion exchange mechanism between selenium and sulphur in adsorption studies using sulphonated cross linked polyethylenimine.

2.5.1.5 Polyethylenimine

In recent years polyethyleimine (PEI) has attracted a lot of attention as an adsorbent for metals. This is because of the large number of primary, secondary and tertiary amine groups along the macromolecular chain (Ma et al. 2014; Li. et al. 2016; Setyono and Valiyaveettil 2016). PEI is charged over a wide pH range.

PEI binds metals either through complexation or electrostatic interaction (Pang et al. 2011a; 2011b). Figure 2.17 shows branched PEI.

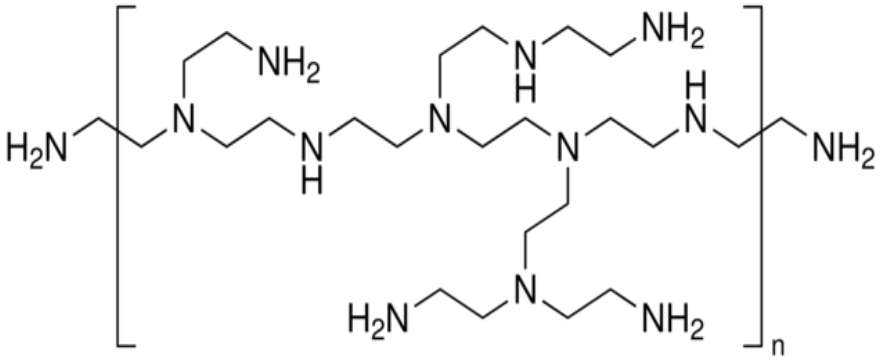


Figure 2.17: Structure of branched polyethylenimine showing primary, secondary and tertiary amine groups (Saad et al. 2011)

PEI is highly soluble in water, which is why it is often immobilised either through cross-linking with polymers that are insoluble in water (Denizli et al. 2003; Ba et al. 2009; Pang et al. 2011a; Say et al. 2002), grafting on biomass (Deng and Ting 2005a; Deng and Ting 2005b), on cellulose (Navarro et al. 1996; Navarro et al. 2001), silica (Wang et al. 2013) or through the use of inorganic supports (An and Gao 2007; Sun et al. 2012). The choice of cross-linker can determine the affinity, selectivity as well as re-use after regeneration (Jia et al. 2014; Saad et al. 2011).

Having a large number of amine groups means that selectivity of PEI is reduced, if applied in contaminated water; metals would be subjected to high competition. For this reason, PEI is often modified to enhance selectivity. Table 2.4 shows some examples of how PEI was modified to target specific analytes. Although most of the target elements are metals, in several studies by Saad et al. 2011; Saad et al. 2012; Saad et al. 2013a; 2013b) PEI was modified with phosphate and sulphonyl functional groups to target arsenic and selenium in mine waste waters. The phosphonated polymer showed 88% efficiency in the removal of arsenic, 81% and 87% efficiency removal for selenium and mercury, respectively, using the sulphonated polymer (Saad et al. 2013a; Saad et al. 2013b). Functionalised

CPEI will therefore be used as a resin for the accumulation of arsenic, selenium and mercury in DGT.

Table 2.4: Examples of PEI modification for enhanced selectivity towards target analytes

Modification	Target analyte(s)	Reference
PEI grafted on mesoporous silica nanoparticles	Cd(II); Ni (II)	Thakur et al. 2017
PEI grafted on aerobic granules	Cr(VI)	Sun et al. 2010
PEI modified biochar	Cr(VI)	Ma et al. 2014
PEI cross-linked with a triazole group	Cu(I); Cu(II)	Movahedi et al. 2015
PEI-functionalised ion-imprinted hydrogel	Cu(II)	Wang and Li 2015
PEI-functionalised paper	Au and Ag nanoparticles, Cr(VI) anions, Ni (II), Cd(II) and Cu(II)	Setyono and Valiyaveettil 2016
PEI modified magnetic porous (SiO_2 and Fe_3O_4) adsorbent	Cu(II); Zn(II); Cd(II)	Pang et al. 2011a
PEI enhanced magnetic carboxymethyl chitosan	Pb(II)	Wang et al. 2011
Phosphonated cross-linked PEI	U; As	Saad et al.2012b; Saad et al. 2013b
Sulphonated cross-linked PEI	Hg; Se	Saad et. 2012a; Saad et al. 2013a
Thiolated cross-linked PEI	Hg	Saad et al. 2013c

Chapter 3: Research aim and objectives

The aim, objectives, research statement and novelty of this study are discussed in this section

3.1 Aim

The aim of this project was to design, develop and optimise a DGT passive sampler for the determination of bioavailable arsenic, selenium and mercury in water.

3.2 Specific objectives

This aim was achieved through the following objectives:

- Synthesis of cross-linked polyethylenimine and functionalising with sulphonyl and phosphate groups.
- Design and construction of DGT sample holder units from PTFE rod
- Development and preparation of the DGT resin and diffusive gel layers.
- Deployment of assembled DGT units under different conditions to study the influence of pH, sample concentration and turbulence on uptake.
- Deployment of optimised DGT passive samplers in environmental samples.
- Determination of the maximum capacity of the newly developed DGT passive sampler in environmental samples.

3.3 Research statement and novelty

One of the biggest concerns arising from AMD is the concomitant release of toxic elements into surface and ground water. Monitoring of surface and ground water within and around the Witwatersrand basin would be important for the long-term evaluation of fate and transport of elements arising from AMD. Amongst these elements are arsenic, selenium and mercury which are potentially toxic and have the ability to bio-accumulate. It is therefore important to find sensitive techniques for monitoring these elements.

DGT technique is a well-studied passive sampling technique and can often be adapted to suit the purpose of the assessment. The binding layer in particular can be varied depending on target analyte(s). To our knowledge, sulphonated and phosphonated cross-linked polyethylenimine (CPEI), which showed potential as remediation adsorbents with the ability to remove arsenic, selenium and mercury with more than 80% efficiency from mine waste water (Saad et al. 2012; 2013a; 2013b), have not been used as binding layers in DGT.

In order for DGT bearing a particular binding layer to be classified as a valid technique it needs to be evaluated for selectivity, recovery reproducibility but most importantly it must be able to work as a kinetic passive sampler, showing linear uptake with deployment time. This work therefore evaluated the DGT passive sampler bearing the sulphonated and phosphonated CPEI as a valid tool for the determination of labile arsenic, selenium and mercury.

Chapter 4: Materials and methods

This chapter outlines the materials and methods used to carry out the research objectives.

4.1 Materials

PTFE rod used for the construction of DGT sample holders was purchased from Maizey plastics (Johannesburg, South Africa). The polyethersulphone (PES) membranes, polyethylenimine (PEI MW 25000), epichlorohydrin, 3-chloropropanesulfonyl chloride ($C_3H_6Cl_2O_2S$), 38% formaldehyde (CH_2O) were all purchased from Merck (Johannesburg, South Africa) and used without further purification. Sodium hydroxide, isopropanol, phosphoric acid, hydrochloric acid, tetrahydrofuran were purchased from Associated Chemical Enterprises (Johannesburg, South Africa). Arsenate, selenite and mercury nitrate used to spike water were prepared from the following salts: Na_3AsO_4, Na_2SeO_3 and $Hg(NO_3)_2$.

4.2 Instrumentation

4.2.1 Elemental analysis

Trace metal and metalloid concentrations were determined using inductively coupled plasma optical emission spectrometry (Spectro Genesis ICP-OES, Kleve, Germany) and the inductively coupled plasma mass spectrometer (Agilent 7900 ICP-MS, Santa Clara, United States).

4.2.2 Anion analysis

Anions in the environmental water samples were analysed using a compact ion chromatography (IC) system (Metrohm 761, Herisau, Switzerland) furnished with a suppressor module, and a Metrosep A Supp 5-150/4.0 column (Metrohm, Herisau, Switzerland) as well as an appropriate guard column.

4.2.3 Fourier transform infrared (FT-IR) spectra

The FT-IR spectra of the polymer resins were characterised using Tensor 27 spectrophotometer (Bruker, Ettlingen, Germany). The spectra were recorded between 4000 and 400 cm^{-1}.

4.2.4 Solid state NMR

The solid state NMR spectra for all cross-linked polyethyleimine (CPEI) based polymers were obtained from Avance III (Bruker, Rheinstetten, Germany) adapted with a 4 mm probe. The ^{13}C CP/MAS, was performed at 500 Hz. Data was processed using MestReNova software.

4.2.5 CHNS analysis

CHNS analysis was performed on the resins using the Vario EL cube elemental analyser, (Langenselbold, Germany). This technique was used to determine the percentage of carbon, hydrogen, nitrogen and sulphur in the polymer samples.

4.2.6 Physico-chemical properties of water

A portable combo meter (Hanna, Rhode Island, United States) that measures pH, conductivity, total dissolved solids (TDS) and temperature was used to measure the physico-chemical properties of water in the field.

4.3 Experimental procedure

4.3.1 Synthesis of polyethylenimine as a sorbent for DGT

4.3.1.1 Cross-linked polyethylenimine (CPEI)

CPEI was prepared using a method adapted from Saad et al. (2011). 10 g of polyethylenimine and 2 g of sodium hydroxide were dissolved in 25 mL deionised water. The mixture was heated under reflux. Once the temperature had stabilised to 65°C, 1.2 mL of epichlorohydrin was added. A white rubbery solid was obtained within 10 minutes. The resulting gel was washed with approximately 750 mL of deionised water followed by approximately 100 mL of isopropanol and left to dry overnight before use.

4.3.1.2 Sulphonated cross-linked polyethylenimine (SCPEI)

The sulphonation of CPEI was performed by dissolving 2.5 g of CPEI in 65 mL of tetrahydrofuran. The mixture was heated under reflux until the temperature had stabilised to approximately 70°C, after which 2.4 mL of 3-chloropropanesulfonyl chloride ($C_3H_6Cl_2O_2S$) was added and the experiment was allowed to proceed overnight. This procedure was adapted from Saad et al. (2012b). An orange-brown rubbery solid was obtained. It was washed with approximately 750 mL of water to remove any unreacted product. The polymer was left to dry overnight.

4.3.1.3 Phosphonated cross-linked polyethylenimine (PCPEI)

The phosphonation of CPEI was carried out by dissolving 2.5 g of CPEI in 80 mL of 6 mol L^{-1} HCl and 19.31 g of phosphoric acid. This method was adapted from Saad et al. (2012a). The reaction mixture was heated under reflux to 90°C. Once the temperature had stabilised, 38 mL of formaldehyde was added drop-wise for one hour, the reaction was then left to proceed overnight. The resulting dark brown solid was washed with deionised water and left to dry overnight.

4.3.2 Batch studies

4.3.2.1 The uptake efficiency of SCPEI-PCPEI polymer mixture

The efficiency of SCPEI-PCPEI to accumulate arsenic, selenium and mercury was determined using two different combinations of the SCPEI and PCPEI resin. In the first combination 80% of SCPEI and 20% of PCPEI resins per 0.8 g total mass were used. The second combination was 20% of SCPEI and 80% of PCPEI per 0.8 g total mass. A solution containing 1 mg L^{-1} arsenic, selenium and mercury was prepared and the pH was adjusted to 3 for one batch and pH 7 for the other. pH 3 and pH 7 were selected because they represent AMD and natural water, respectively. Afterwards, 20 mL of the respective pH solutions were poured into 25 mL sample vials. 0.3 g of each resin combination was added to the sample vials. The samples representing each resin combination were prepared in triplicate. The samples were left on a shaker for 1.5 hours, after which they were filtered. The remaining resins were desorbed using 5 mol L^{-1} nitric acid (Saad et

al. (2012b; 2013b). The filtrates before and after desorption were analysed using ICP-MS.

4.3.2.2 The uptake factor

The uptake efficiency was expressed in terms of the uptake factor (f_u) which was calculated using Equation (4.1) below:

$$f_u = \frac{M_i - M_f}{M_i} \quad (4.1)$$

Where M_i and M_f are the initial mass and mass remaining in solution, respectively (Davison, 2016).

4.3.2.3 Elution efficiency of different eluents

It is important for elution to be accurate and reproducible. This is because the elution factor (f_e) as previously shown in Equation (2.5) and (2.6) is required for the determination of mass accumulated by DGT (Zhang and Davison, 1995). The elution efficiencies of different eluents were determined following the procedure outlined below: Resin gel discs (resin that was embedded in agarose and cut into discs after the polymerisation) were prepared and each disc was deployed in 20 mL deionised water containing 1 mg L^{-1} of arsenic, selenium and mercury. After 12 hours the resin gels were removed and rinsed with deionised water and placed into different sample vials containing 20 mL of either 5 or 7 mol L^{-1} nitric acid. The resin gels were removed after 12 hours, the remaining solutions were filtered and analysed using ICP-MS. The above mentioned procedure was repeated using 0.25 and 0.5 mol L^{-1} of either sulphuric, phosphoric acid or thiourea (dissolved in 0.5 mol L^{-1} hydrochloric acid). This procedure was again repeated using 1 mol L^{-1} of either nitric, sulphuric, phosphoric, hydrochloric acid, thiourea (dissolved in 1 mol L^{-1} hydrochloric acid) and sodium hydroxide as the eluents. The samples were analysed using ICP-MS.

4.3.2.4 The elution factor

The elution factor is expressed as a percentage. The elution factor was calculated using Equation (4.2) below:

$$f_e = \frac{M_e}{M_i - M_f} \quad (4.2)$$

Where M_e is mass eluted, M_i and M_f are the initial mass and mass remaining in solution, respectively (Davison 2016).

4.3.3 Construction of passive sampler

4.3.3.1 Construction of sample holders

DGT sample holder units used in this study were manufactured from a 3.0 cm diameter polytetrafluoroethylene (PTFE) rod (Figure 4.1). The dimensions used in the construction of the units were based on those described for commercial DGT; the cap was 2.5 cm in diameter with a 2.0 cm exposure window (DGT Research Ltd., UK). The cap was modified by introducing groves that would act as a grip, allowing the cap to be removed and replaced multiple times.



Figure 4.1: PTFE rod used in the construction of DGT sample holder units

4.3.3.2 Preparation of resin embedded in agarose

The receiving layer in commercial DGT comprises of the Chelex® resin embedded into an agarose-derivative gel (Zhang and Davison 1995). Based on this concept, 0.5 g of SCPEI-PCPEI mixture was evenly spread out in a square Perspex container. 1.5 % of warm agarose was poured on the resin mixture, ensuring that the resin was completely covered. This was left to polymerise at room temperature, on an even surface.

4.3.3.3 Preparation of diffusive gel layer

An agarose-based diffusive gel was made from 1.5% (w/v) of agarose. Briefly, the required amount of agarose was weighed into a 250 mL Erlenmeyer flask and dissolved with deionised water and sealed with a 50 mL Erlenmeyer flask. The agarose was placed in a conventional microwave oven and allowed to dissolve. Once dissolved, the hot mixture was poured into a Perspex mould with 0.08 cm plastic spacers. The Perspex mould was sealed with a lid to ensure an even surface. Once polymerised, the agarose gel was cut into 2.5 cm discs using a 2.5 cm custom-made disc cutter. Gel thickness was measured using a digital caliper. On average the thickness of the agarose diffusive gel ranged between 0.068 cm and 0.08 cm. The gel discs were kept hydrated until use.

4.3.4 Assembly and deployment of DGT passive sampler

SCPEI-PCPEI based DGT passive samplers were assembled using two alternative methods. In the first, resin gel discs comprising of SCPEI-PCPEI resin mixture embedded in agarose, were used. In the second, 0.8 g of SCPEI-PCPEI resin mixture in its loose polymer form was placed directly on the DGT piston base. The rest of the steps were the same, whereby an agarose diffusive gel was placed directly on top of the resin layer followed by a PES membrane. To complete the assembly, the modified DGT cap was used to enclose all the DGT components, ensuring a water-tight seal. These steps are summarised in Figure 4.2.

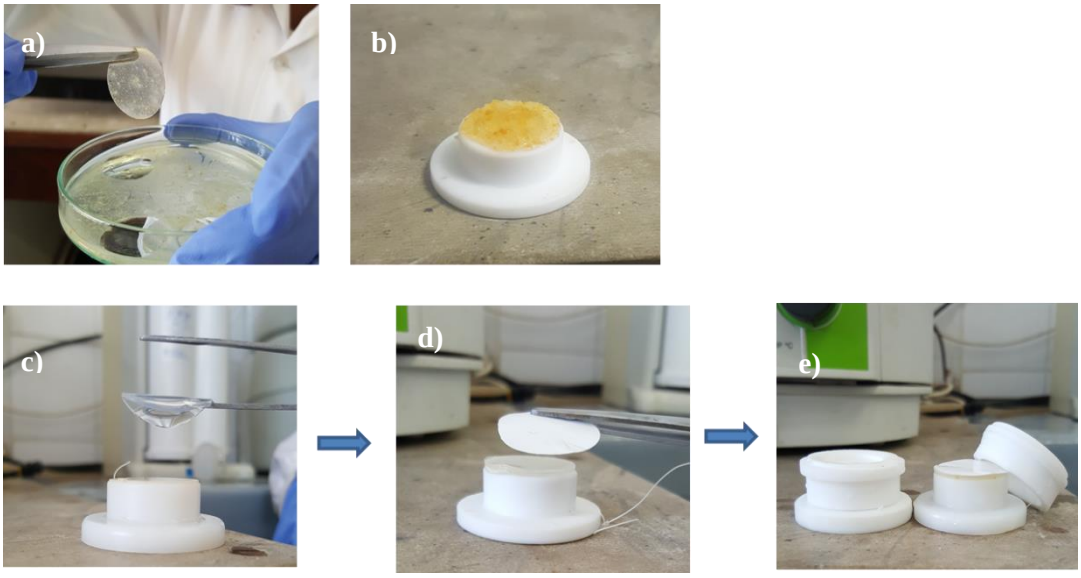


Figure 4.2: a) SCPEI-PCPEI resin gel discs used as DGT binding layers, alternatively b) 0.8 g of the SCPEI-PCPEI resin mixture in the loose polymer form was used as the binding layer. Either binding layer was placed directly on the piston base followed by the c) diffusive gel disc. d) A PES membrane was positioned on top of the diffusive gel e) the assembly was completed by sealing with the modified DGT cap.

SCPEI-PCPEI based DGT passive samplers were deployed in 6 L borosilicate glass containers filled with 5 L solutions spiked with a known concentration of arsenic, selenium and mercury. Depending on whether stirring was required; the containers were placed on magnetic stirrers (stirred at 60 rpm) and deployed for a prescribed number of days. This experimental set-up is shown in Figure 4.3.



Figure 4.3: Laboratory-based deployment of passive samplers in Spiked deionised water.

4.3.5 Calibration of DGT passive sampler

4.3.5.1 Effect of SCPEI as DGT binding layer

Due to the ubiquity of sulphur and its strong association with multiple elements SCPEI was the initial resin of choice. In preliminary studies, a simple experiment was set up by weighing 0.4 g of SCPEI resin and placing it directly on the DGT piston base, a PES membrane was placed on top of the SCPEI resin. These contents were sealed with the modified DGT cap. Two more DGT devices were assembled this way and deployed for 12 days in a solution spiked with arsenic, selenium and mercury with a final concentration of 1 mg L^{-1}. A DGT sampling device was removed after 6, 9 and 12 days. Prior to analysis the resins were removed from the DGT base, rinsed and placed in sample vials containing 20 mL of 1 mol L^{-1} sulphuric acid and left overnight at room temperature. The samples were filtered and analysed using ICP-OES.

4.3.5.2 Effect of SCPEI-PCPEI resin mixture dispersed in agarose gel

SCPEI-PCPEI resin gels embedded in agarose were prepared as described in section 4.3.3.2. The side with the gravity-deposited resin was placed facing upwards on the DGT piston. A PES membrane was placed on top of the resin gel layer and sealed with the modified DGT cap. These DGT devices were deployed

in a solution containing 1 mg L^{-1} of arsenic, selenium and mercury at pH 3. The passive samplers were deployed for 15 days with samplers removed in triplicate every 3 days. Prior to analysis, the resin gels were removed, rinsed and placed in sample vials containing 20 mL of 1 mol L^{-1} sulphuric acid. The sample vials were left overnight at room temperature. The samples were filtered and analysed using ICP-OES.

4.3.5.3 Effect of SCPEI-PCPEI resin mass on DGT capacity

The mass of the SCPEI-PCPEI resin mixture was varied in order to improve the capacity of arsenic, selenium and mercury. The resin mixture was not impregnated in agarose gel but instead used in its loose polymer form. An arbitrary mass of 0.4 g was selected since this was the minimum amount that could provide complete coverage of the DGT piston base. Furthermore, 0.8 g was the maximum amount that could be used while still allowing the DGT cap in the assembled unit to close with a tight seal.

The resin layer was prepared by using either 0.4 g or 0.8 g of the SCPEI-PCPEI resin mixture in the loose polymer form and placing it directly onto the DGT piston base. This layer was smoothed out as much as possible before placing a PES membrane and sealing with a DGT cap. The passive samplers were deployed in a solution containing 1 mg L^{-1} of arsenic, selenium and mercury, at pH 3 for 15 days. Sampling devices were removed in triplicate every 3 days. Prior to analysis the resin layers were removed from the DGT base and placed in sample vials (Figure 4.4), 20 mL of 1 mol L^{-1} sulphuric acid was poured into each sample vial and the samples were left overnight at room temperature. The samples were filtered and the filtrate analysed using ICP-OES.



Figure 4.4: Sample vials containing the SCPI-PCPEI resin mixture in the loose polymer form after exposure to spiked solution with arsenic, selenium and mercury, prior to desorption using 1 mol L^{-1} sulphuric acid.

4.3.5.4 Effect of the diffusive gel in SCPEI-PCPEI based DGT

The role of the agarose diffusive gel was assessed using two different methods of DGT device assembly. In the first method a PES membrane was placed directly on top of 0.4 g SCPEI-PCPEI resin mixture and sealed with the DGT cap. In the second method, an agarose diffusive gel was placed between the resin mixture and a PES membrane before sealing with the DGT cap, the diffusive gel was 0.07 cm. The passive samplers were deployed in deionised water spiked with 1 mg L^{-1} arsenic, selenium and mercury at pH 3. The passive samplers were deployed for 6 days, and removed in triplicate after day 1; day 3 and day 6. Prior to analysis the resin gels were removed from the DGT base and placed in 20 mL of 1 mol L^{-1} sulphuric acid and left overnight at room temperature. The samples were filtered and analysed using ICP-OES.

4.3.5.5 The diffusive gel thickness and flux

The effect of the diffusive gel thickness on flux was determined by assembling DGT sampling units as described in section 4.3.4. The thickness of the diffusive

gels was varied between 0.06, 0.08, 0.1 and 0.12 cm. These devices were deployed in deionised water containing 1 mg L^{-1} of arsenic, selenium and mercury at pH 3, for 3 days. The resins were removed from the DGT sample holders and placed in sample vials containing 20 mL of 1 mol L^{-1} sulphuric acid and left overnight at room temperature. The samples were filtered and analysed using ICP-OES. The experiments were performed in triplicate.

The flux can be determined using the concentration, C_{DGT} (mg L^{-1}) obtained from DGT using Equation 4.3:

$$M = \left(\frac{C_{DGT}\,(v+V)}{0.8 \times A}\right)\frac{1}{x} \tag{4.3}$$

where *v* and *V* are the extractant and gel volume (mL), respectively. *x* is the atomic number of the element, 0.8 represents the elution factor and A is the exposure area (cm^2). Using deployment time *t* (seconds), Flux, F (nmol cm^{-2} s^{-1}) can be calculated as follows:

$$F = \frac{M}{t \times A} \tag{4.4}$$

Table A.2 in the appendix provides more detail.

4.3.5.6 The effect of turbulence on DGT uptake

SCPEI-PCPEI based DGT passive samplers were assembled using the steps as described in section 4.3.4 using 0.8 g of the SCPEI-PCPEI resin mixture in its loose polymer form. SCPEI-PCPEI based DGT passive samplers were deployed in 5 L deionised water containing 1 mg L^{-1} of arsenic, selenium and mercury at pH 3, for a total of 12 days, with samplers removed in triplicate every 3 days. Before analysis the resins were placed in sample vials containing 20 mL of 1 mol L^{-1} sulphuric acid and left overnight at room temperature. The samples were filtered and analysed using ICP-OES. Experiments were carried out under both stirred and stagnant conditions.

Under stirred conditions, solution agitation was achieved by using a FMH STR-MG140 magnetic stirrer (Midrand, South Africa) with the speed of 60 rpm. This stirring rate was selected because it was considered representative of quiescent water which would be encountered during field applications.

4.3.5.7 The effect of sample concentration on DGT uptake

Assembled SCPEI-PCPEI based DGT passive samplers were deployed in solutions containing either 0.25 mg L^{-1}, 0.5 mg L^{-1} or 1 mg L^{-1} of arsenic, selenium and mercury, at pH 3. The total deployment period was 12 days and sampling devices were removed in triplicate every 3 days. Prior to analysis the resins were placed in sample vials containing 20 mL of 1 mol L^{-1} sulphuric acid and left overnight at room temperature. The samples were filtered and analysed using ICP-OES.

4.3.5.8 The effect of pH on DGT uptake

The pH plays an important role in the speciation of arsenic, selenium and mercury. It was important to ensure that SCPEI-PCPEI based DGT can operate in both AMD and natural water for extended periods. The DGT passive samplers were assembled and deployed in deionised water containing 1 mg L^{-1} arsenic, selenium and mercury set at either pH 3 or 5, which are representative of AMD and natural water, respectively. The DGT sampling units were deployed for 15 days, with devices removed in triplicate every 3 days. The pH of the water solutions was checked every few days to ensure that no significant changes had taken place. Prior to analysis the resins were placed in sample vials containing 20 mL of 1 mol L^{-1} sulphuric acid and left overnight at room temperature. The samples were filtered and analysed using ICP-OES.

4.3.6 Determination of diffusion coefficients and diffusive boundary layer

4.3.6.1 The diffusion coefficient (*D*) in agarose gel

SCPEI-PCPEI DGT passive samplers were deployed in deionised water spiked with 1 mg L^{-1} of arsenic, selenium and mercury. The total deployment time was

16 hours and DGT sampling devices were removed in triplicate after 4 hours then every 2 hours after that until the experiment was complete. The resin was removed from the DGT sampler holders, desorbed overnight in 20 mL of 1 mol L^{-1} sulphuric acid, filtered and the filtrate analysed using ICP-OES. The diffusion coefficient was calculated using Equation 2.12.

4.3.6.2 The diffusive boundary layer (DBL)

The thickness of the DBL (δ) was determined by deploying SCPEI-PCPEI DGT devices with varying diffusive gel thickness (0.06, 0.08, 0.1 and 0.12 cm) in deionised water spiked with arsenic, selenium and mercury (1 mg L^{-1}) at pH 3. The DGT sampling devices were deployed for 3 days, afterwards the resins were removed from the sample holders, desorbed overnight in 20 mL of 1 mol L^{-1} sulphuric acid, filtered and the filtrate analysed using ICP-OES. The DBL was calculated using Equation 2.14.

4.3.7 Determination of the blank and method detection limit (MDL)

SCPEI-PCPEI based DGT passive samplers were assembled using the steps as described in section 4.3.4 using 0.8 g of the SCPEI-PCPEI resin mixture in its loose polymer form. The DGT units were deployed in deionised water for 24 hours, the resins were retrieved and desorbed overnight with 20 mL of 1 mol L^{-1} sulphuric acid, after which they were filtered and the filtrate analysed using ICP-OES. The method detection limit was calculated as three times the standard deviation of the blank.

4.3.8 Field deployment of optimised SCPEI-PCPEI based DGT

4.3.8.1 Construction of sampling cages

The passive sampling cages were designed and constructed from affordable, easily accessible material. These cages would protect the passive samplers during field deployments. The skeleton was made of threaded steel rods, a plastic mash was wrapped around the steel rod structure in order to seal the cage while allowing the free flow of water. During field deployment, the DGT passive

samplers were suspended on the steel rods via a thin strip of polypropylene rope. It was important to fully submerge the DGT passive samplers together with the sampling cages. Figure 4.5 shows the constructed sampling cages.

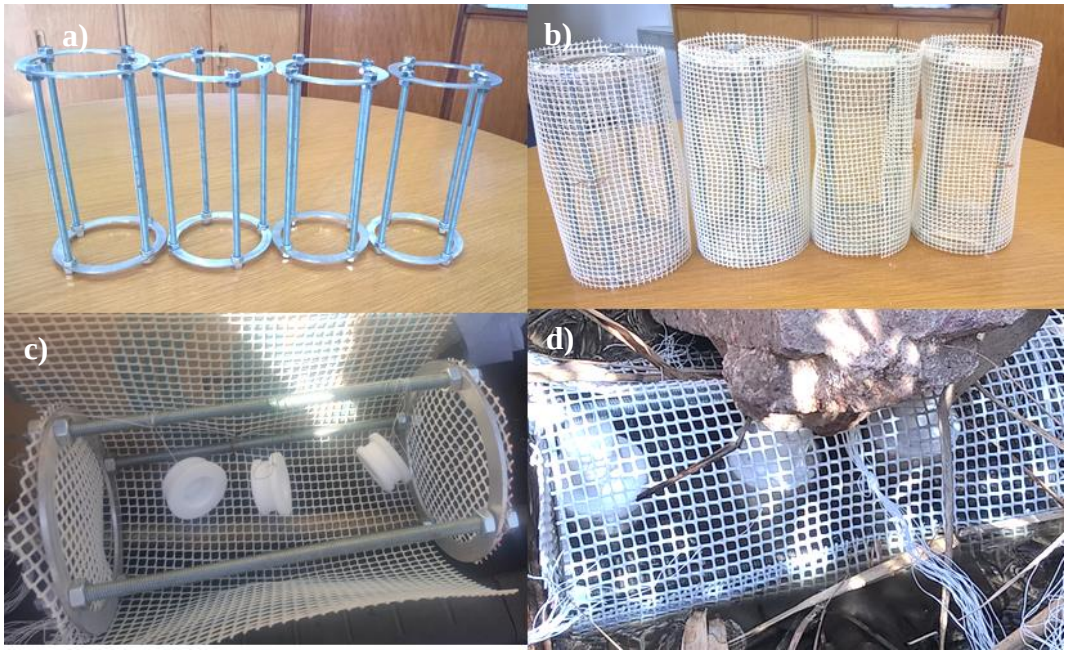


Figure 4.5: a) The steel rods used as the skeleton of the sampling cages. b) The fully constructed sampling cages used to house the passive samplers during field deployments, c) DGT passive samplers attached to the sampling cage d) DGT passive samplers deployed in the field.

4.3.8.2 Description of sampling sites

DGT passive samplers were deployed at two different sites affected by previous mining activities. Both sampling sites are found in Roodepoort, West of Johannesburg, with mine tailings in clear view (Figure 4.6). The first sampling site was near a mine tailing (GPS coordinates: 26°11'07.8"S 27°52'51.2"E) with active AMD production. The second sampling site was Fleurhof Dam (GPS coordinates: 26°11'53.4"S 27°54'33.5"E).



Figure 4.6: a) Arial view of the area where water samples and DGT passive samplers were deployed: b) site A is the site with active AMD seepage and c) site B is Fleurhof Dam, which is in close proximity to mine tailings and active AMD.

Physico-chemical properties of the sampled water such as temperature, pH, redox potential and conductivity were obtained on site and in the lab. From each sampling site, 25 L of water was collected; however no preservative measures were taken as this would alter the pH prior to deployment of the DGT passive samplers.

4.3.8.3 DGT deployment in Fleurhof Dam water

SCPEI-PCPEI based DGT units were assembled as described in section 4.3.4 a day prior to the sampling expedition and kept hydrated at 4°C. The DGT devices were deployed in Fleurhof Dam for a total of 15 days. The physico-chemical properties of the water were measured on site. DGT sampling devices were removed in triplicate after 3, 6, 9 and 15 days.

For the laboratory-based experiments 30 L of Fleurhof Dam water was collected and used immediately. Two laboratory-based experiments were set up. In the first, two 6 L containers with 5 L of the Fleurhof Dam water spiked with arsenic, selenium and mercury to a final concentration of 0.5 mg L^{-1}. 6 DGT sampling devices were place in each container and they were deployed for a total of 9 days, with DGT devices removed in triplicate after 3, 6 and 9 days.

In the second experiment 6 L borosilicate containers were filled with 5 L of Fluerhof dam water. DGT devices were deployed for a total of 9 days with samplers removed after 3, 6 and 9 days.

Prior to analysis, the resins were retrieved and placed in sample vials containing 20 mL of 1 mol L^{-1} sulphuric acid. These vials were left at room temperature over-night, filtered and analysed using ICP-OES and IC-MS.

4.3.8.4 Deployment in dissolved efflorescent crusts

Dissolved efflorescent crusts were used to mimic AMD water in order to assess matrix effects and bioavailable fractions of arsenic, selenium and mercury. The solution was prepared by dissolving 50 g of the efflorescent crust in 5 L of deionised water. This solution was spiked with arsenic, selenium and mercury to a final concentration of 1 mg L^{-1}. DGT devices were deployed for 19 days and DGT devices were removed in triplicate every 3 days. The pH, redox potential, conductivity, anion concentration and background metals were analysed. The dry and ground efflorescent crust along with the experimental set up are shown in Figure 4.7. Prior to analysis using ICP-OES, solutions were filtered several times using 0.45 µm syringe filter.

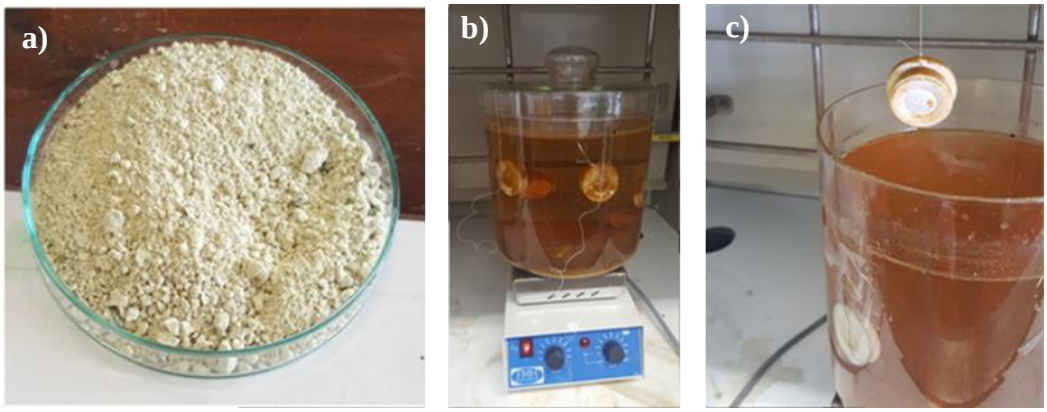


Figure 4.7: a) The efflorescent crust used in this study. b) SCPEI-PCPEI based DGT sampling devices deployed in the dissolved efflorescent crust.

4.3.8.5 Passive sampler deployment in AMD

AMD water collected from site A (Figure 4.6) was used in laboratory-based experiments. This water sample was spiked with arsenic, selenium and mercury to a final concentration of 0.5 mg L^{-1}. DGT devices were only deployed for 5 days (Figure 4.8) to avoid significant precipitation of the drainage water. DGT sampling devices were simultaneously deployed at site A for 5 days. The resins were desorbed with 20 mL of 1 mol L^{-1} of sulphuric acid and the samples analysed using ICP-MS.



Figure 4.8: Experimental set up of SCPEI-PCPEI based DGT sampling devices in AMD water.

4.3.9 PHREEQC modelling software

PHREEQC Interactive Code is a tool used in aquatic chemistry including surface, groundwater, interactions between solids and gaseous phases. It can be used to conduct speciation, reactive transport, inverse and forward modelling (Parkhurst and Wissmeier, 2015). The main application for this study was on speciation modelling. The physico-chemical parameters such as pH, redox potential, conductivity measured in the field were used in the simulation models, together with concentrations obtained from ICP-OES. The Minteq.v4 database was used in all simulations. Figure 4.9 shows a PHREEQC input script.

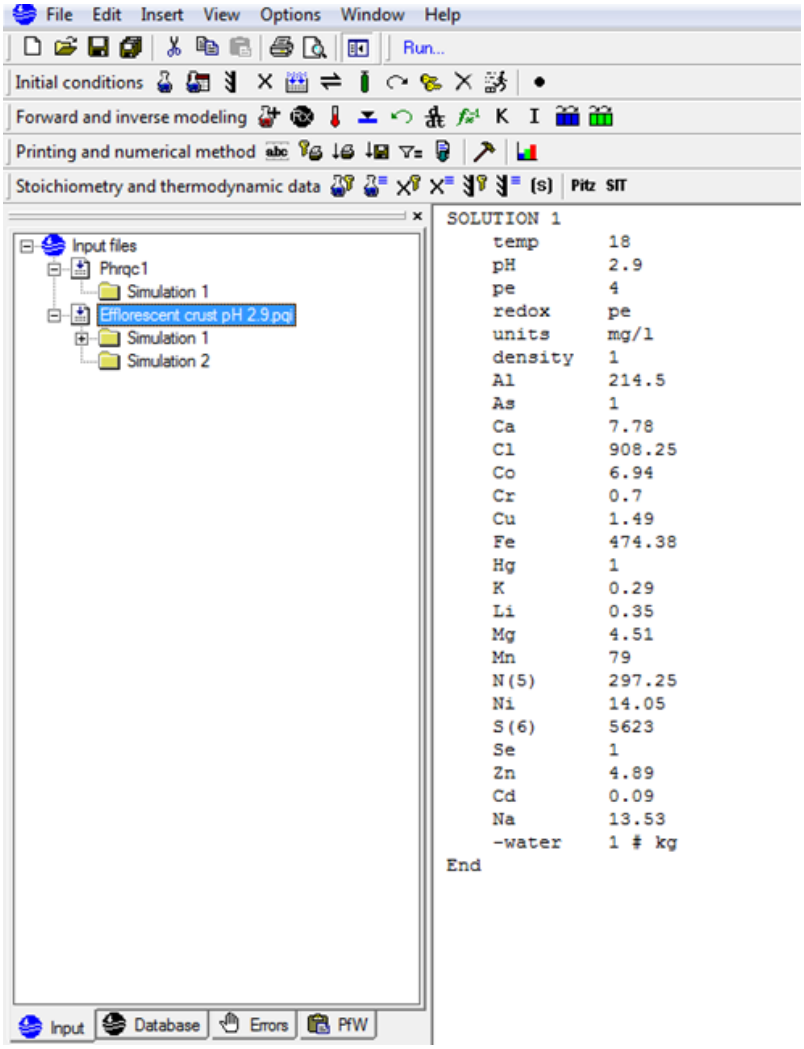


Figure 4.9: PHREEQC input script

Chapter 5: Results and discussion

This chapter describes the findings of this work and how the results relate to the main aim and objective of this work.

5.1 Characterisation of functionalised CPEI

CPEI is a transparent amorphous solid that turns white over time, whereas SCPEI and PCPEI are characteristically orange and dark brown in colour, respectively (Figure 5.1). All three resins are rubbery and extremely sticky in nature. Upon contact with water they swell up, implying that they are also hygroscopic.

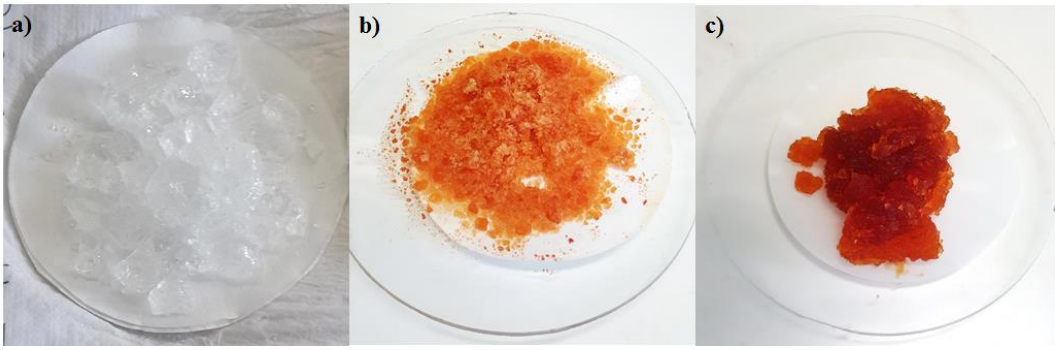


Figure 5.1: a) CPEI b) sulphonated and c) phosphonated CPEI derivatives shortly after synthesis.

5.1.1 FT-IR analysis

Figure 5.2 shows the spectral differences between CPEI, SCPEI and PCPEI. The absorption bands of the relevant functional groups are summarised in Table 5.1. The FT-IR spectrum of CPEI has amine group absorption bands at 3317, 1633 and 1031 cm^{-1}. In addition, there is an alcohol group represented by an absorption band at 1315 cm^{-1}. These main features are in accordance with the structure of CPEI as shown in Figure 2.17. These bands were further compared to those typically obtained for PEI, the building block of CPEI. PEI has a characteristic N-H band between 1559 and 1592 cm^{-1} (Thakur et al. 2017; Ma et al. 2014; Wang et al. 2015) and another N-H band is usually observed between 3100 and 3700 (Wang et al. 2015). In addition, Pang et al. (2011a) also quotes a characteristic C-N band at 1267 cm^{-1} which appeared at 1031 cm^{-1} in CPEI. The absorption bands obtained for PEI and CPEI are in agreement with each other.

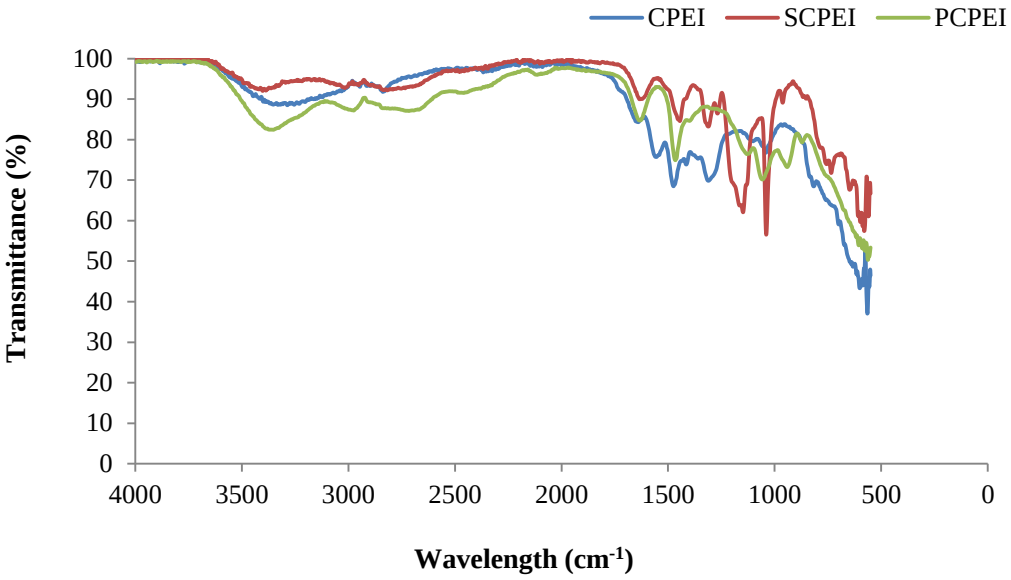


Figure 5.2: FT-IR spectra of CPEI, sulfonated CPEI, phosphonated CPEI.

Table 5.1: Description of the absorption bands observed in Figure 5.3

Wavenumber (cm^{-1})			
CPEI	**SCPEI**	**PCPEI**	**Bond and functional group**
3317	3408	3371	N-H stretch; 1°, 2° amines and amides
1633	1670	1627	N-H bend, 1° amine
1550	-	-	N-O asymmetric stretch, nitro compound
1473	1423	1465	N-O asymmetric stretch
1315	1315	-	C-O stretch alcohols
-	1147	-	CH_2X where X = (SO_3)
1031	1039	1066	C-N aliphatic amine
-	-	947	P-OH

Upon functionalisation of CPEI, the absorptions bands for the primary, secondary and tertiary amine groups, as well as the N-O asymmetric stretch bond and the C-N bond were retained. There was however, loss of the N-O asymmetric stretch bond at 1550 cm^{-1} in both SCPEI and PCPEI, suggesting that this bond could have a role in functionalisation. The C-O stretch bond at 1315 cm^{-1} found in both CPEI and SCPEI spectra was not observed in the PCPEI. Furthermore, SCPEI has an absorption band at 1147 cm^{-1} (CH_2X) which is not present in either CPEI or PCPEI. This band most likely represents the (CH_2-SO_3H) of the sulphonyl group. Similarly, PCPEI has a band at 947 cm^{-1} which is not present in the CPEI and

SCPEI spectra. This band corresponds to the one obtained by Saad et al. (2013a) for the phosphate group in PCPEI.

Shifts in absorption bands of PEI as a result of functionalisation have been documented in previous studies: Ma et al. (2014) showed that modification of PEI with biochar resulted in a shift of the N-H stretch band from 1559 to 3398 cm^{-1}. When Mady et al. (2011) studied the interaction between DNA and PEI, a phosphate absorption band was observed at 1236 cm^{-1}. Conversely, in Table 5.1, the absorption band related to the phosphate group was observed at a lower frequency. This could be attributed to the fact that the phosphate groups are in different environments; Mady et al. (2011) studied the phosphate groups that may have belonged to DNA whereas in the current study they are attached to a CPEI backbone. Based on the distinct differences in the spectra of CPEI, SCPEI and PCPEI, it can be assumed that functionalisation of CPEI was successful.

5.1.2 Solid state NMR

^{13}C solid state NMR was used instead of solution NMR for structural analysis because CPEI, SCPEI and PCPEI are insoluble in most solvents. The ^{13}C NMR spectra of SCPEI and PCPEI are shown in Figure 5.3a. The spectrum for SCPEI appears broad and unresolved suggesting a more amorphous structure whereas the sharper lines observed in the PCPEI spectrum suggests a less amorphous, slightly crystalline structure. In addition, there is a strong correlation between the predicted chemical shifts (Figure 5.3b) and actual measurements: SCPEI shows a unique peak near 30 ppm (peak 2), according to the prediction software this peak belongs to ^{18} C and ^{21}C, which are in close proximity to the sulphonyl groups. Shielding by the sulphonyl groups causes the peak to appear at a lower chemical shift. The obvious differences between the two spectra suggest two different functional groups; ($–SO_3H$) and ($–PO_4^{-2}$). To further validate this notion it would have been ideal to assess PCPEI using ^{31}P solid state NMR.

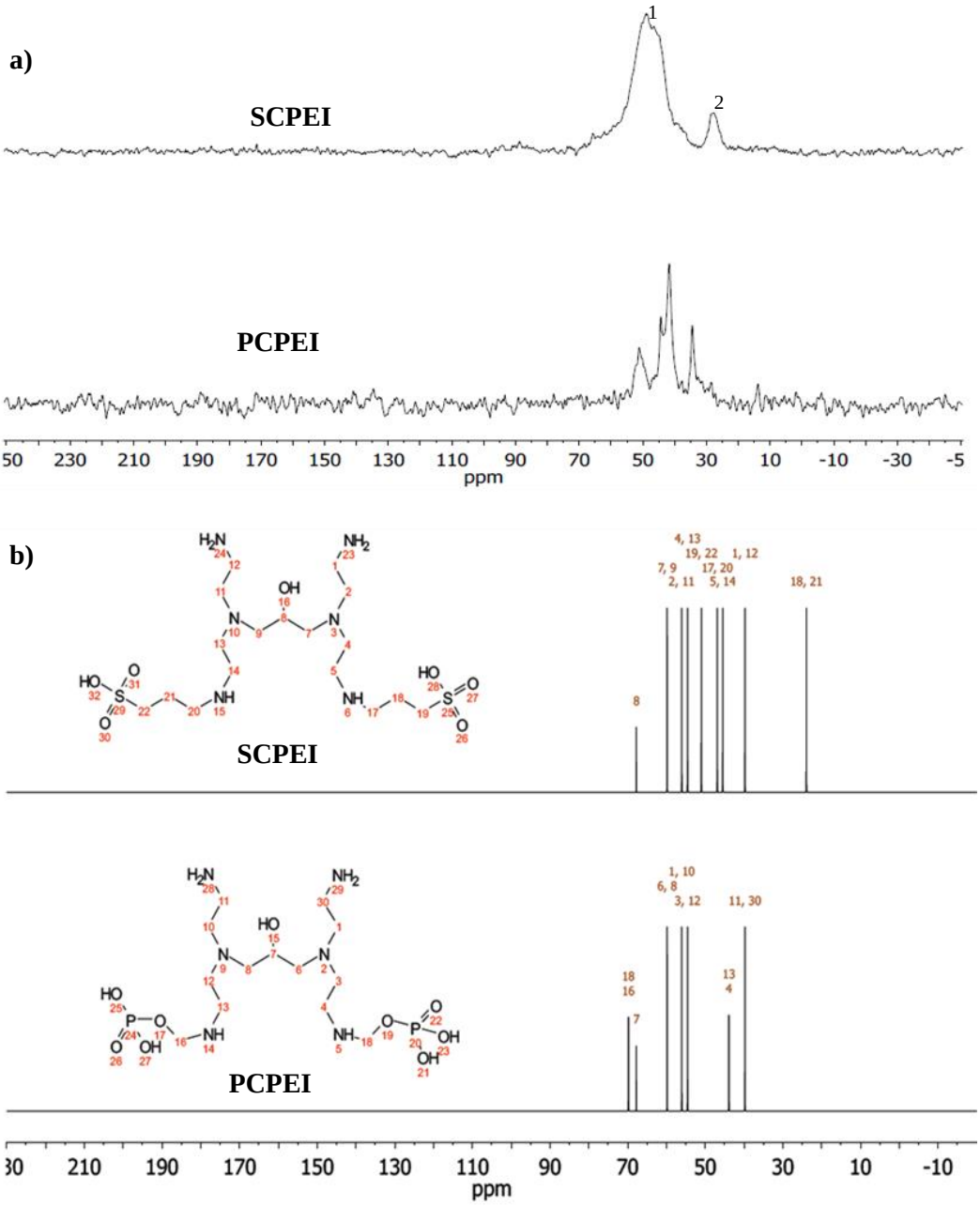


Figure 5.3: a) ^{13}C solid state NMR spectra for SCPEI and PCPEI b) the predicted chemical structures and spectra of SCPEI and PCPEI.

5.1.3 CHNS analysis

Elemental analysis of CPEI, SCPEI and PCPEI shows that CPEI has the highest percentage of carbon (32.8%), hydrogen (8.16%) and nitrogen (14.6%) compared

to SCPEI and PCPEI (Table 5.2). According to the polymeric structure of CPEI (Figure 2.17) this is correct. Alternatively, SCPEI had the highest sulphur content due to the incorporation of the sulphonyl functional group. Additionally, the sum of the percentage values were not close to 100% and this could be attributed to poor combustion since the resin is a polymer and not a pure solid.

Table 5.2: Elemental analysis of the polymers

Sample	C (%)	H (%)	N (%)	S (%)
CPEI	32.8	8.16	14.6	0.034
SCPEI	29.5	7.38	11.2	6.47
PCPEI	26.3	7.81	9.87	0.042
SCPEI-PCPEI mixture*	28.2	7.53	10.9	4.66

C = carbon, H = hydrogen, N = nitrogen, S = sulphur

** Mixture is a combination of SCPEI and PCPEI in an 80% to 20% ratio*

5.2 Batch studies

5.2.1 Uptake factors of different SCPEI and PCPEI resin mixtures

Batch studies were performed using different ratios of the sulphonated and phosphonated resins for the simultaneous uptake of arsenic, selenium and mercury. According to Figure 5.4, at pH 3 the mixture with the higher sulphonated resin component (80% SCPEI : 20% PCPEI) resulted with high mercury uptake and lower uptake for arsenic and selenium. Alternatively, increasing the ratio of the phosphonated resin by using 20% SCPEI : 80% PCPEI, the uptake factor of arsenic was higher compared to selenium but still lower than mercury. A similar trend was observed at pH 7.

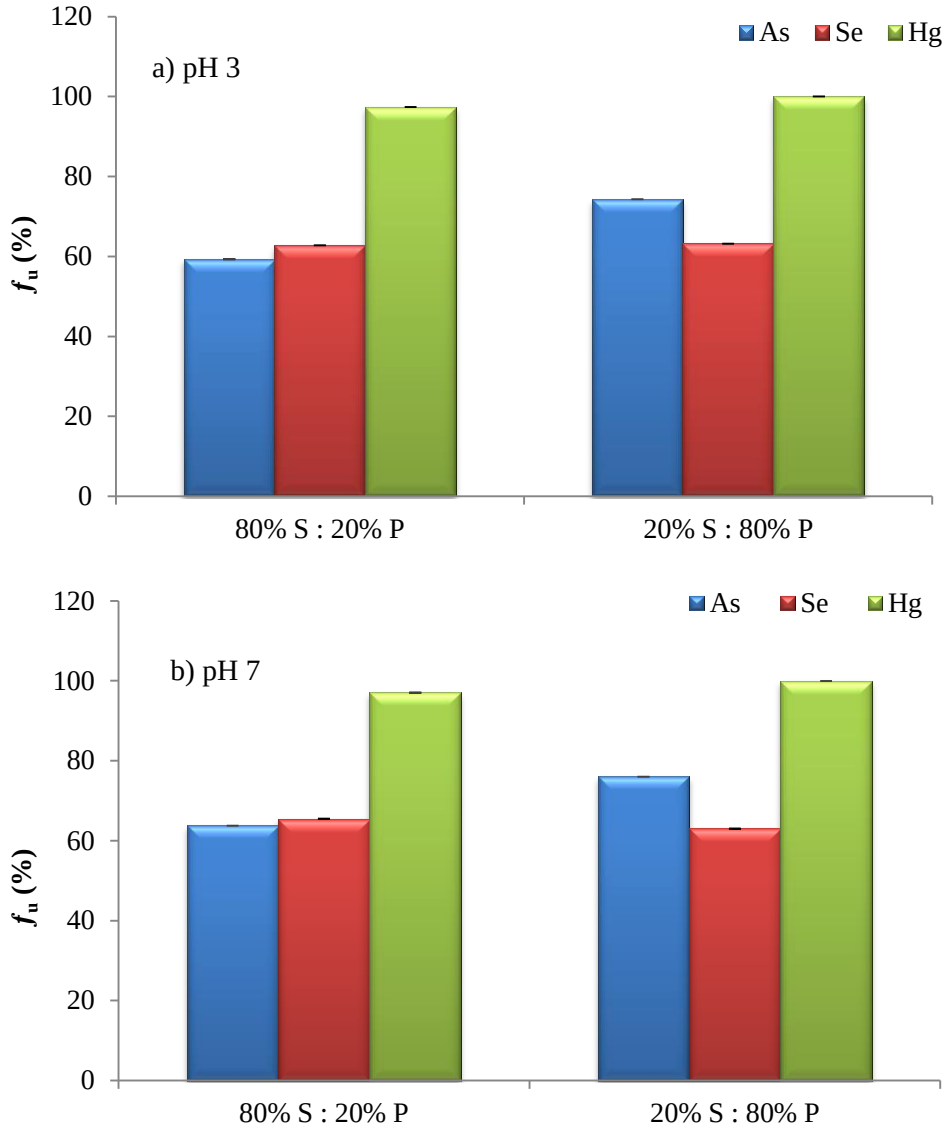


Figure 5.4: The influence of mixing the sulphonated (S) and phosphonated (P) CPEI resins in different ratios on uptake at a) pH 3 and b) pH 7 (n = 3, RSD < 5%).

It is generally accepted that $\%f_u$, values should be greater than 85% for successful DGT (Davison 2016). For example, the f_u for arsenate, arsenite, selenite and selenate with the Ferrihydrite binding layer were 100, > 95, 96.5 and 19.3%, respectively (Bennett et al. 2010). This indicates good adsorption for all arsenic species and selenite by Ferrihydrite. According to Figure 5.4, success was attained for mercury because 100% adsorption was achieved whereas arsenic was between

60 and 75%. Selenium seemed unaffected by the different proportions of SCPEI and PCPEI in the resin mixture. The lack of notable differences between results obtained from 80% SCPEI : 20% PCPEI and 20% SCPEI : 80% PCPEI for all three elements did not warrant further investigate into other ratios.

Saad et al. (2012, 2013a; 2013b) showed that the Freundlich isotherm best described the data on the adsorption of arsenic on PCPEI as well as selenium and mercury on SCPEI. Data obtained from their thermodynamic studies further suggested that all three elements adsorbed on a heterogenous surface via chemisorption. Furthermore, as previously pointed out by Saad et al. (2012b), the adsorption of mercury by SCPEI is based on the hard-soft Lewis acid-base theory whereby Hg^{2+} acts as a Lewis acid and the sulphur in the sulphonyl group as a Lewis base (Figure 5.5a). On the other hand arsenic and selenium are adsorbed via an anion exchange mechanism with the phosphate and sulphonyl groups, respectively, as shown in Figure 5.5b and 5.5c (Saad et al. 2013a; 2013b).

These different modes of adsorption could possibly impact the ease by which uptakes takes place. It is possible that the complexation of mercury to the sulphonyl group takes place first. This means that the anion replacement of selenium may not take place as effectively, affecting its adsorption. Conversely, arsenic is not competing for any binding sites but could be subjected to steric hindrance.

Mason et al. (2005) suggested that one of the drawbacks of using mixed binding layers is uneven distribution of the binding sites. This could result in some analytes having to travel further to reach their binding sites, than they would in a single resin binding layer. The combination of SCPEI and PCPEI enhanced the selectivity towards arsenic, selenium and mercury. Moreover, the addition of PCPEI did not significantly compromise the capacity of SCPEI for selenium and mercury. Batch studies using PCPEI resin alone were not performed since it would only target arsenic.

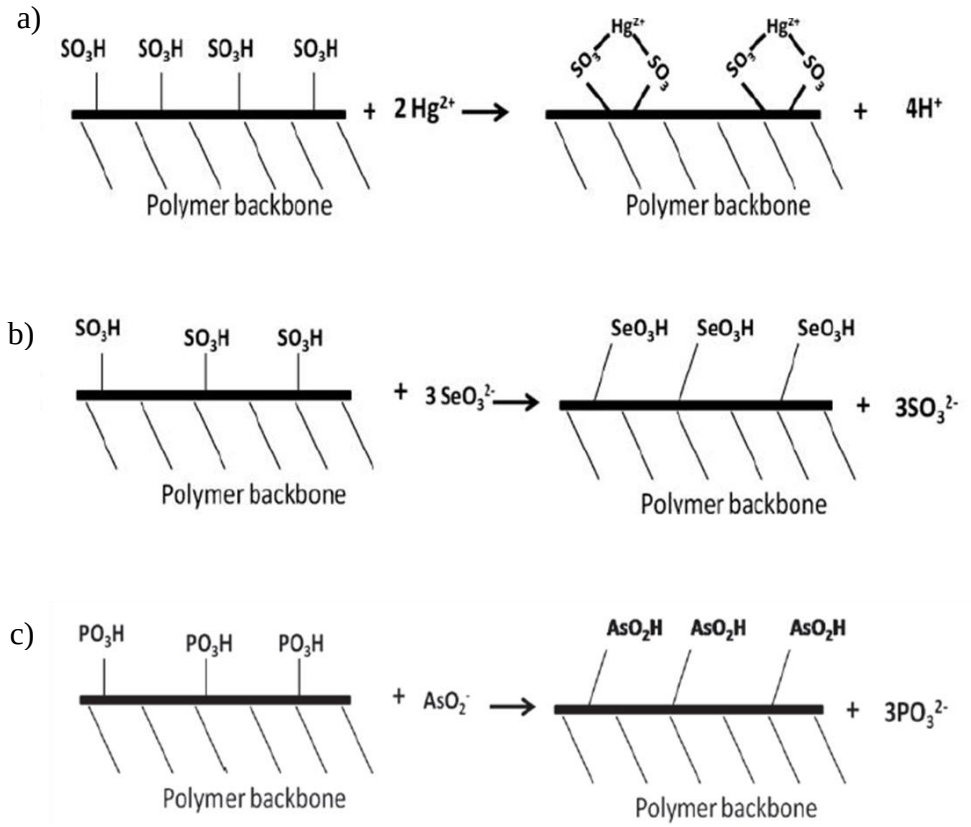


Figure 5.5: The different modes of adsorption by the SCPEI and PCPEI polymers as hypothesised by Saad et al. (2013a; 2013b). a) Mercury forms a complex with the sulphur in the SO_3^{2-} group and b) the selenium anion replaces the SO_3^{2-} group in SCPEI, c) arsenic replaces the phosphate group during adsorption.

5.2.2 Elution factor (f_e)

Saad et al. (2011) recommended nitric acid as the best eluent for CPEI, SCPEI and PCPEI. This recommendation was based on the individual resins and not their combination. The extraction of arsenic, selenium and mercury from SCPEI-PCPEI using 5 and 7 mol L^{-1} resulted in the lowest $\%f_e$ values for selenium compared to the values obtained for arsenic and mercury (Figure 5.6). The extraction of arsenic and mercury using both 5 and 7 mol L^{-1} nitric acid was highly effective. For selenium, 5 mol L^{-1} produced better results compared to 7 mol L^{-1}, an observation also made by Saad et al. (2011). Either concentration of

nitric acid could not be considered a suitable eluent since all 3 elements were not effectively removed from the resin mixture.

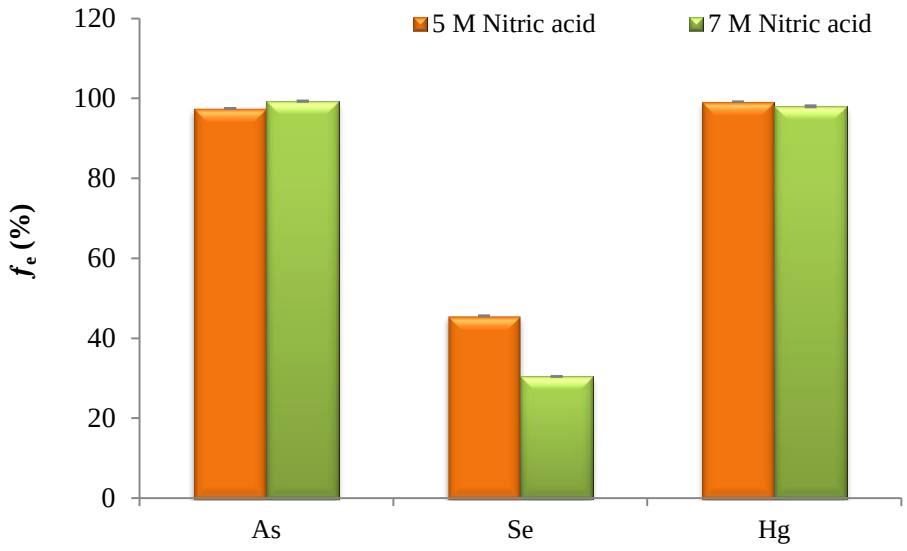


Figure 5.6: The elution factors of arsenic, selenium and mercury using 5 and 7 mol L^{-1} of nitric acid (n = 3, RSD < 5%).

Other eluents were explored at lower concentrations (Figure 5.7). The best eluent for mercury was thiourea, at both 0.25 and 0.5 mol L^{-1}. Arsenic was best extracted using 0.25 mol L^{-1} of thiourea and phosphoric acid. This is justified considering the association arsenic has with sulphur and phosphate groups. Extraction of selenium was generally low, particularly with thiourea. Thiourea is a frequently used spot test reagent for the determination of selenium. It reduces SeO_3^{2-} anion to Se^0 (Gopalan 2009). Se^0 is generally characterised as being insoluble, implying that some of the selenium could have been lost during filtration, prior to analysis of the samples. This could be the likely cause of the reduced extraction efficiency. Moreover, 0.25 mol L^{-1} sulphuric acid produced slightly higher elution for arsenic and selenium compared to 0.5 mol L^{-1}. The expectation was that higher elution would be obtained with increasing eluent concentration. Results obtained from 0.5 mol L^{-1} therefore deviate from this possible trend, which could simply be a

consequence of experimental error. Overall, these eluents showed potential but were still not effective enough for the removal of all three target elements.

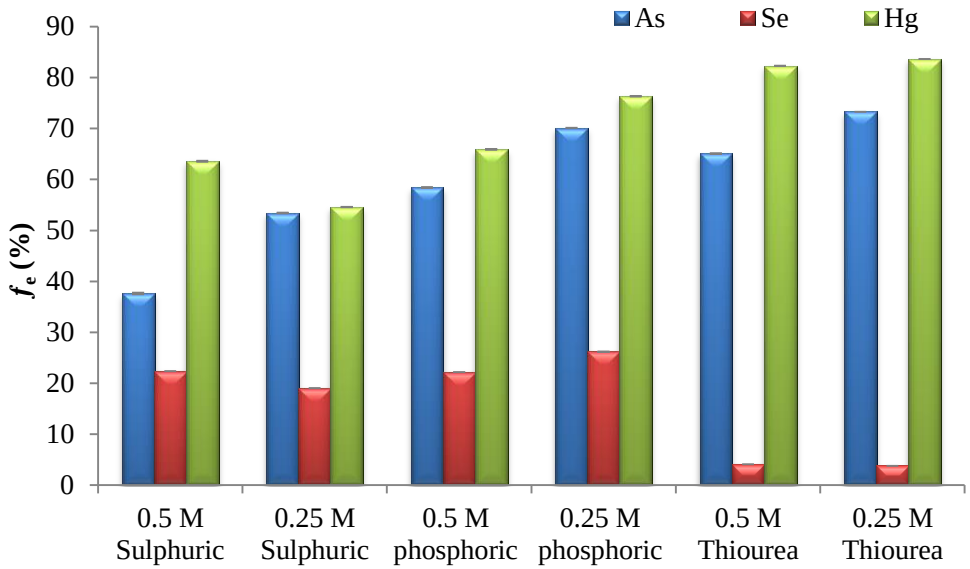


Figure 5.7: Extraction efficiencies of arsenic, selenium and mercury using different eluents at different concentrations (n = 3, RSD < 5%).

Following the results shown in Figure 5.7, using the same eluents, 1 mol L^{-1} concentration was considered (Figure 5.8). At this concentration better results were obtained, particularly for selenium. Sulphuric and phosphoric acid produced $\%f_e$ values higher than 80% for both arsenic and selenium compared to the other eluents. At this concentration, nitric acid could also be considered a good eluent but less effective. Thiourea, hydrochloric acid and sodium hydroxide were the least favourable at eluting selenium. Sodium hydroxide was previously successful at eluting arsenic and selenium from titanium dioxide based DGT with high efficiency (Bennett et al. 2010). This just shows that the selection of eluent is also dependent on the adsorbent. Elution factors for mercury were not determined as

the ICP-MS was not available due to breakdown. However, based on previous results, elution efficiencies higher the 80% are expected.

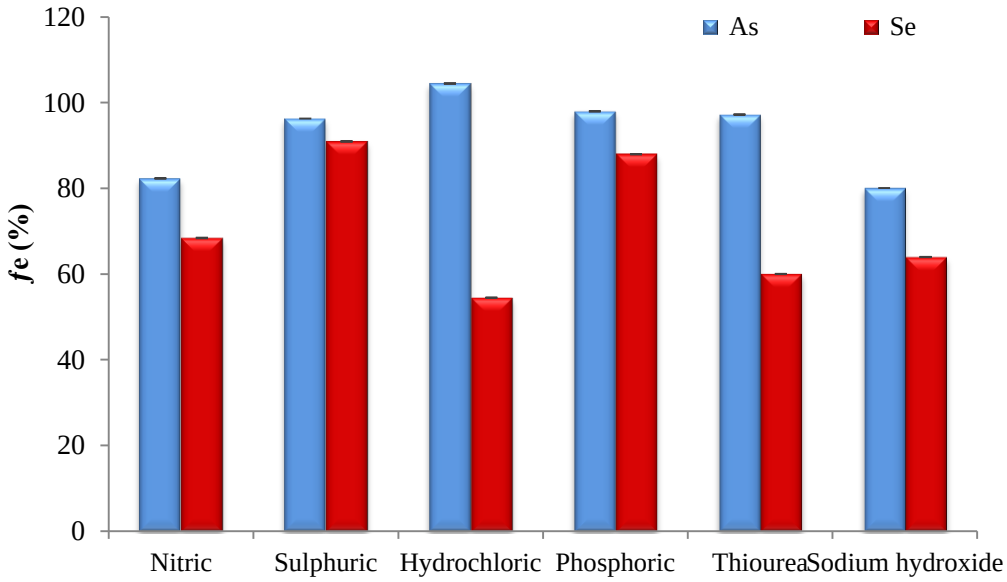


Figure 5.8: The elution factors of arsenic and selenium obtained using 1 mol L^{-1} of different eluents (n = 3, RSD < 5%).

In the current study 20 mL was used as the elution volume instead of 1 mL commonly used during the extraction of the resin layer (Zhang and Davison 1995; Devillers et al. 2017). Devillers et al. (2017) showed that higher f_e values were obtained when higher elution volumes were used. This is because they eliminate errors usually associated with smaller elution volumes. This is especially true if the concentration of the extraction solvent is low. Higher volumes could however, dilute the analytes, which could be a problem for analytes in very low concentrations.

5.3 Design and manufacture of DGT sample holders

DGT sample holders were designed and manufactured from PTFE rods according to the dimensions specified for commercial DGT. The cap in commercial DGT is

disposable; to resolve this issue a re-usable cap was designed by introducing groves that would allow removal and replacement of the cap without damage or leakage. Figure 5.9 compares the structural designs of the manufactured DGT sample holder with a commercial DGT holder. All other sampler dimensions were kept similar to commercial DGT. Figure 5.9d to f shows the slit in commercial DGT cap where a screwdriver is inserted during the retrieval of the resin gel.

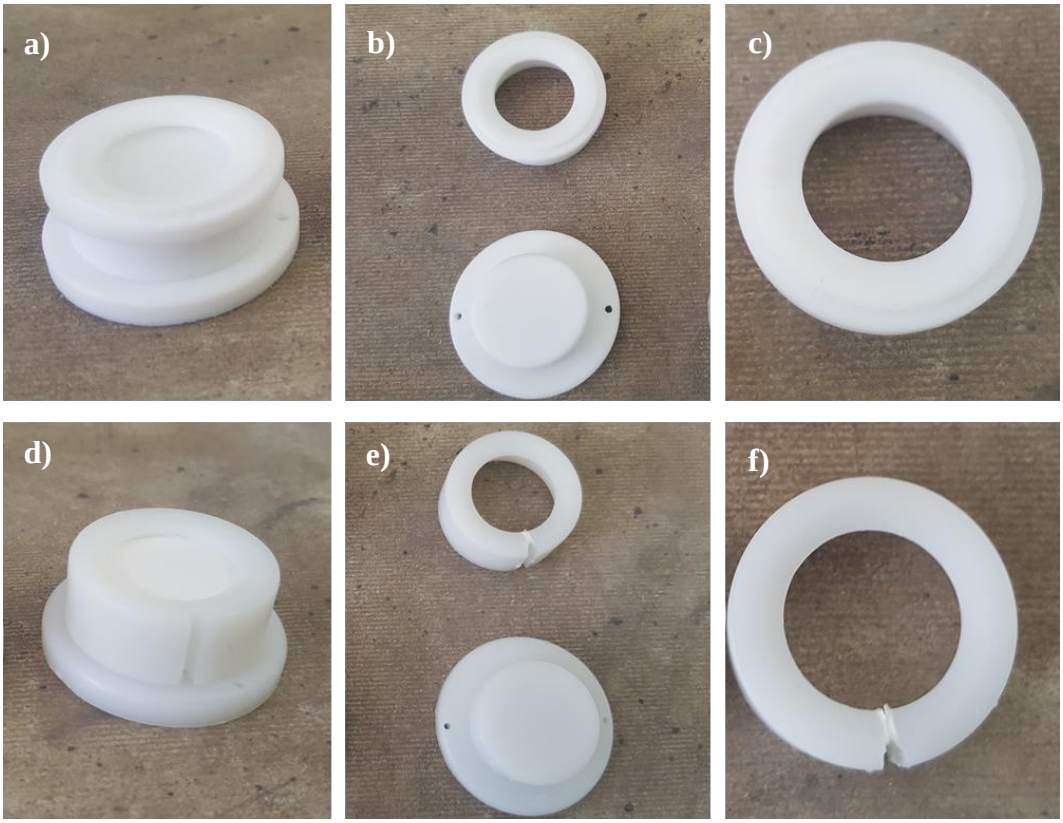


Figure 5.9: a) fully assembled unit of the new DGT sample holder, b) the modified DGT cap and the piston base c) close-up of the modified DGT cap with groves. d) fully assembled commercial DGT sample holder unit, e) the commercial DGT and piston base, f) close up of commercial DGT cap.

One of the main attributes of commercial DGT sample holders is their ability to have a water-tight seal that ensures analytes only enter through the sampling window. In a similar manner, the design of this new DGT cap maintained a water-

tight seal. Entry into the passive sampler was therefore exclusively via the DGT cap window.

Ding et al. (2016) also designed new DGT sample holders. For sample holders that had a similar configuration to commercial DGT, they did not carry out any performance tests because they assumed that the behaviour would be the same. Similarly, for this study, the addition of groves on the cap was not expected to have any major implications on DGT uptake trends. However, because a new resin was used calibration studies were performed.

5.4 Calibration of DGT passive sampler

5.4.1 Effect of SCPEI as DGT binding layer

SCPEI was initially considered as the exclusive resin for DGT, however, results showed better selectivity towards selenium and poor selectivity for arsenic and mercury (Figure 5.10). Although the amount of selenium increased with time, the uptake trend deviated from linearity. The amount of arsenic accumulated was low but showed a linear trend (Figure 5.10a). Conversely, mercury did not display any mass increase with deployment time (Figure 5.10c).

The results for mercury indicate low adsorption and retention. In their batch studies Saad et al. (2012b) demonstrated strong selectivity of SCPEI sulphonyl group for mercury. In the presence of selenium, the sulphonyl groups are replaced with the selenite anion. Mercury has been shown to bind selenium with high affinity (Berry and Ralston 2008; Dyrssen and Wedborg 1991); therefore the replacement of the sulphonyl group with selenite in SCPEI is not expected to affect the binding of mercury. Arsenic does seem to bind SCPEI however, the mass adsorbed was low. Alternatively, Saad et al. (2013 a) recommends PCPEI as the best option for arsenic. Subsequent experiments therefore involved a combination of SCPEI and PCPEI.

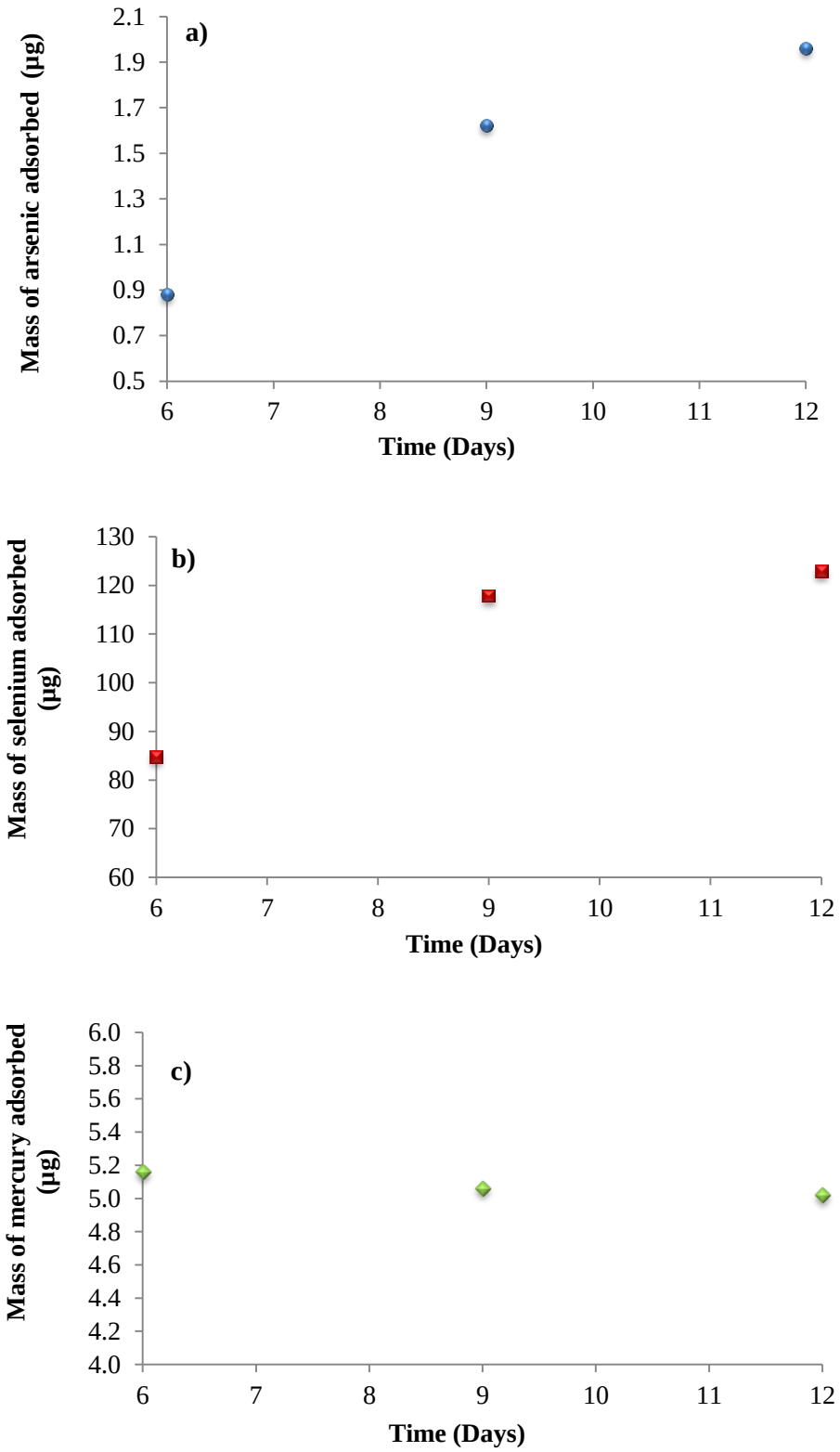


Figure 5.10: Preliminary study showing the mass accumulated for a) arsenic b) selenium and c) mercury by SCPEI-based DGT.

5.4.2 Effect of SCPEI - PCPEI resin mixture dispersed in agarose gel

Dispersing the SCPEI-PCPEI resin mixture in agarose reduced the capacity for arsenic and selenium beyond day 9 (Figure 5.11). Initially, between day 3 and day 9 the mass of arsenic and selenium increased linearly. After day 9 both arsenic and selenium began to decline, implying that the analytes were moving out of the passive sampler. Mercury results are not available due to the breakdown of ICP-MS used for its analysis.

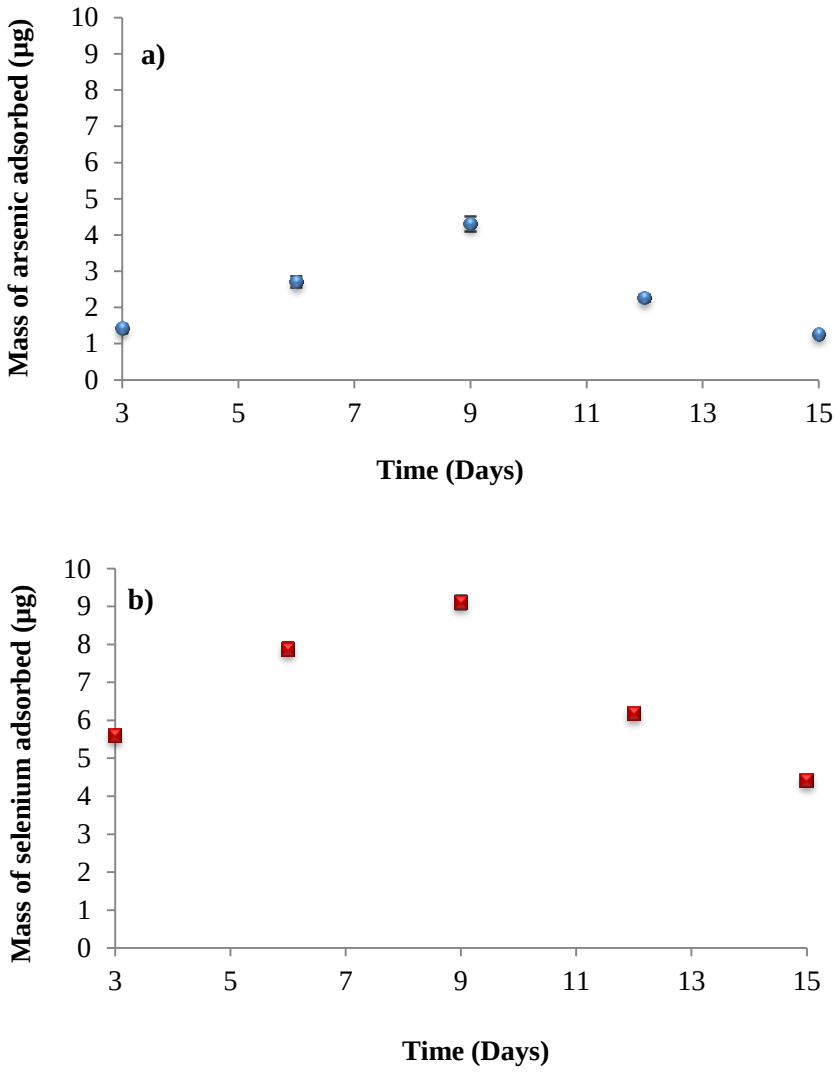


Figure 5.11: Accumulation of a) arsenic and b) selenium in SCPEI-PCPEI resin mixture embedded in agarose gel (n = 3, RSD < 10 %).

According to the principles of passive sampling (Figure 2.8), when a passive sampler has reached maximum capacity it attains equilibrium with the surrounding medium. The trends in Figure 5.11 are therefore unusual.

Uptake of DGT requires rapid adsorption in order to maintain zero analyte concentration on the resin surface. This can only happen if the binding layer has high affinity and capacity for its target analytes. Once bound the target molecules should be able to diffuse to the rest of the resin. Zero concentration at the resin-diffusive gel interface helps develop and maintain a constant concentration gradient from the bulk solution through the diffusive layer (Zhang and Davison 1995). This means that on day 9, the concentration at the resin-diffusive gel interface had increased due to the reduced rate of analyte adsorption. This caused the concentration gradient to favour the bulk solution instead of the DGT resin, leading to the desorption of arsenic and selenium.

Mongin et al. (2013) further explained that during extended deployment periods, as more binding sites are occupied, the uptake deviates from linearity as the net flux decreases towards equilibrium with the bulk solution. Since equilibrium was not attained, SCPEI-PCPEI resin was not just facing a capacity issue but reduced affinity for arsenic and selenium as well. The assumption is that the agarose gel obstructed some of the adsorption sites on the SCPEI-PCPEI resin mixture, since it was not in the loose polymer form.

Furthermore, when SCPEI-PCPEI resin is exposed to water, it physically swells up. As previously pointed out, gels with a high predisposition to swell will have a high proportion of free water (Khare and Peppas 1993; Quinn et al. 1988; Qu et al. 2000; Zhang and Davison 1993). Impregnation in agarose gel seems to restrict the swelling of SCPEI-PCPEI and somehow this affected the extent of adsorption. Sampling units with the resin mixture embedded in agarose are only effective for deployment periods of 9 days or less. Therefore subsequent experiments used the resin in the loose polymer form.

5.4.3 Effect of SCPEI-PCPEI resin mass on DGT capacity

In order for DGT to function in accordance to Equation (2.10) the DGT binding phase has to demonstrate a linear mass accumulation over exposure time (Hutchins et al. 2012). By increasing the resin mass from 0.4 to 0.8 g the linear region extended from 6 days to 15 for both arsenic and selenium (Figure 5.12). No results were obtained for mercury due to the breakdown of the ICP-MS instrument required for analysis. Consequently, 0.8 g of resin was considered optimum as it showed better uptake compared to 0.4 g.

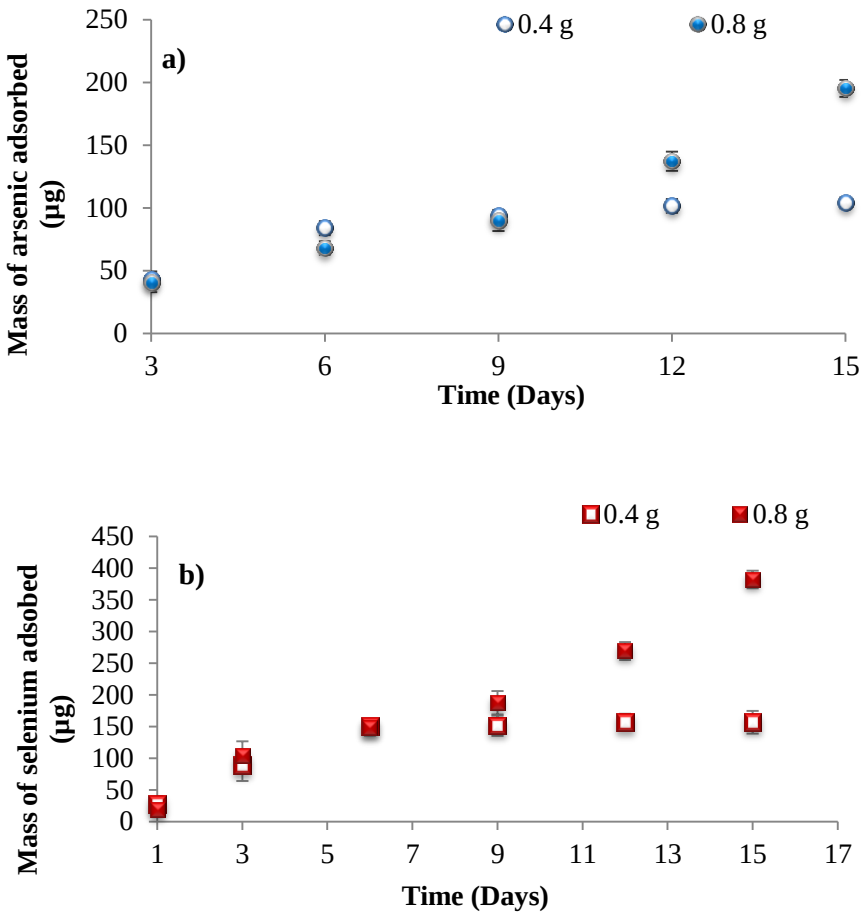


Figure 5.12: The influence of SCPEI-PCPEI resin mass on the capacity of a) arsenic and b) selenium (n = 3, RSD < 10%).

5.4.4 Effect of the diffusive gel in SCPEI-PCPEI based DGT

Fine tuning the sampling rate is a key feature in DGT and all passive samplers because it guarantees longer deployment times and the subsequent determination of TWA concentrations (Namieśnik et al. 2005). A diffusive gel of known thickness will affect the sampling rate, ensuring that transport into DGT is exclusively by molecular diffusion (Davison and Zhang 1994; Zhang and Davison 1995). Results in Figure 5.13 show that the inclusion of a diffusive gel led to a slower uptake rate compared to DGT without a diffusive gel. In the absence of a diffusive gel, DGT approaches equilibrium much faster. It is also apparent that the inclusion or exclusion of the diffusive gel has no bearing on the capacity since the amount accumulated was the same in both cases. These results also highlight the reproducibility of the technique. The results for mercury were not determined due to same reason stated earlier.

Arsenic and selenium generally exist as oxyanions in solution depending on the conditions (Pourbaix diagrams Figure 2.1 and 2.3). Wang et al. (2016) observed that at low ionic strength, the fixed negative charges on agarose are enough to cause weak repulsion of oxyanions. Even if this was the case, in the current study, the extent was not severe since both elements were able to cross the diffusive layer and accumulate within the SCPEI-PCPEI resin.

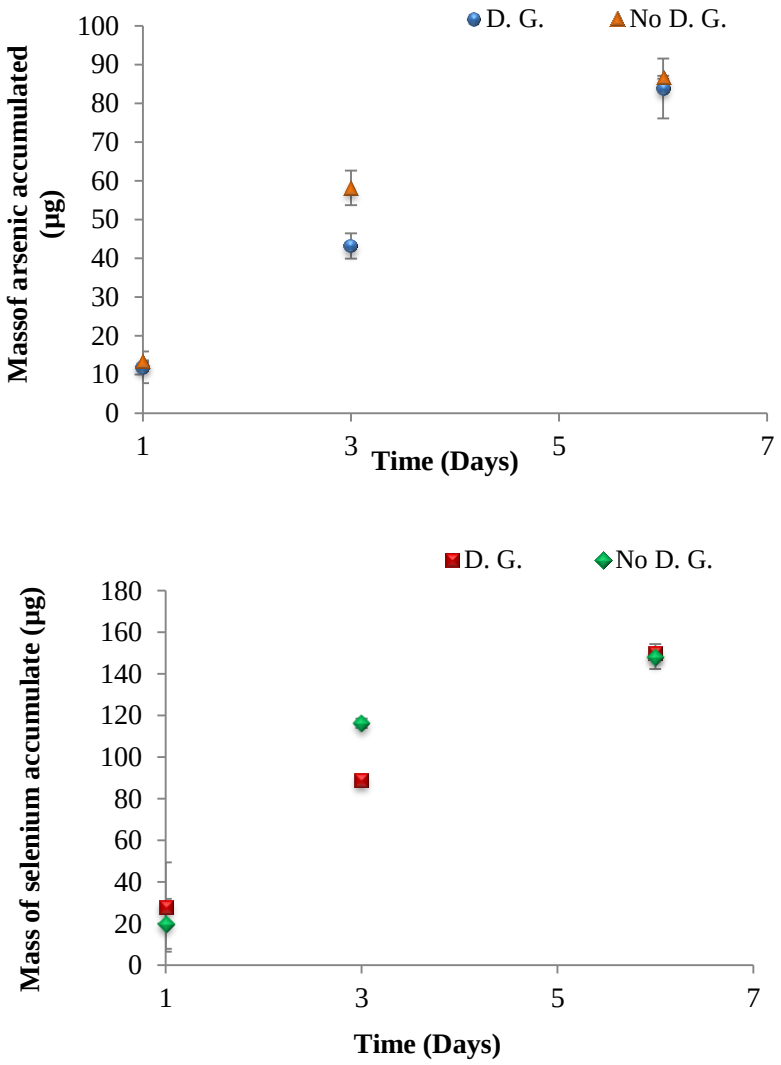


Figure 5.13: The effect of the agarose diffusive gel (D. G.) on the uptake of arsenic and selenium using 0.4 g of SCPEI-PCPEI resin (n = 3, RSD < 10%).

5.4.5 The diffusive gel thickness

It was important to evaluate the optimum thickness range as it would influence the ability of labile species to pass through the diffusive layer. This effect was evaluated by calculating flux at different diffusive gel thickness as shown in Figure 5.14. When the diffusive gel is 0.12 cm, there is a noticeable decrease in the flux for arsenic and selenium. This is because a thicker diffusive gel increases the distance analytes need to travel, subsequently reducing the mass accumulated.

The optimum diffusive gel thickness range was between 0.069 and 0.08 cm for selenium, and 0.069 and 0.1 cm for arsenic.

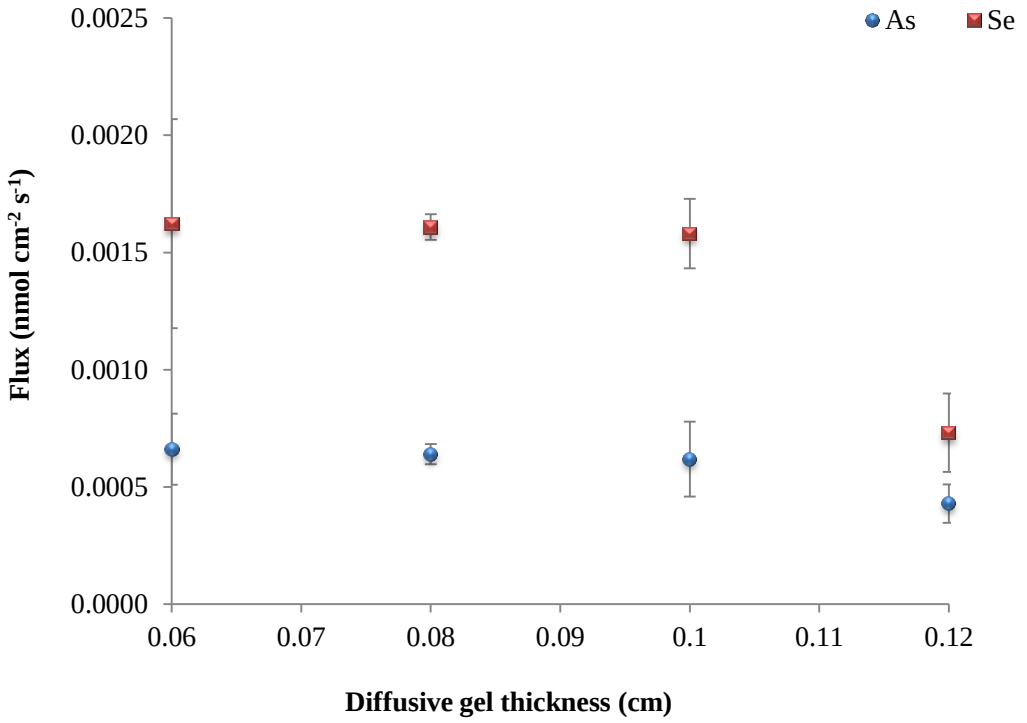


Figure 5.14: The changes in flux as a result of increasing diffusive gel thickness (n = 3).

5.4.6 The effect of turbulence on DGT uptake

Turbulence addresses the molecular dynamics of the solution and how it can affect analyte accumulation, especially in field applications. DGT must be able to operate in both fast moving water bodies such as a river, or in quiescent water at the bottom of a lake, once it is optimised. DGT directly measures a flux, which is dependent on the kinetics of the solution, this allows it to measure labile fractions in solution and not kinetically inert species (Zhang and Davison 1995). Table 5.3 shows how the flux was affected by turbulent and stagnant conditions: in the stirred solutions the flux was higher compared to the stagnant solutions. The effects were more pronounced for selenium compared to arsenic.

Table 5.3 Flux differences between turbulent and stagnant solutions after 6 days of deployment.

Flux for arsenic (nmol $cm^{-2}s^{-1}$)		Flux for selenium (nmol $cm^{-2}s^{-1}$)	
Turbulent	**Stagnant**	**Turbulent**	**Stagnant**
6.76×10^{-4}	3.17×10^{-4}	1.12×10^{-3}	8.51×10^{-4}

The influence of turbulence on the overall performance of DGT with deployment time is shown Figure 5.15. As expected, under stagnant conditions, the rate of mass accumulation was slower. These conditions seemed to encourage a slow and steady increase of arsenic with time, as evidenced by the linear curve. On the other hand solution agitation resulted in faster movement of analytes which would ultimately result in DGT approaching equilibrium by day 6. It should be noted that for this experiment 0.4 g total mass of SCPEI-PCPEI resin was used instead of 0.8 g, which could explain the lower capacity. The trend observed for selenium in both stirred and stagnant solutions was the same: selenium approaches equilibrium after the same number of days irrespective of the fluid dynamics. These results suggest that this passive sampler can operate under stagnant environmental conditions, the slower uptake kinetics imply that it will take longer for the sampler to reach equilibrium. This is particularly important for analytes that exist in trace concentrations.

The mass of selenium accumulated with time is generally higher than arsenic. It is possible that selenium diffuses at a faster rate into the passive sampler compared to arsenic occupying majority of the adsorption sites. This sterically hinders the arsenic from binding effectively. This could also explain why arsenic reached full capacity at a lower mass. The influence of turbulence on accumulation of mercury could not be determined due to the breakdown of the ICP-MS instrument.

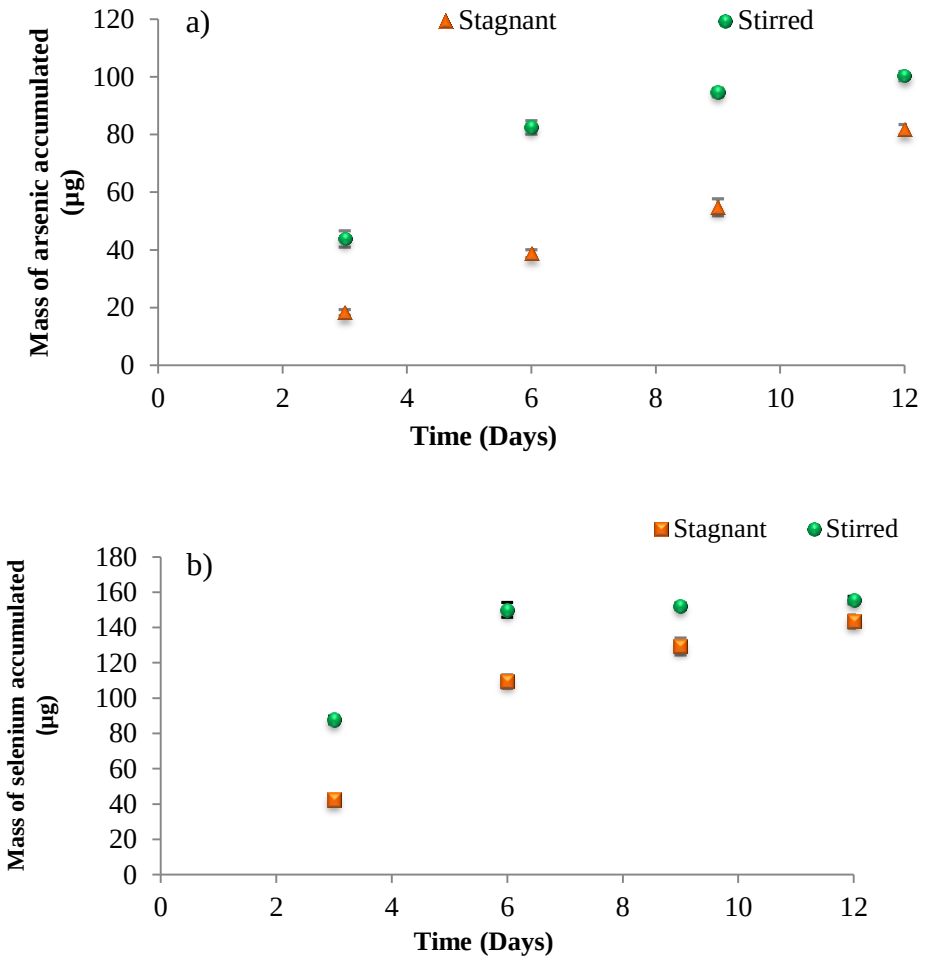


Figure 5.15: The effect of turbulence on mass uptake of a) arsenic and b) selenium (0.4 g of SCPEI-PCPEI; 60 rpm stirring rate; n = 3, RSD < 5%).

5.4.7 The effect of sample concentration on DGT uptake

Operation of DGT relies on the establishment of a concentration gradient between the aqueous solution and DGT resin. When the concentration in the bulk solution is higher, there is a faster rate of diffusion into DGT resin. DGT samplers exposed to solutions containing 1 mg L^{-1} of arsenic and selenium showed a faster response compared to those exposed to lower concentrations (Figure 5.16). Nonetheless, for a kinetic passive sampler, the final amount accumulated at maximum capacity as well as the sampling rates and uptake kinetics should be independent of sample concentration. This allows the optimised passive sampler to be able to estimate

the TWA independent of sample concentration. It seems DGT with SCPEI-PCPEI resin mixture is influenced by sample concentration, especially when deployed in solutions higher than 0.5 mg L^{-1}. For SCPEI-PCPEI based DGT to operate as a kinetic passive sampler, it is best deployed in dilute samples with concentrations of target analytes below 0.5 mg L^{-1}. The influence of sample concentration on mercury accumulation could not be determined due to the breakdown of the ICP-MS instrument.

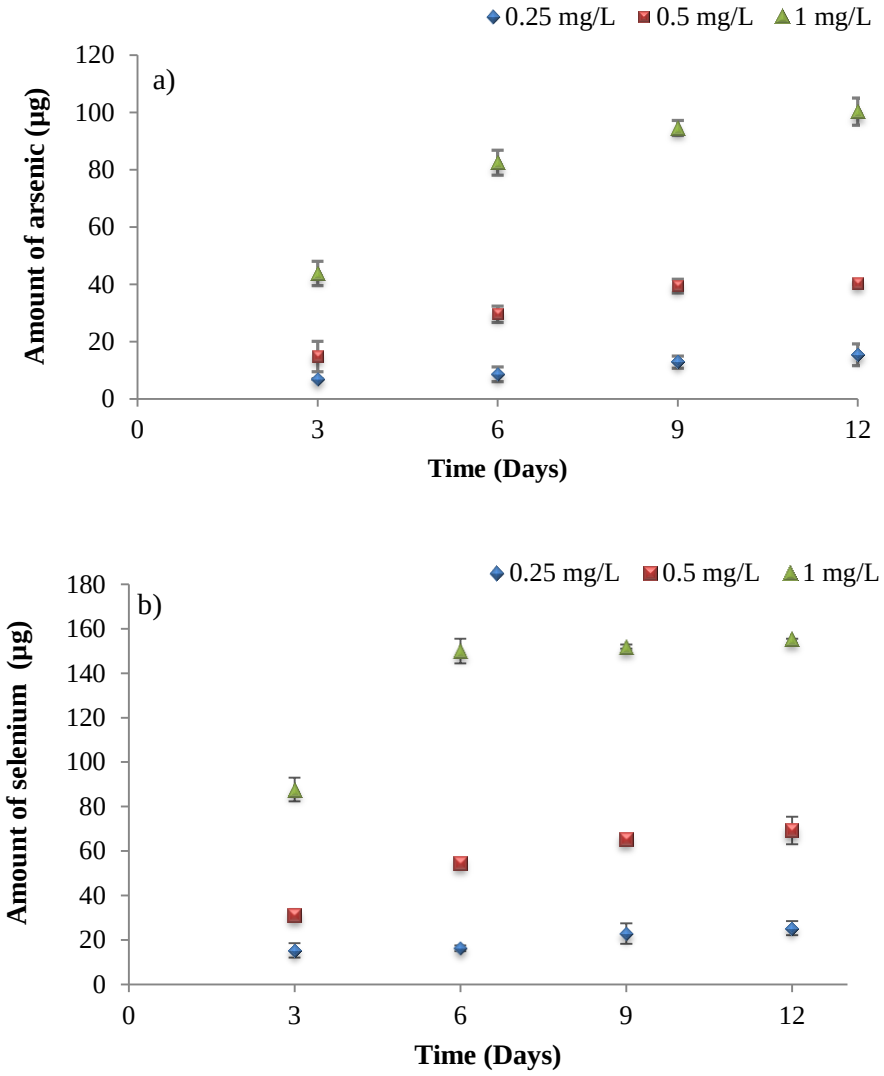


Figure 5.16: The effect of sample solution concentration on uptake of a) arsenic and b) selenium in SCPEI-PCPEI DGT (0.4 g of SCPEI-PCPEI resin; n = 3, RSD < 10%).

5.4.8 The effect of pH on DGT uptake

SCPEI-PCPEI DGT passive samplers were designed for application in AMD and natural water, whose pH is around 3 and 6.5, respectively. Experiments were carried out to study whether the passive sampler's performance would be affected by sample pH (Figure 5.17). At pH 3, arsenic and selenium are accumulated linearly for the 15 day deployment time. On the other hand mercury shows a linear uptake trend for the first 9 days, after which the passive sampler seems to be approaching equilibrium. The plots for arsenic and selenium at pH 5 follow the uptake trend of a typical passive sampler; there is a distinct linear region between day 1 and day 9, after which the passive sampler approaches equilibrium. Upon closer examination, between day 1 and day 9 the slopes of the arsenic and selenium curves at pH 5 appear to be higher compared to the ones obtained at pH 3. This suggests faster accumulation.

Figure 5.17 also shows that the capacity is not significantly affected by pH. The pH does however; seem to affect the rate at which arsenic and selenium are accumulated in the sampler. At pH 3, there is a slow and steady increase of arsenic and selenium in SCPEI-PCPEI DGT. According to Li et al. (2005) and Mongin et al. (2013) this is because at low pH the functional groups in the binding layer are acidic, due to strong competition with protons which reduce the binding strength. At pH 5 the uptake rate is faster (SCPEI-PCPEI DGT reaches equilibrium on day 9) and it can be assumed that this is due to partial protonation of the functional groups as a result of the reduced proton concentration. Partial protonation of arsenic and selenium means a more efficient anion exchange mechanism between SO_3^{2-} and SeO_3^{2-}; and $HAsO_4^{2-}$ with PO_4^{2-} (Saad et al. 2013a; 2013b). SCPEI-PCPEI can operate effectively between pH 3 and 5. Although results for mercury were not obtained at pH 5, it can be assumed that the passive sampler will still accumulate mercury successfully.

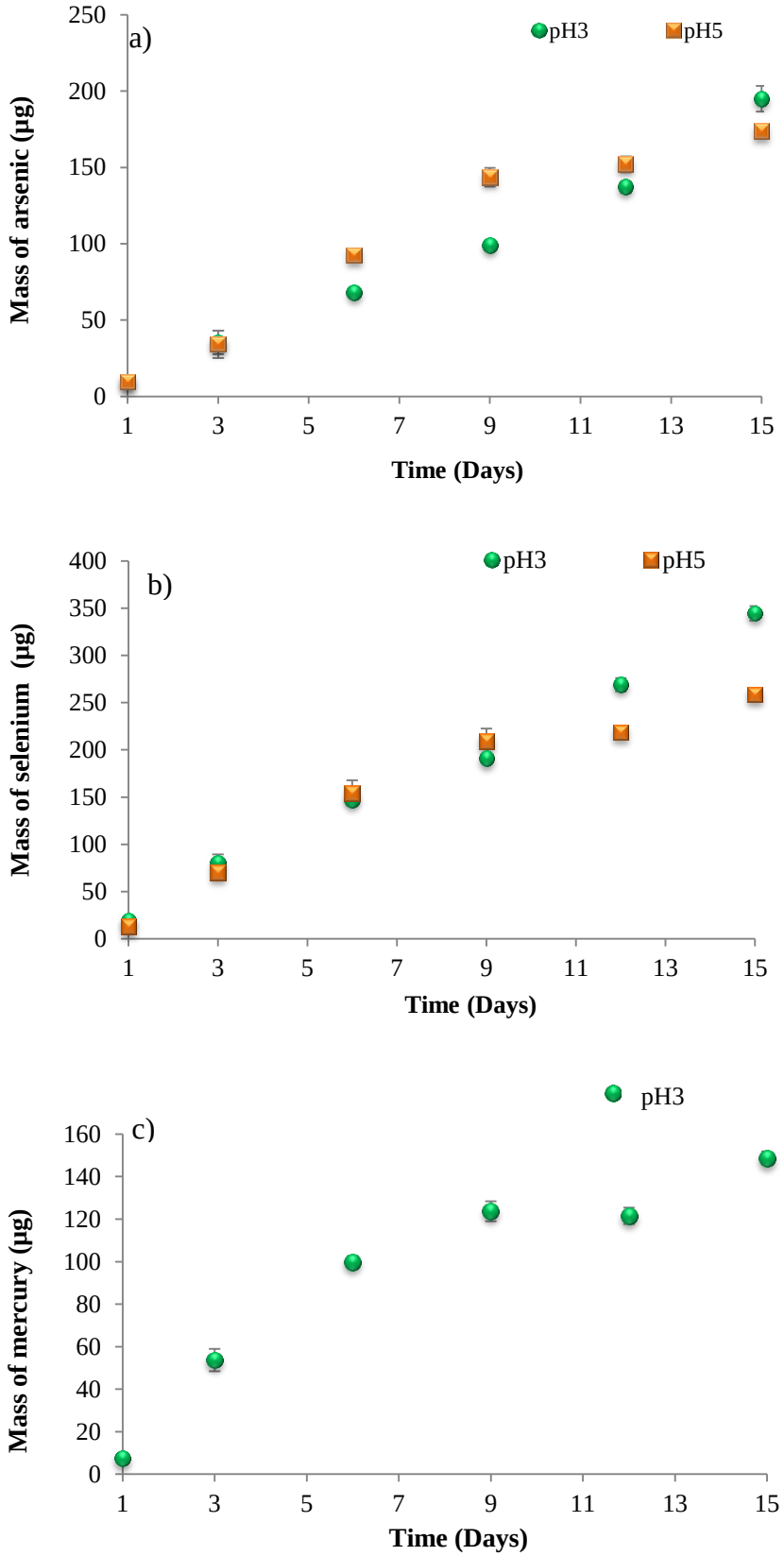


Figure 5.17: Influence of pH on the mass of a) arsenic and b) selenium c) the accumulation of mercury at pH 3 (0.8 g SCPEI-PCPEI resin; n = 3, RSD < 5%).

5.5 Determination of diffusion coefficients and DBL thickness

5.5.1 The diffusion coefficient in agarose gel

The diffusion coefficients of arsenic and selenium at pH 3 were calculated from the slopes of the linear curves in (Figure 5.18). Both arsenic and selenium followed a linear uptake and the mass of selenium was generally higher compared to arsenic. The diffusion coefficient for mercury could not be determined due to instrument breakdown.

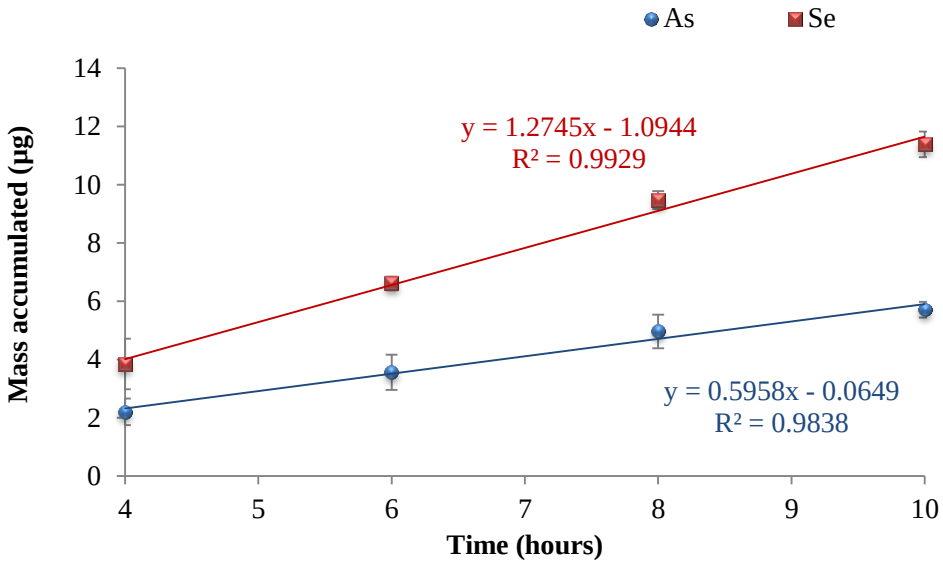


Figure 5.18: Mass of arsenic and selenium accumulated over time. The slopes of these plots were used to calculate the diffusion coefficients in spiked deionised water (n = 3).

Using information obtained from Figure 5.18, the diffusion coefficients were calculated as outlined in Table 5.4. The values of *D* at 22ºC were calculated as 6.41×10^{-5} and 8.29×10^{-5} cm^2 s^{-1} for arsenic and selenium, respectively. These values were compared to those found in literature (Table 5.5).

Table 5.4: Determination of the diffusion coefficient (*D*) from the slope of a linear plot of the mass against time (22ºC)

Equation of line	R^2	Slope (µg hr^{-1})	Slope (µg s^{-1})	Δg (cm)	C_{soln} (mg L^{-1})	C_{soln} (µg cm^{-3})	A (cm^2)	D (cm^2 s^{-1})
y = **0.5958***x* - 0.0649	0.9838	0.88	2144	0.083	0.88	884000	3.14	6.41×10^{-5}
y = **1.2745***x* - 1.0944	0.9929	1.27	4588	0.083	1.46	1463333	3.14	8.29×10^{-5}

Table 5.5: Comparison of arsenic and selenium diffusion coefficients (cm^2 s^{-1})

Method	Hydrogel	As (III)	As (V)	Se (IV)	Se (VI)	References
SCPEI-PCPEI DGT	Agarose	-	6.41×10^{-5}	8.29×10^{-5}	-	Current study
Zr-oxide	Agarose	-	6.56×10^{-6}	-	6.75×10^{-6}	Wang et al. 2016
TiO_2 DGT	APA	10.5×10^{-6}	6.83×10^{-6}	8.91×10^{-6}	*bdl*	Bennett et al. 2010
Mercapto-silica and Ferrihydrite	APA	10.1×10^{-5}	7.09×10^{-6}	-	-	Bennett et al. 2011
Ferrihydrite DGT	APA	-	5.25×10^{-6}	-	5.83×10^{-6}	Luo et al. 2010
Ferrihydrite DGT	APA	1.01×10^{-5}	6.28×10^{-6}	-	-	Moreno-Jiménez et al. 2013
Ferrihydrite DGT	APA	5.3×10^{-6}	4.90×10^{-6}	-	-	Panther et al. 2008
Ferrihydrite DGT	APA	-	-	6.37×10^{-6}	6.28×10^{-6}	Peng et al. 2017
Diffusion in water (D_{water})	-		9.05×10^{-6}		9.46×10^{-6}	Li and Gregory 1974

APA= agarose cross-linked polyacrylamide

"-" No values available for that specie

For SCPEI-PCPEI DGT diffusion coefficients are for total arsenic and selenium since no speciation studies were performed

The diffusion coefficient values reflect the trend that has been observed thus far where the mass of selenium is generally higher than arsenic. Selenium is able to move at a faster rate from the bulk solution through the diffusive gel. This also supports the notion that selenium occupies the adsorption sites first, subsequently hindering arsenic to bind on adjacent sites.

The diffusion coefficients in the current study are an order of magnitude higher than values previously reported in agarose, agarose cross-linked polyacrylamide and in water (Table 5.5). The only exceptions were the values obtained by Moreno-Jiménez et al. (2013) (1.01×10^{-5} cm^2 s^{-1}) and Bennette et al. (2011) (10.05×10^{-5} cm^2 s^{-1}) for arsenite. Although these values are the same order of magnitude, the actual diffusion coefficients vary considerably.

At pH 3 arsenic and selenium both exist as the uncharged species H_3AsO_3 and Se^0, respectively. It has been suggested by Li and Gregory (1974) that molecules with a large hydration layer of water molecules are retarded to a greater extent. The lack of charge could mean a smaller hydration layer as well as little repulsion from the negative agarose surface charges Wang et al. (2016). The pores in 1.5% agarose gels are described as having an open structure, yielding pore sizes greater than 20 nm (Zhang and Davison 1999), resulting in diffusion coefficients similar to those in water (Chramback 1985; Attwood et al.1981). The diffusion coefficients in the current study are however, higher than those obtained in water.

The diffusion rate in SCPEI-PCPEI DGT is also influenced by the filter membrane. Wang et al. (2016) conducted experiments to evaluate the role of the filter membrane on the diffusion of analytes. They found that filter membranes enhanced the diffusion rate, which could be a result of the larger pore size in the filter membrane compared to agarose. In their study, arsenic diffusion rates were improved with the addition of either cellulose nitrate or PES filter membrane (Wang et al. 2016). Alternatively, Scally et al. (2006) showed that the diffusion coefficient in the filter membrane is not statistically different from one in the diffusive gel.

The time series method for determining *D* is often used because the measurement conditions are the same as ones encountered during DGT deployment (Wang et al. 2016; Price et al. 2013; Scally et al. 2006; Shiva et al. 2015). However, it would have been ideal to measure the diffusion coefficient using a diffusion cell for comparative purposes even though the use of diffusion cell is only recommended for quality control purposes (Shiva et al. 2015).

5.5.2 The DBL (δ)

The DBL values were determined from the slopes of the plots shown in Figure 5.19. The equations obtained for these plots were: $y = 0.0427x + 0.0216$ and $y = 0.0063x + 0.0091$ for arsenic and selenium, respectively. The DBL values were calculated as 0.51 cm for arsenic and 1.44 cm for selenium.

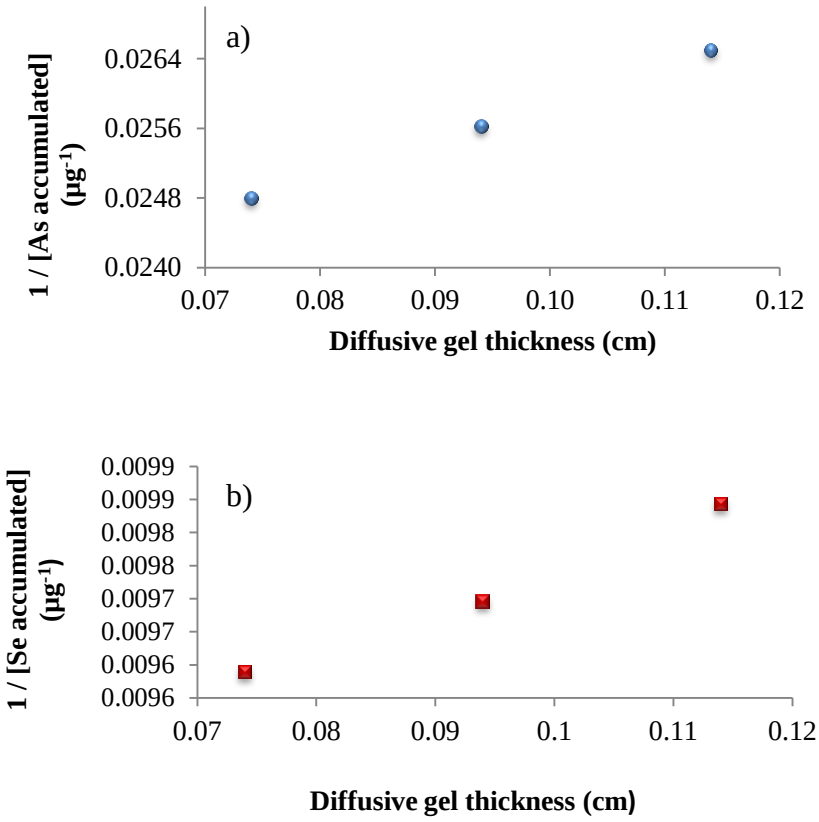


Figure 5.19: The reciprocal mass of a) arsenic and b) selenium accumulated by DGT (μg^{-1}) with varying diffusive layer thickness.

If a plot of 1/mass against Δg is non-linear, then it means a DBL is present and should be considered in calculations (Davison and Zhang 1994; Warnken et al. 2006). On average, the thickness of the filter membrane and diffusive gel combined was 0.092 cm; the DBL values are much higher than this. According to Warnken et al. (2006) this means that the DBL should be considered in the calculation of C_{TWA}. Warnken et al. (2006) studied the effects of stirring rate under laboratory settings on the DBL thickness. The DBL was 0.044 cm for solutions stirred at 60 rpm and 0.150 cm under stagnant solutions.

5.6 Determination of resin blanks and method detection limits

Resin blanks were important for the verification of SCPEI-PCPEI DGT technique. The resin blanks were 0.33± 0.002 µg (17 µg L^{-1}) and 0.32 ± 0.001 µg (16 µg L^{-1}) for arsenic and selenium, respectively. The MDL values which are 3 times the standard deviation of the blanks were 50 µg L^{-1} for arsenic and 48 µg L^{-1} for selenium. The MDL values are very low which means SCPEI-PCPEI DGT is suitable for trace analysis.

5.7 Comparison of DGT resin sorbents and maximum deployment time

In most studies, success has been attained by incorporating resin in a gel solution. It should be noted that some DGT devices prepared in this manner were not deployed for more than 48 hours in the laboratory and 7 days in the field (Table 5.6). This is because some passive samplers are calibrated and better suited for shorter deployment times. These passive samplers are ideal for deployed after recent discharge of pollutants whereby analyte concentrations are high. When the concentration of target analytes is low, longer deployment times are usually required.

Table 5.6: Some examples of how some resin gels were prepared and the maximum number of days the DGT passive samplers were deployed

Target analyte (s)	Composition of resin / binding gel	Maximum deployment period in the laboratory	Maximum deployment in the field	References
Arsenic and selenium	**1 g** titanium dioxide in **10 mL** of gel solution	24 hours	4 days	Bennett et al. (2010)
Nitrate	4 g anion exchange resin (SIR-100-HP) **11 mL** agarose	48 hours	20 hours	Cai et al. (2017)
Illicit drugs	**2 g** XAD18 in **10 mL** agarose gel	24 hours	7 days	Guo et al. (2017)
Mercury	**3 g** of: 1) 3-Mercaptopropyl functionalized SBA-15 2) 3-mercaptopropyl functionalized ethenylene bridged periodic mesoporous organosilica 3) Sumichelate Q10R 4) 3-mercaptopropyl functionalized silica gel 5) Chelex-100 resin Each resin was dissolved in **10 mL** of gel solution	24 hours	2 days	Gao et al. (2011)
Antibiotics	**1g** of either XDA-1, LX-1180, XDA-600, LX-4027, D296, NKA-9, CAD-40 or XAD-18 resin in **10 mL** agarose	12 hours	8 hours	Xie et al. (2017)
Arsenic, selenium and mercury	**0.8 g SCPEI-PCPEI** loose polymer mixture in a 80% SCPEI and 20% PCPEI	15 days	15 days	Current study

5.8 Deployment of optimised SCPEI-PCPEI based DGT in field samples

5.8.1 DGT uptake in laboratory-based experiments using dam water

5.8.1.1 Composition of dam water

The pH and conductivity of Fleurhof Dam water were 6.3 and 0.50 mS cm^{-1}, respectively. The redox potential was 324 mV, implying an oxidising water environment. The anion and metal composition are shown in Table 5.7. The low conductivity of the Fleurhof Dam water correlates with the low concentration of dissolved anions and metals: concentrations of the sulphate and chloride anions were 139 and 19.7 mg L^{-1}, respectively. Sodium and magnesium were the highest metals, with concentrations as high as 138 and 132 mg L^{-1}, respectively. The concentration of iron was 0.143 mg L^{-1}. The concentrations of arsenic and selenium were 0.022 and 0.032 mg L^{-1}, respectively, which correspond with those found in natural water; arsenic is usually between 0.15 and 0.45 µg L^{-1} (Smedley and Kinniburg 2002) and selenium 0.02 µg L^{-1} (Fernández-Martínez and Chalet 2009).

Fleurhof Dam is in close proximity to mine tailings. It has two streams bringing water to the dam. One stream passes near tailing dumps, which feeds AMD into the stream. The second stream comes from a residential area. The streams intersect before entering the dam. Both streams are wetland-based, which helps in retaining most of the pollutants. In addition, at pH 6, majority of metals would have precipitated. This explains why the general concentrations in the dam were low. Concentrations in acidic water tend to be higher due to conditions favouring the release of metals from surrounding rock and sediments.

Table 5.7: Anion and metal composition of water sampled at Fleurhof Dam.

	Concentration (mg L^{-1})
F^-	0.109
Cl^-	19.7
NO_3^-	6.92
SO_4^{2-}	139
Ca	29.6
K	48.0
Mg	132
Na	138
Co	0.077
Cu	2.98
Fe	0.143
Mn	0.532
Ni	0.114
As	0.022
Se	0.032

5.8.1.2 Deployment of DGT in dam water under laboratory conditions

Deployment of the optimised passive sampler in dam water under laboratory conditions was done to study the influence of sample matrix. Two tests using Fleurhof Dam water were carried out. In the first test the water was spiked at 0.5 mg L^{-1} with arsenic, selenium and mercury. In the second test the water collected from Fleurhof Dam was used without spiking.

SCPEI-PCPEI based DGT showed a linear uptake trend for the accumulation of arsenic, selenium and mercury, from spiked Fleurhof Dam water (Figure 5.20a; b and c). On day 9 the accumulation rate had slowed down for arsenic and selenium.

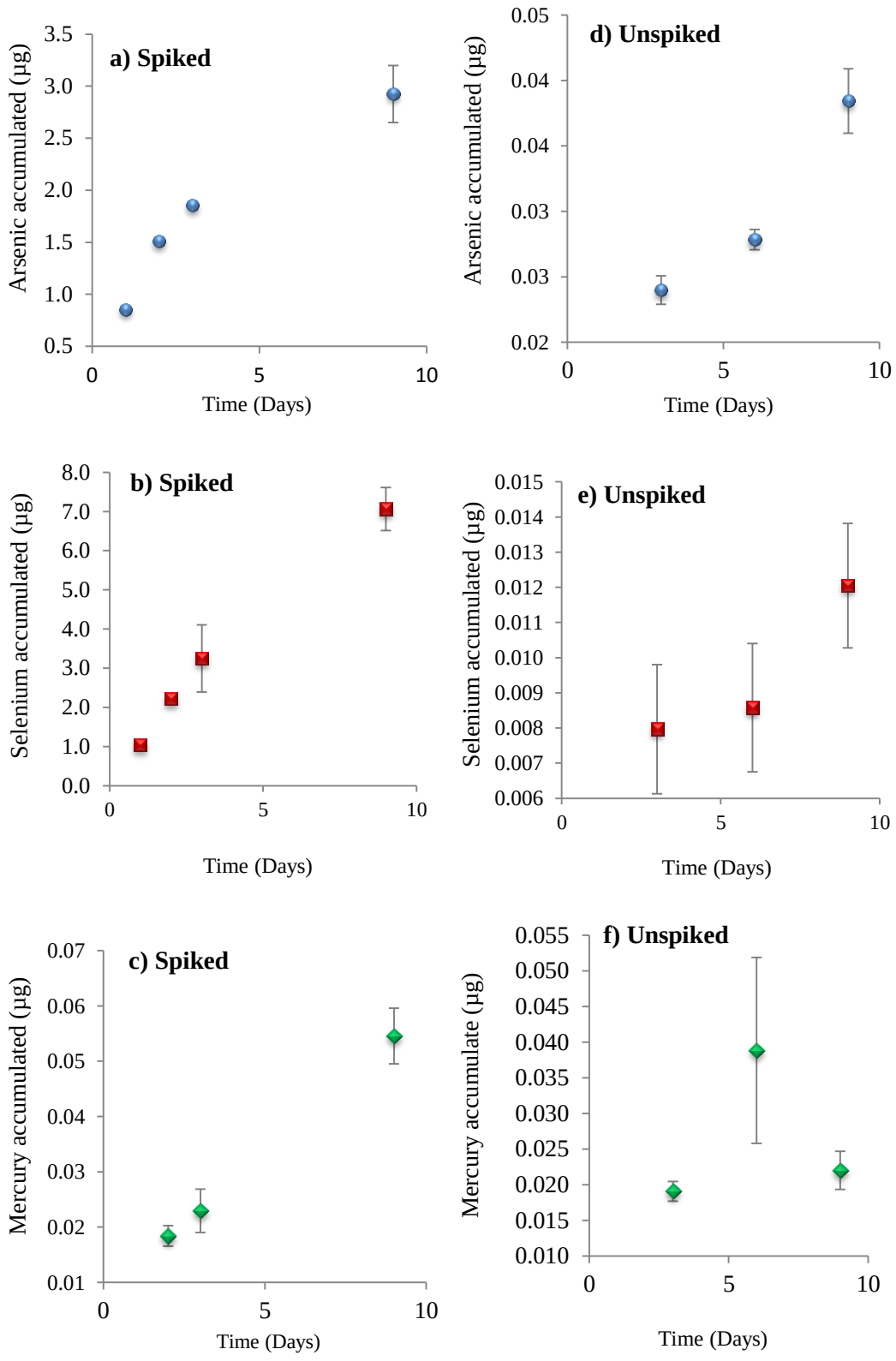


Figure 5.20: Uptake of a) arsenic; b) selenium; c) mercury in spiked and d) arsenic; e) selenium; f) mercury in unspiked dam water.

In un-spiked dam water the passive sampler was able to accumulate arsenic and selenium, even so, the trend deviated from linearity (Figure 5.20d; e). On the other hand, the uptake of mercury was not linear, nor did it increase with time, perhaps due to matrix effects.

The concentration of arsenic, selenium and mercury in the spiked samples were sufficiently high enough to allow an effective concentration gradient to be established. This is why a steady increase in analyte is observed. In the un-spiked sample however, the overall concentrations were generally low, this was compounded by precipitation of the water sample with time. This decreased the concentration of bioavailable analytes in solution.

5.8.1.3 Uptake of other cations from Fleurhof dam water

After deployment in the dam water sample, the passive sampler was also analysed for other metal ions (Figure 5.21). There was no clear uptake trend. This is expected as the passive sampler has capacity issues and these metals exist in relatively high concentrations. The sampler could have attained full capacity within a short space of time.

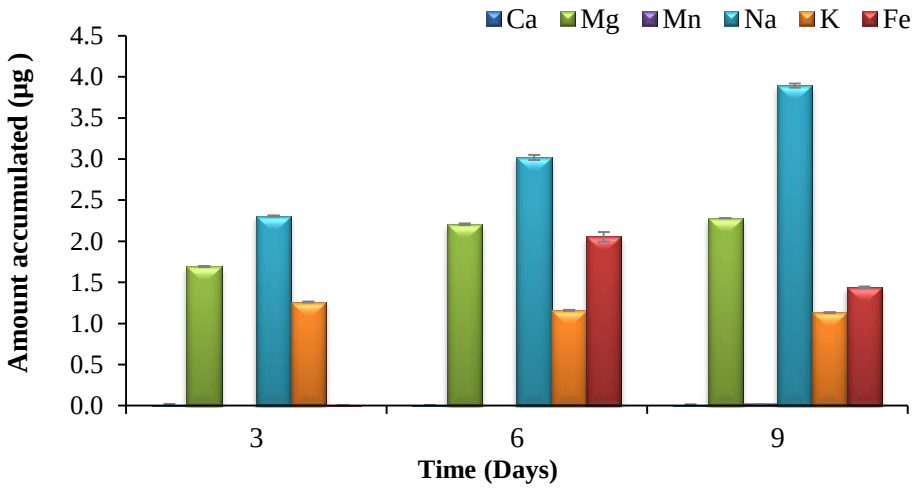


Figure 5.21: Accumulation of background metals by DGT in the laboratory-based experiments using dam water (n = 3, RSD < 5%).

PEI, the primary constituent in CPEI, has a large number of primary and secondary amine groups (Spell 1969), which are effective at adsorbing metals, either through complexation or electrostatic interactions (Pang et al. 2011a; 2011b). The lack of specific binding sites for metals other than the amine groups in PEI means that competition amongst the metal ions is very high. For example, in a study by Saad et al. (2011) CPEI was able to remove chromium, zinc, iron, nickel, manganese and lead from water. Wang and Li (2015) used a PEI-functionalised ion imprinted hydrogel for the selective removal of Cu (II) from water; however, the adsorbent also targeted lead, cadmium and nickel from solution. The lack of selectivity would also explain why metals do not follow the typical uptake trend followed by passive samplers (Figure 2.8).

5.8.1.4 Changes in the physico-chemical properties of dam water

The physico-chemical properties of un-spiked dam water were measured over 12 days and the results are summarised in Table 5.8. Changes in the physico-chemical properties are observed. Most notable is the significant decrease in the pH. Table 5.7 shows that iron was present in the water sample. This iron could have reacted with water in the following way, concomitantly reducing the solution pH:

$$Fe(H_2O)_6^{3+} + H_2O \rightarrow Fe(H_2O)_5OH^{2+} + H_3O^{+} \quad (5.1)$$

The conductivity, redox potential as well as total dissolved solids all seemed to increase with time. The increase in acidity caused any adsorbed metals to desorb, which could have possibly led to the increase in conductivity and total dissolved solids. The concentration of anions remained fairly constant except for nitrates, which seem to increase with the number of days. The increase in redox potential also highlights the increased possibility of nitrogen reacting with oxygen to form nitrates.

Table 5.8: Changes in the physico-chemical properties of dam water with time

Parameters	Day 0	Day 3	Day 5	Day 9	Day 12
pH	6.4	5.7	5.0	3.9	2.4
Conductivity (mS cm^{-1})	0.36	0.39	0.4	0.44	0.99
Total dissolved solids (ppt)	0.16	0.19	0.22	0.3	0.48
Redox potential (mV)	317	325	335	353	385
F^- (mg L^{-1})	0.11	0.09	0.089	0.09	0.082
Cl^- (mg L^{-1})	19.7	20.4	21.3	20.2	20.5
Br^- (mg L^{-1})	0.053	0.059	0.073	0.067	0.06
SO_4^{2-} (mg L^{-1})	139	140	148	142	144
NO_3^- (mg L^{-1})	6.92	21.4	27.4	21.01	79.9

5.8.2 Deployment in the dam

5.8.2.1 Uptake of target analytes during field deployment

During field deployment arsenic was accumulated linearly (Figure 5.22). Conversely, accumulation of selenium in the field was unsuccessful considering that the mass was the highest at the beginning of the experiment but decrease and remained constant. The mass of mercury also declined between day 3 and day 6, after which no distinct trend is observed. The trends observed for selenium and mercury could be attributed to matrix effects.

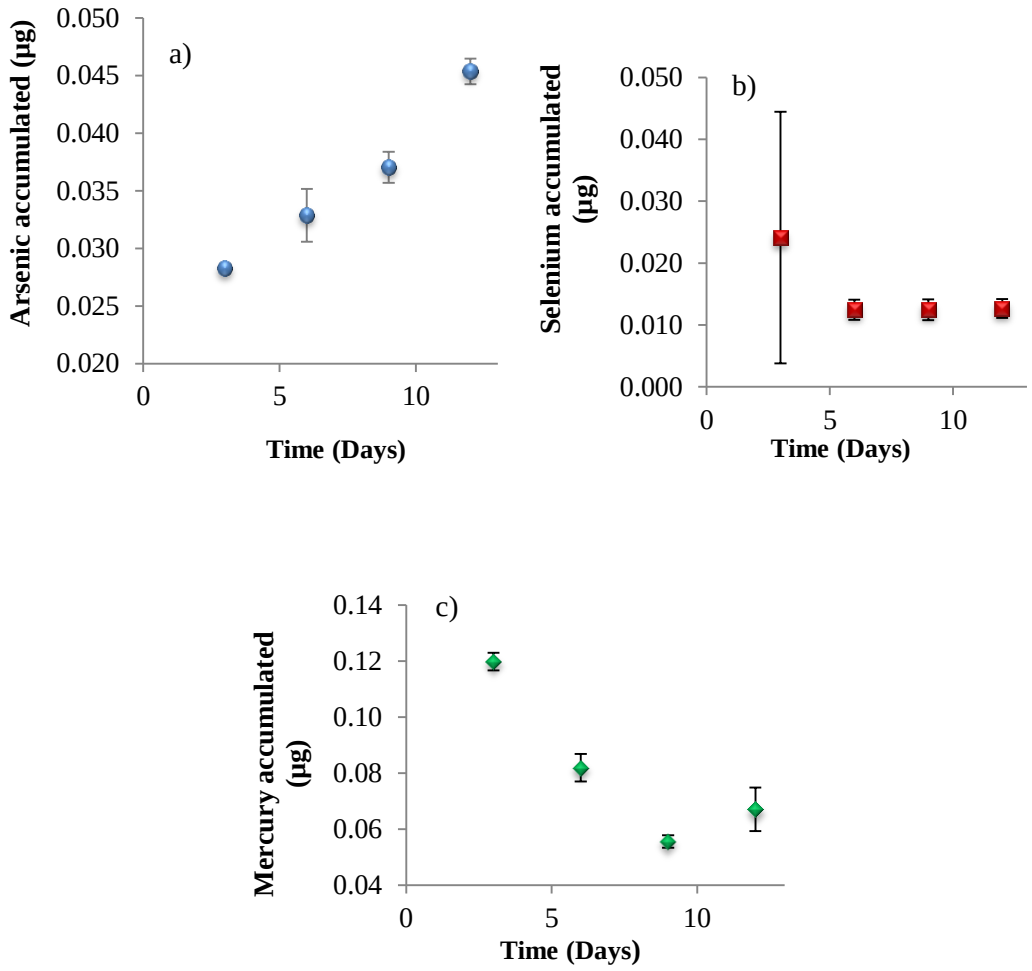


Figure 5.22: Accumulation of a) arsenic b) selenium c) mercury in Fluerhof dam

5.8.2.2 Accumulation of other metals during field deployments

Analysis of DGT after field deployments shows that the passive sampler accumulated other metals besides mercury. The mass of iron accumulated was relatively higher (Figure 5.23). Iron was also higher than the amount accumulated during the laboratory-based experiments (Figure 5.21). This is because in the field there was a higher concentration of bioavailable iron whereas in the laboratory this was reduced due to precipitation. No linear uptake was observed for these metals due to poor capacity of the resin.

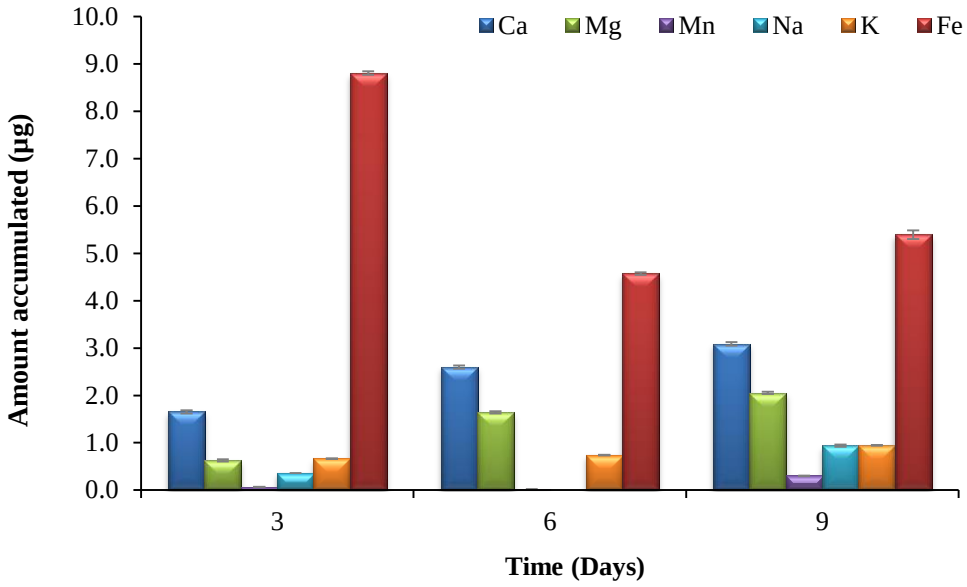


Figure 5.23: Metals accumulated in SCPEI-PCPEI DGT during field deployments (n = 3, RSD < 10%).

5.8.3 Deployment of DGT in dissolved efflorescent crust

5.8.3.1 Composition of dissolved efflorescent crust

The dissolved efflorescent crust formed a highly acidic solution with a pH value of 2.3. The measured conductivity was 5.30 mS cm^{-1}. In a study on efflorescent crusts, Camden-Smith et al. (2013) also obtained EC values ranging between 5.7 and 6.4 mS cm^{-1} for crust solutions with a high quantity of observable insoluble mass. Indeed, after re-hydration, the crust solution was very cloudy and precipitated significantly within a few hours of preparation (Figure 4.7). Conversely, for solutions that were completely dissolved, Camden-Smith et al. (2013) obtained conductivity values as high as 10 mS cm^{-1}.

The composition of the dissolved efflorescent crust (Table 5.9) shows elevated concentrations of sulphate, chloride, iron, nitrate, aluminium and manganese. Concentrations of major cations calcium, potassium, lithium, magnesium and sodium, as well as the transition metals cadmium, cobalt, chromium, copper,

nickel and zinc were relatively lower compared to the rest of the constituents. Arsenic and selenium were below the detection limit.

High sulphate and iron concentrations are consistent with AMD samples because they are by-products of sulphide mineral oxidation (Equation 2.13 to 2.16). Alternatively, the high nitrate concentration suggests the source of the efflorescent crust was close to an industrial site since high nitrate levels found in surface and ground water, are usually associated with factors such as the use of fertilizers and treated municipal waste water (Nolan and Hitt, 2006; Thorburn et al. 2003). The concentration of chloride ions, together with the other metals present in the crust will depend on the composition of the sulphide mineral being oxidised as well as the chemical reactions that took place in the original water source (Camden-Smith et al. 2013; Cheng et al. 2009).

Efflorescent crusts have different colours depending on their mineralogy (Camden-Smith et al. 2013; Naicker et al. 2003). Camden-Smith et al. (2013) studied the composition of efflorescent crusts (Table 5.10) and found that crusts classified as white with bright green had the highest iron content. The crust in the current study had a white-greenish colour based on the classification used by Camden-Smith et al. (2013). When comparing the general composition of the two white-greenish crusts it is apparent that they shared similar mineralogy trends: The crust studied by Camden-Smith et al. (2013) had elevated iron and aluminium concentrations. The crust in this study also had high concentrations of iron and aluminium.

Table 5.9 :Anion and metal analysis of the dissolved efflorescent crusts. Concentrations are described in (mg L^{-1})

	Cl^-	NO_3^-	SO_4^{2-}	Al	Ca	K	Li	Mg	Na	Cd	Co	Cr	Cu	Fe	Mn	Ni	Zn	As	Se
Dissolved crust	908.3	297.3	5623	214.5	7.78	0.29	0.35	4.51	13.53	0.09	6.94	0.70	1.49	474.4	79.00	14.05	4.89	*bdl*	*bdl*

bdl = below the detection limit

Table 5.10: Mole percentages of metals found in efflorescent crusts (Camden-Smith et al. 2013).

Colour of crust	Al	Ca	Cr	Co	Cu	Fe	K	Mg	Mn	Na	Ni	Tl	Zn
Yellow white	56.9			0.6	0.3		0.6	39.1	1.0		0.9		0.7
Beige	51.4			0.4	0.3	0.3	0.5	43.9	1.2	0.7	0.7		0.6
Green-yellow	38.7			0.5	0.9	29.8	2.0	26.6	0.6		0.6		0.4
Pink yellow	50.4		0.1	0.5	0.7	6.6	0.6	38.7	1.0		0.8		0.6
Orange-brown	43.6	2.0		0.4	0.5	7.5	1.4	41.7	0.8		0.6	1.0	0.4
White with bright green	**14.6**	**0.1**	**0.1**	**0.2**	**0.3**	**71.9**	**0.5**	**11.4**	**0.3**		**0.2**	**0.3**	**0.1**

Bold = colour of crust used in current study

5.8.3.2 DGT deployment in dissolved efflorescent crust

A linear uptake trend is an indication that DGT has successfully accumulated analytes at a constant and definable rate, within the constraints of the kinetic regime. The dissolved efflorescent crust was spiked with arsenic, selenium and mercury (1 mg L^{-1}), however, only arsenic could be determined from this study. The accumulation of labile arsenic fractions from the spiked dissolved efflorescent crust solution followed a linear regression between day 3 and day 15 (Figure 5.24). Nonetheless, after day 15, the curve began to slightly deviate from a linearity, indicating that equilibrium between the passive sampler and solution had been established.

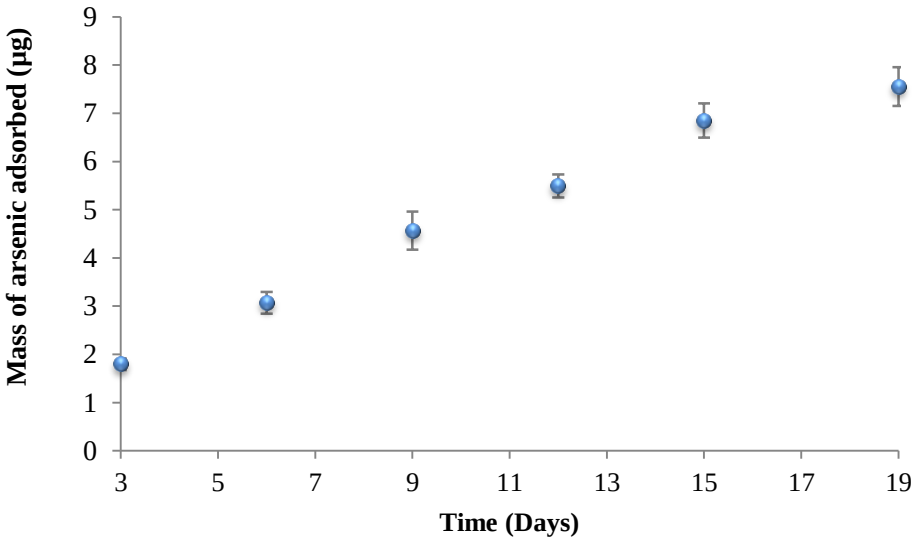


Figure 5.24: Time series experiment in the dissolved crust spiked with arsenic (1 mg L^{-1}) using 0.8 g of SCPEI-PCPEI resin (n = 3).

The maximum mass of arsenic accumulated (Figure 5.24) was 8 µg. This mass represents the labile and bioavailable fraction of arsenic in the dissolved crust solution. This amount is relatively low considering that the intended initial concentration of arsenic, selenium and mercury was 1 mg L^{-1}. However, after

spiking, the measured concentration was 0.34 ± 0.01 mg L^{-1} for arsenic and the concentrations of selenium and mercury could not be determined due to the breakdown of ICP-MS. The large discrepancy between the spiked and measured arsenic could be attributed to the high proportion of precipitate arising from the dissolved efflorescent crust.

SCPEI-PCPEI resin targets arsenic and selenium through an anion replacement mechanism based on the premise that they are ionic in solution (Saad et al. 2013a; 2013b). Mercury is adsorbed via a complexation mechanism (Saad et al. 2012b). Based on their respective Poubaix diagrams (Figure 2.1; 2.3 and 2.5) at pH 2.9, under the redox potential of surface water, arsenic is expected to exist as $H_3AsO_3^0$ (arsenite) or $H_2AsO_4^-$ (arsenate oxyanion), conversely, selenium predominates as Se^0. The mercury specie that predominates is either Hg (I) or $HgCl_2$. This information was validated using PHREEQC. According to PHREEQC, at pH 2.9, 100% of arsenite exists as $H_3AsO_3^0$ and 89% of arsenate as $H_2AsO_4^-$, with the uncharged arsenite specie predominating. On the other hand, selenide (H_2Se) was the main selenium specie in the efflorescent crust at approximately 86% followed by selenite ($HSeO_3^-$). Selenite was much lower compared to selenide. Majority of mercury was elemental mercury, the proportion of inorganic mercury was very low and the predominating specie was ($HgCl_2$) at 71%.

The speciation information stated above shows that at pH 2.9, majority of arsenic and selenium do not exist in their oxyanion forms. This suggests that the anion replacement mechanism was most probably limited. The proportion that is charged is found in much lower concentrations. With regards to arsenic, this is the fraction that is likely to be pre-concentrated by SCPEI-PCPEI via the anion replacement mechanism. More so considering that no phosphate anions were detected in the dissolved crust solution as these could have limited arsenic adsorption on SCPEI-PCPEI. Regarding the selenium oxyanion, the anion replacement mechanism was restricted by the extremely high sulphate concentration and the extremely low selenium oxyanion concentration: even if selenium was able to replace a single sulphonyl anion, due to the high sulphate concentration it would be replaced right back. Additionally, the likelihood of

mercury being adsorbed by SCPEI-PCPEI is low considering that majority of mercury was $HgCl_2$. The high concentration of chloride in the dissolved crust meant that complexation would favour chloride in solution instead of the sulphonyl group in within the SCPEI-PCPEI resin.

5.8.3.3 Uptake of other cations by DGT

Similar to passive samplers deployed in dam water, cations were also accumulated by SCPEI-PCPEI DGT (Figure 5.25). Iron, aluminium and magnesium showed the highest uptake. Regarding iron and aluminium, this was expected since their concentration in the dissolved crust was high (Table 5.9). In Figure 5.25 only aluminium shows linearity between day 6 and day 19. The rest of the metals do not show a specific trend in uptake with increasing deployment time.

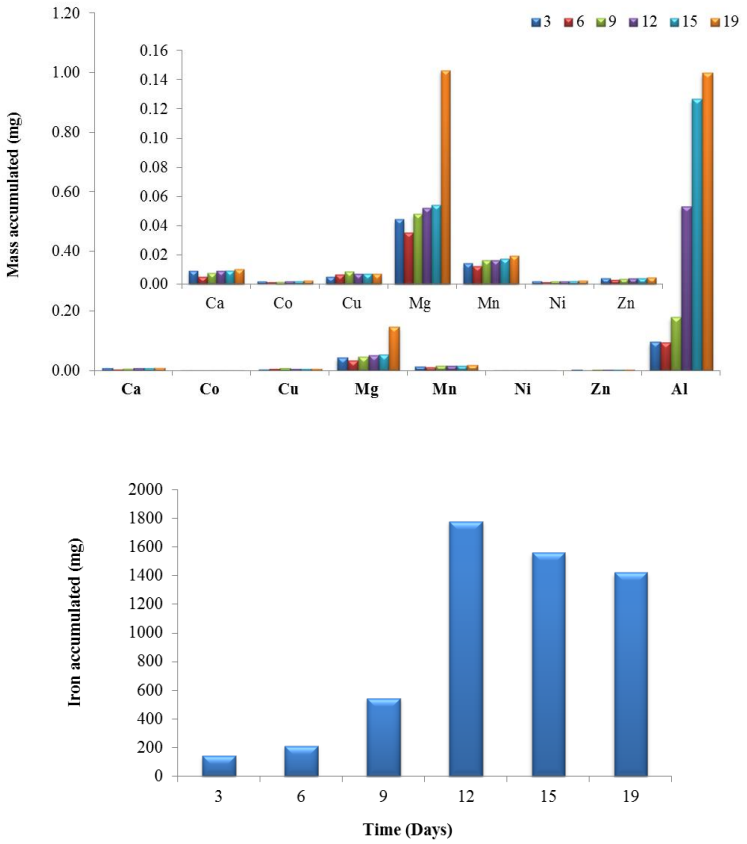


Figure 5.25: a) The mass of the major cations accumulated from the dissolved crust b) mass of iron accumulated.

According to PHREEQC, the majority of iron exists as Fe^{2+} and $FeSO_4$, while the predominant aluminium species are $AlSO_4^+$; $Al(SO_4)^{2-}$ and Al^{3+}. Magnesium, which was the third highest metal adsorbed by SCPEI-PCPEI DGT existed mainly as Mg^{2+} and $MgSO_4$. Manganese also predominated as Mn^{2+} and $MnSO_4$. The only difference between magnesium and manganese was that the concentration of free magnesium ion in solution was higher compared to manganese, hence the higher uptake. Uptake of iron and aluminium were enhanced due to their high concentrations in solution.

5.8.4 Uptake in laboratory-based experiments using AMD drainage water

The sampled AMD drainage water was highly acidic at pH 2.4 and had a high conductivity (10.5 mS cm^{-1}) which can be attributed to the higher concentration of dissolved metals and anions, in particular sulphate anions. The redox potential (366 mV) corresponds with redox potentials of most surface (Zhang et al. 2017).

5.8.4.1 Composition of AMD

The composition of the AMD drainage water was determined using ICP-OES. The trend as observed in Table 5.11 shows elevated sulphate (4319 mg L^{-1}) and iron (3793 mg L^{-1}) concentrations. The concentrations of aluminium (570 mg L^{-1}), magnesium (395 mg L^{-1}), calcium (376 mg L^{-1}) and manganese (97.5 mg L^{-1}) were relatively high, so were the concentrations of the trace metals cobalt (34.94 mg L^{-1}), nickel (32.32 mg L^{-1}). AMD water contains a high fraction of dissolved components. The concentration of mercury could not be determined due to the breakdown of ICP-MS.

Table 5.11: Anion and metal composition in AMD water

	Concentration (mg L^{-1})
Cl^-	42.47
SO_4^{2-}	4319
Al	570
Ca	376
Co	34.94
Cr	1.91
Cu	17.38
Fe	3793
Mg	395
Mn	97.5
Ni	32.32
Zn	*bdl*
As	0.554
Se	*bdl*

5.8.4.2 Accumulation in AMD drainage water

The AMD water sample was spiked with arsenic, selenium and mercury (0.5 mg L^{-1}). SCPEI-PCPEI DGT devices were deployed for 5 days. After 5 days, a thin layer had formed on top the water (Figure 5.26a). Figure 5.26b shows that by day 5, fouling from iron colloid particles had occurred. The high iron content also caused changes within the passive sampler interior (Figure 5.26c): the SCPEI-PCPEI resin changed colour and iron colloids had formed within the binding layer.

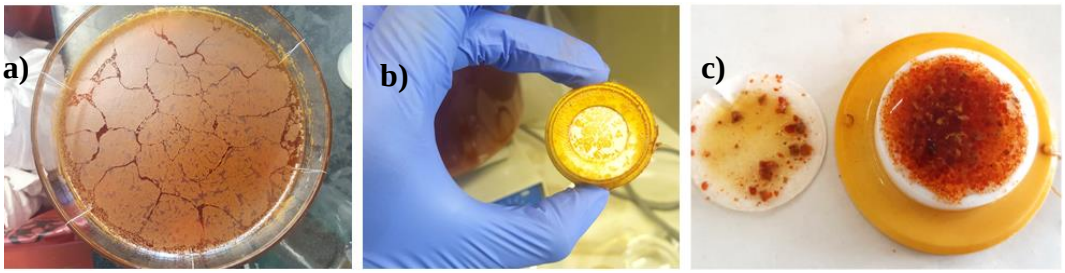


Figure 5.26: a) The formation of a thin layer on top of the AMD drainage water after 5 days. b) Fouling on DGT after deployment in AMD water c) passive sampler interior shows the colour change that took place on the resin and the formation of iron colloids

Figure 5.27 shows the accumulation of arsenic in AMD water. A linear uptake trend is observed. Linearity is more precise between day 2 and day 5. On day 5 there is no indication that maximum capacity for arsenic has been attained.

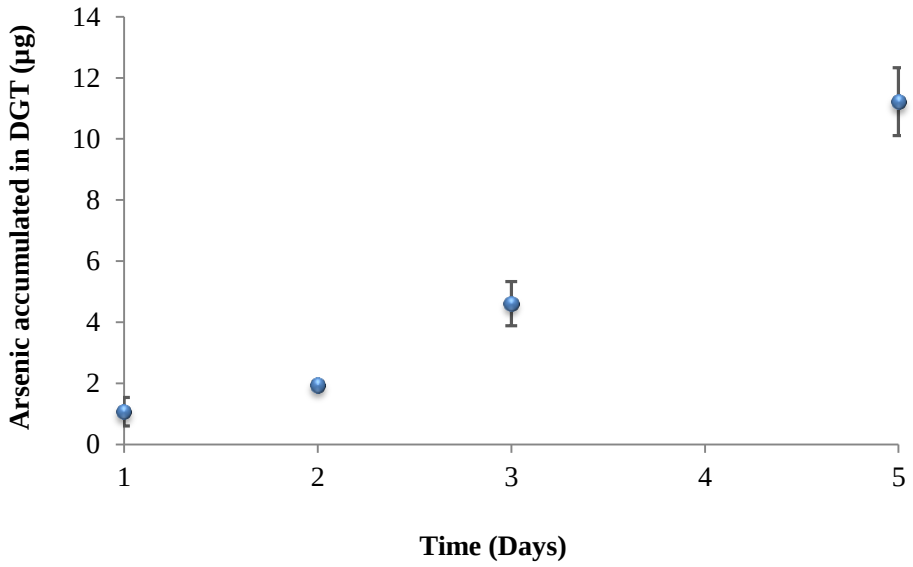


Figure 5.27: The accumulation of arsenic by DGT in water collected from AMD affected site spiked with arsenic (0.5 mg L^{-1}; n=3).

The amount of selenium and mercury accumulated could not be determined due to ICP-MS breakdown. Selenium and mercury were below the detection limit of the ICP-OES. The species of arsenic, selenium and mercury existing in solution were similar to those found in the dissolved efflorescent crust, due to similarities in pH and background components. Majority of arsenic was uncharged arsenite (H_3AsO_3); the concentration of charged arsenate specie ($H_2AsO_4^-$) was extremely low.

Selenium was overwhelmed by the high concentration of sulphate which is why it was not retained by DGT. Similarly, majority of mercury was complexed with chloride ions, according to PHREEQC, which is why it could not accumulate in DGT.

5.8.4.3 Simultaneous uptake of other cations

It has already been established that SCPEI-PCPEI DGT will simultaneously accumulate cations from solution. Figure 5.28 shows high accumulation of iron, aluminium, calcium and magnesium, respectively, in accordance to their concentrations in the AMD solution (Table 5.11). The mass of iron increased with deployment time as the mass of aluminium decreased.

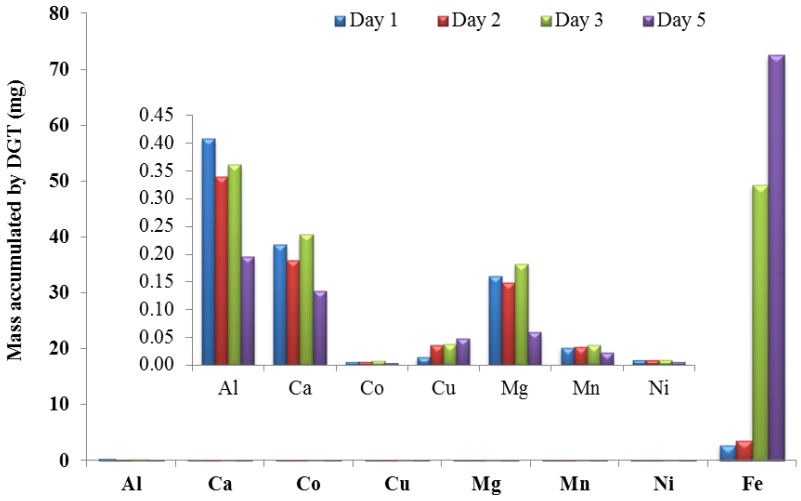


Figure 5.28: Metals accumulated from AMD water

Figure 5.26c) shows the SCPEI-PCPEI DGT resin after deployment for 5 days. The resin had changed colour and iron colloids had started to form. During deployment, metals slowly occupied the binding sites, however, because the concentration of iron was so high, it occupied majority of the sites. This probably increased competition for binding sites with other metals, particularly aluminium, which is why aluminium slowly decreased with deployment time and the other metals do not show a distinct uptake pattern. Ultimately, the binding sites became saturated with iron. This led to the formation of iron colloid particles within the binding layer. These colloid particles acted as a secondary binding site for any additional metals that entered DGT. This could possibly explain why some metals showed a non-specific uptake trend (Figure 5.28).

During calibration experiments using spiked deionised water, the SCPEI-PCPEI resin mixture showed great abilities as a DGT binding layer resin. However, deployments in environmental samples highlighted the low capacity of the resin mixture in the presence of competing ions. In their batch studies, Saad et al. (2012b; 2013a; 2013b) the maximum exposure time for SCPEI and PCPEI was 120 minutes. In comparison, this modified DGT was exposed to the target analytes for a minimum of 3 days. This shows differences in behaviour of the polymers when used as adsorbents and as binding layer components. These effects in SCPEI-PCPEI resin mixture are especially obvious for selenium and mercury compared to arsenic. The non-specific binding from the CPEI backbone also decreased the capacity of the passive sampler significantly. Successful arsenic uptake was achieved in both spiked deionised water and environmental samples.

Chapter 6: Conclusions and recommendations

This chapter briefly summarises the main findings of this study. Conclusions are also presented along with recommendations for future work.

6.1 Conclusions

This study focused on developing and evaluating a modified DGT passive sampler that would be robust enough to handle highly contaminated water compartments such as those affected by AMD. The suitability of functionalised cross-linked PEI as a DGT binding layer was investigated in the modified DGT sampler. A polymer mixture consisting of sulphonate and phosphonated cross-linked PEI was used as a DGT binding layer. The DGT sample holders used in this study were manufactured in our workshop and consisted of groves which allowed the cap to be re-used unlike conventional DGT sample holders. The performance of these devices was assessed in time series experiments using arsenate, selenite and mercury (II) solutions as well as dam water, dissolved efflorescent crust and AMD water under controlled laboratory conditions. The DGT devices were ultimately deployed in dam water during field tests for the determination of labile arsenic, selenium and mercury.

According to the laboratory-based experiments using spiked deionised water, SCPEI-PCPEI based DGT can operate in stagnant conditions under the pH range of natural water. SCPEI-PCPEI based DGT particularly showed better performance in dilute solutions. Results from field deployments highlighted reduced selectivity and capacity for the target analytes in the presence of competing ions. This could result from the concomitant adsorption of other metal ions from dam water. The accumulation of background metals did not show a specific trend due to limited capacity of the resin. In AMD water, the high metal concentration affected the accumulation of target elements. Not only did iron reduce the bioavailable fraction of arsenic, selenium and mercury through adsorption, but its entry into the passive sampler caused the formation of colloid particles. These particles behaved as secondary adsorption sites within the passive sampler, affecting uptake trends of target elements.

This study shows that good adsorbents, as determined by batch studies do not necessarily make good resins or binding layer components for DGT, especially polymeric ones in this case. Moreover, sorbents such as SCPEI and PCPEI

whereby adsorption occurs on a heterogenous surface, swelling could lead to a significant reduction in sorbent capacity. Sorbents with high adsorption capacity for target metals are thus favoured. Secondly, high selectivity is important, especially for longer deployments as that ensures that target analytes do not desorb from the resin. Therefore, SCPEI-PCPEI resin mixture is better suited for dilute solutions with concentrations below 0.5 mg L^{-1}.

Deployment in environmental samples resulted with uptake of other metals along with the target analytes. This is because CPEI has a high affinity for metals due to the large number of amine groups. Consequently, if a polymeric adsorbent is to be selected for application in DGT, the base polymer used for functionalisation must be inert in order to avoid high adsorption of background elements.

In commercial DGT, the Chelex-100 resin is embedded in a hydrogel. This study shows that not all resins require impregnation in a gel solution, especially polymeric ones. With regards to the DGT binding layer polymeric adsorbents are particularly challenging to work with; this is because they do not form defined particles that can be easily incorporated in a gel so that target compounds are uniformly adsorbed. Accordingly, different approaches on binding layer preparation need to be considered. However, uniformity and defined particles still need to be a priority to ensure that the polymer has high capacity.

It can be concluded that SCPEI-PCPEI based DGT was successfully developed, optimised and applied for arsenic. The capacity and retention abilities for selenium and mercury were limited, and this was demonstrated by deployment in environmental samples. Thus, the developed DGT passive sampler is best suited for dilute solutions with little competing metal ions.

6.2 Recommendations

This study will pave the way for more sorbents to be explored as long as the basic principles in passive sampler design and assembly are honoured. From this study, the following recommendations are suggested:

- To determine the bioavailable fraction of potential metals in various water samples and compare with total concentration for each deployment site to show that the developed DGT sampler can work well.
- Explore various sorbents that would be robust and selective enough to withstand conditions in AMD. This is very important as most developed DGT samplers have been applied in river water or surface waters. An example of such a sorbent could be thiolated CPEI which can specifically target mercury as well as gold fractions within AMD leachates.
- For long term studies it would be ideal to find a sorbent that has a lower propensity to swell as this could affect uptake during extended deployment.
- Redesign a DGT cap that would allow the use of enough sorbent for maximum capacity.
- Laboratory-based optimisation should be concurrent with field deployments in order to assess the selectivity of the resin layer.

References

Abad-Valle, P., Álvarez-Ayuso, E., Murciego, A., Muñoz-Centeno, L.M., Alonso-Rojo, P. and Villar-Alonso, P., 2018. Arsenic distribution in a pasture area impacted by past mining activities. *Ecotoxicology and Environmental Safety*, 147, pp.228-237.

Aguilar-Martinez, R., Palacios-Corvillo, M.A., Greenwood, R., Mills, G.A., Vrana, B. and Gómez-Gómez, M.M., 2008. Calibration and use of the Chemcatcher® passive sampler for monitoring organotin compounds in water. *Analytica Chimica Acta*, 618(2), pp.157-167.

Ahmed, E.M., 2015. Hydrogel: Preparation, characterization, and applications: A review. *Journal of Advanced Research*, 6(2), pp.105-121.

Ali, M. S., 2011. Remediation of acid mine waters. *International Mine Water Association Proceedings:" Mine Water–Managing the Challenges", Aachen, Germany*, 253–258.

Akcil, A. and Koldas, S., 2006. Acid mine drainage (AMD): causes, treatment and case studies. *Journal of Cleaner Production*, 14(12-13), pp.1139-1145.

Akpor, O.B. and Muchie, M., 2010. Remediation of heavy metals in drinking water and wastewater treatment systems: Processes and applications. International *Journal of Physical Sciences*, 5(12), pp.1807-1817.

Allan, I.J., Knutsson, J., Guigues, N., Mills, G.A., Fouillac, A.M. and Greenwood, R., 2008. Chemcatcher® and DGT passive sampling devices for regulatory monitoring of trace metals in surface water. *Journal of Environmental Monitoring*, 10(7), pp.821-829.

Allan, I.J., Mills, G.A., Vrana, B., Knutsson, J., Holmberg, A., Guigues, N., Laschi, S., Fouillac, A.M. and Greenwood, R., 2006a. Strategic monitoring for the European water framework directive. *TrAC Trends in Analytical Chemistry*, 25(7), pp.704-715.

Allan, I.J., Vrana, B., Greenwood, R., Mills, G.A., Roig, B. and Gonzalez, C., 2006b. A “toolbox” for biological and chemical monitoring requirements for the European Union's Water Framework Directive. *Talanta*, 69(2), pp.302-322.

Almeida, M.I.G., Cattrall, R.W. and Kolev, S.D., 2012. Recent trends in extraction and transport of metal ions using polymer inclusion membranes (PIMs). *Journal of Membrane Science*, *415*, pp.9-23.

Almeida, M.I.G., Cattrall, R.W. and Kolev, S.D., 2017. Polymer inclusion membranes (PIMs) in chemical analysis-A review. *Analytica Chimica Acta*, 987, pp.1-14.

AMAP/UNEP, 2013. Technical background report for the global mercury assessment 2013. *Arctic Monitoring and Assessment Programme, Oslo, Norway/UNEP Chemicals Branch Geneva, Switzerland*.

An, F. and Gao, B., 2007. Chelating adsorption properties of PEI/SiO2 for plumbum ion. *Journal of Hazardous Materials*, 145(3), pp.495-500.

Anawar, H.M., Akai, J. and Sakugawa, H., 2004. Mobilization of arsenic from subsurface sediments by effect of bicarbonate ions in groundwater. *Chemosphere*, *54*(6), pp.753-762.

Anderson, C.S., 2013. Minerals Yearbook–Selenium and Tellurium (Advance Release). US Geological Survey, Reston, VI, USA.

Aposhian, H.V. and Aposhian, M.M., 2006. Arsenic toxicology: five questions. *Chemical Research in Toxicology*, *19*(1), pp.1-15.

Appelo, C.A.J., Van der Weiden, M.J.J., Tournassat, C. and Charlet, L., 2002. Surface complexation of ferrous iron and carbonate on ferrihydrite and the mobilization of arsenic. *Environmental Science & Technology*, *36*(14), pp.3096-3103.

Arai, Y., Sparks, D.L. and Davis, J.A., 2004. Effects of dissolved carbonate on arsenate adsorption and surface speciation at the hematite− water interface.

Environmental Science & Technology, 38(3), pp.817-824.

Arnott, S., Fulmer, A.S.W.E., Scott, W.E., Dea, I.C.M., Moorhouse, R. and Rees, D.A., 1974. The agarose double helix and its function in agarose gel structure. *Journal of Molecular Biology*, 90(2), pp.269-284.

Attwood, D., Johansen, L., Tolley, J.A. and Rassing, J., 1981. A new ultrasonic method for the measurement of the diffusion coefficient of drugs within hydrogel matrices. *International Journal of Pharmaceutics*, 9(4), pp.285-294.

Ba, C., Langer, J. and Economy, J., 2009. Chemical modification of P84 copolyimide membranes by polyethylenimine for nanofiltration. *Journal of Membrane Science*, 327(1-2), pp.49-58.

Balistrieri, L.S. and Chao, T.T., 1990. Adsorption of selenium by amorphous iron oxyhydroxide and manganese dioxide. *Geochimica et Cosmochimica Acta*, *54*(3), pp.739-751.

Barkay, T., Gillman, M. and Turner, R.R., 1997. Effects of dissolved organic carbon and salinity on bioavailability of mercury. *Applied and Environmental Microbiology,* 63(11), pp.4267-4271.

Barrow, N.J. and Cox, V.C., 1992. The effects of pH and chloride concentration on mercury sorption. I. By goethite. *Journal of Soil Science*, 43(2), pp.295-304.

Bednar, A.J., Garbarino, J.R., Ranville, J.F. and Wildeman, T.R., 2002. Preserving the distribution of inorganic arsenic species in groundwater and acid mine drainage samples. *Environmental Science & Technology*, *36*(10), pp.2213-2218.

Bednar, A.J., Garbarino, J.R., Ranville, J.F. and Wildeman, T.R., 2005. Effects of iron on arsenic speciation and redox chemistry in acid mine water. *Journal of Geochemical Exploration*, *85*(2), pp.55-62.

Bennett, W.W., Teasdale, P.R., Panther, J.G., Welsh, D.T. and Jolley, D.F., 2010. New diffusive gradients in a thin film technique for measuring inorganic arsenic and selenium (IV) using a titanium dioxide based adsorbent. *Analytical*

Chemistry, 82(17), pp.7401-7407.

Bennett, W.W., Teasdale, P.R., Panther, J.G., Welsh, D.T. and Jolley, D.F., 2011. Speciation of dissolved inorganic arsenic by diffusive gradients in thin films: selective binding of AsIII by 3-mercaptopropyl-functionalized silica gel. *Analytical Chemistry*, 83(21), pp.8293-8299.

Bennett, W.W., Teasdale, P.R., Panther, J.G., Welsh, D.T., Zhao, H. and Jolley, D.F., 2012. Investigating arsenic speciation and mobilization in sediments with DGT and DET: a mesocosm evaluation of oxic-anoxic transitions. *Environmental Science & Technology*, 46(7), pp.3981-3989.

Benoit, J.M., Gilmour, C.C., Mason, R.P. and Heyes, A., 1999. Sulfide controls on mercury speciation and bioavailability to methylating bacteria in sediment pore waters. *Environmental Science & Technology*, 33(6), pp.951-957.

Bergeron, M.J., Clemençon, B., Hediger, M.A. and Markovich, D., 2013. SLC13 family of Na+-coupled di-and tri-carboxylate/sulfate transporters. *Molecular Aspects of Medicine*, *34*(2-3), pp.299-312.

Berry, M.J. and Ralston, N.V., 2008. Mercury toxicity and the mitigating role of selenium. *EcoHealth*, *5*(4), pp.456-459.

Bicak, N. and Sherrington, D.C., 1995. Mercury sorption by "non-functional" crosslinked polyacrylamides. *Reactive and Functional Polymers*, 27(3), pp.155-161.

Bissen, M. and Frimmel, F.H., 2003. Arsenic—a review. Part I: occurrence, toxicity, speciation, mobility. *Acta Hydrochimica et Hydrobiologica*, 31(1), pp.9-18.

Bjørklund, G., Aaseth, J., Ajsuvakova, O.P., Nikonorov, A.A., Skalny, A.V., Skalnaya, M.G. and Tinkov, A.A., 2017a. Molecular interaction between mercury and selenium in neurotoxicity. *Coordination Chemistry Reviews*, *332*, pp.30-37.

Bjørklund, G., Dadar, M., Mutter, J. and Aaseth, J., 2017b. The toxicology of mercury: Current research and emerging trends. *Environmental Research*, *159*,

pp.545-554.

Blom, L.B., Morrison, G.M., Kingston, J., Mills, G.A., Greenwood, R., Pettersson, T.J. and Rauch, S., 2002. Performance of an in situ passive sampling system for metals in storm water. *Journal of Environmental Monitoring*, 4(2), pp.258-262.

Blowes, D.W., Ptacek, C.J., Jambor, J.L. and Weisener, C.G., 2003. The geochemistry of acid mine drainage. *Treatise on Geochemistry*, 9, p.612.

Bodek, I., 1988. *Environmental Inorganic Chemistry: Properties, Processes, and Estimation Methods*. Pergamon.

Brack, W., Dulio, V., Ågerstrand, M., Allan, I., Altenburger, R., Brinkmann, M., Bunke, D., Burgess, R.M., Cousins, I., Escher, B.I. and Hernández, F.J., 2017. Towards the review of the European Union Water Framework Directive: recommendations for more efficient assessment and management of chemical contamination in European surface water resources. *Science of the Total Environment*, *576*, pp.720-737.

Brammer, H. and Ravenscroft, P., 2009. Arsenic in groundwater: a threat to sustainable agriculture in South and South-east Asia. *Environment International*, 35(3), pp.647-654.

Branch, U.C., 2008. The global atmospheric mercury assessment: sources, emissions and transport. *Geneva: UNEP-Chemicals*.

Broka, D., Ditzel, E., Quach, S. and Camenisch, T.D., 2016. Methylation of inorganic arsenic by murine fetal tissue explants. *Drug and Chemical Toxicology*, *39*(3), pp.279-283.

Brown, D.J.A. and Sadler, K., 1989. Fish survival in acid waters. *Acid Toxicity and Aquatic Animals*, *34*, pp.31-44.

Brown, K.M. and Arthur, J.R., 2001. Selenium, selenoproteins and human health: a review. *Public Health Nutrition*, 4(2b), pp.593-599.

Brozmanová, J., Mániková, D., Vlčková, V. and Chovanec, M., 2010. Selenium: a double-edged sword for defense and offence in cancer. *Archives of Toxicology*, 84(12), pp.919-938.

Brumbaugh, W.G., Petty, J.D., May, T.W. and Huckins, J.N., 2000. A passive integrative sampler for mercury vapor in air and neutral mercury species in water. *Chemosphere-Global Change Science*, 2(1), pp.1-9.

Bullock Jr, O.R., 2000. Modeling assessment of transport and deposition patterns of anthropogenic mercury air emissions in the United States and Canada. *Science of the Total Environment*, 259(1-3), pp.145-157.

Burger, J. and Gochfeld, M., 2012. Selenium and mercury molar ratios in saltwater fish from New Jersey: individual and species variability complicate use in human health fish consumption advisories. *Environmental Research*, 114, pp.12-23.

Buzier, R., Charriau, A., Corona, D., Lenain, J.F., Fondanèche, P., Joussein, E., Poulier, G., Lissalde, S., Mazzella, N. and Guibaud, G., 2014. DGT-labile As, Cd, Cu and Ni monitoring in freshwater: toward a framework for interpretation of in situ deployment. *Environmental Pollution*, 192, pp.52-58.

Buzier, R., Tusseau-Vuillemin, M.H. and Mouchel, J.M., 2006. Evaluation of DGT as a metal speciation tool in wastewater. *Science of the Total Environment*, 358(1-3), pp.277-285.

Cai, C., Williams, P.N., Li, H., Davison, W., Wei, T.J., Luo, J., Zhu, Y.G. and Zhang, H., 2016. Development and application of the diffusive gradients in thin films technique for the measurement of nitrate in soils. *Analytical Chemistry*, 89(2), pp.1178-1184.

Camden-Smith, B., Johnson, R., Richardson, R., Billing, D. and Tutu, H., 2013. Investigating the potential impact of efflorescent mineral crusts on water quality: complementing analytical techniques with geochemical modelling. Brown A, Figueroa L, and Wolkersdorfer Ch (eds.), *Reliable Mine Water Technology*, 1.

Castle, G.D., Mills, G.A., Bakir, A., Gravell, A., Schumacher, M., Townsend, I., Jones, L., Greenwood, R., Knott, S. and Fones, G.R., 2018. Calibration and field evaluation of the Chemcatcher® passive sampler for monitoring metaldehyde in surface water. *Talanta*, 179, pp.57-63.

Chan, Y.T., Kuan, W.H., Chen, T.Y. and Wang, M.K., 2009. Adsorption mechanism of selenate and selenite on the binary oxide systems. *Water Research*, 43(17), pp.4412-4420.

Chan, Y.T., Liu, Y.T., Tzou, Y.M., Kuan, W.H., Chang, R.R. and Wang, M.K., 2018. Kinetics and equilibrium adsorption study of selenium oxyanions onto Al/Si and Fe/Si coprecipitates. *Chemosphere*, *198*, pp.59-67.

Cheng, H., Hu, Y., Luo, J., Xu, B. and Zhao, J., 2009. Geochemical processes controlling fate and transport of arsenic in acid mine drainage (AMD) and natural systems. *Journal of Hazardous Materials*, 165(1-3), pp.13-26.

Chapman, P.M., Adams, W.J., Brooks, M.L., Delos, C.G., Luoma, S.N., Maher, W.A., Ohlendorf, H.M., Presser, T.S. and Shaw, D.P., 2009. Ecological assessment of selenium in the aquatic environment: Summary of a SETAC Pellston Workshop. *Society of Environmental Toxicology and Chemistry, Pensacola*.

Chrambach, A., 1985. *Practice of Quantitative Gel Electrophoresis*. VCH.

Ciardelli, M.C., Xu, H. and Sahai, N., 2008. Role of Fe (II), phosphate, silicate, sulfate, and carbonate in arsenic uptake by coprecipitation in synthetic and natural groundwater. *Water Research*, *42*(3), pp.615-624.

Clarkson, T.W., 2002. The three modern faces of mercury. Environmental Health Perspectives, 110(Suppl 1), p.11.

Coes, A.L., Paretti, N.V., Foreman, W.T., Iverson, J.L. and Alvarez, D.A., 2014. Sampling trace organic compounds in water: A comparison of a continuous active sampler to continuous passive and discrete sampling methods. *Science of the Total Environment*, 473, pp.731-741.

Coetzee, H., Hobbs, P.J., Burgess, J.E., Thomas, A., Keet, M., Yibas, B., Van Tonder, D., Netili, F., Rust, V., Wade, P. and Maree, J., 2010. Mine water management in the Witwatersrand Gold Fields with special emphasis on acid mine drainage. *Report To The Inter-Ministerial Committee on Acid Mine Drainage*, pp.1-128.

Cole, R.F., Mills, G.A., Hale, M.S., Parker, R., Bolam, T., Teasdale, P.R., Bennett, W.W. and Fones, G.R., 2018. Development and evaluation of a new diffusive gradients in thin-films technique for measuring organotin compounds in coastal sediment pore water. *Talanta, 178*, pp.670-678.

Combs Jr, G.F. and Gray, W.P., 1998. *Chemopreventive agents: selenium. Pharmacology & Therapeutics*, 79(3), pp.179-192.

Combs Jr, G.F., 2000. Food system-based approaches to improving micronutrient nutrition: The case for selenium. *Biofactors*, 12(1-4), pp.39-43.

Coquery, M., Cossa, D. and Sanjuan, J., 1997. Speciation and sorption of mercury in two macro-tidal estuaries. *Marine Chemistry*, 58(1-2), pp.213-227.

Cossa, D. and Gobeil, C., 2000. Mercury speciation in the lower St. Lawrence Estuary. *Canadian Journal of Fisheries and Aquatic Sciences*, 57(S1), pp.138-147.

Cotter, J. and Brigden, K., 2006. *Acid mine drainage: the case of the Lafayette mine*, Rapu Rapu (Philippines).

Cullen, W.R. and Reimer, K.J., 1989. Arsenic speciation in the environment. *Chemical Reviews*, 89(4), pp.713-764.

Da Silva, J.F. and Williams, R.J.P., 2001. *The Biological Chemistry of the elements: the inorganic chemistry of life*. Oxford University Press.

Das, S., Hendry, M.J. and Essilfie-Dughan, J., 2013. Adsorption of selenate onto ferrihydrite, goethite, and lepidocrocite under neutral pH conditions. *Applied Geochemistry*, 28, pp.185-193.

Daus, B., Mattusch, J., Paschke, A., Wennrich, R. and Weiss, H., 2000. Kinetics of the arsenite oxidation in seepage water from a tin mill tailings pond. *Talanta*, *51*(6), pp.1087-1095.

Davison, W. and Zhang, H., 1994a. In situ speciation measurements of trace components in natural waters using thin-film gels. *Nature*, 367(6463), p.546.

Davison, W. and Zhang, H., 2012. Progress in understanding the use of diffusive gradients in thin films (DGT)–back to basics. *Environmental Chemistry*, 9(1), pp.1-13.

Davison, W. ed., 2016. *Diffusive gradients in thin-films for environmental measurements*. Cambridge University Press.

Davison, W., Fones, G., Harper, M., Teasdale, P. and Zhang, H., 2000. Dialysis, DET and DGT: in situ diffusional techniques for studying water, sediments and soils. *In Situ Monitoring of Aquatic Systems: Chemical Analysis and Speciation.*, pp.495-569.

Davison, W., Lin, C., Gao, Y. and Zhang, H., 2015. Effect of gel interactions with dissolved organic matter on DGT measurements of trace metals. *Aquatic Geochemistry*, 21(2-4), pp.281-293.

Davison, W., Zhang, H. and Grime, G.W., 1994. Performance characteristics of gel probes used for measuring the chemistry of pore waters. *Environmental Science & Technology*, 28(9), pp.1623-1632.

de Magalhães, M.E.A. and Tubino, M., 1995. A possible path for mercury in biological systems: the oxidation of metallic mercury by molecular oxygen in aqueous solutions. *Science of the Total Environment*, 170(3), pp.229-239.

Deng, S. and Ting, Y.P., 2005a. Characterization of PEI-modified biomass and biosorption of Cu (II), Pb (II) and Ni (II). *Water Research*, 39(10), pp.2167-2177.

Deng, S. and Ting, Y.P., 2005b. Polyethylenimine-modified fungal biomass as a high-capacity biosorbent for Cr (VI) anions: sorption capacity and uptake

mechanisms. *Environmental Science & Technology*, 39(21), pp.8490-8496.

Deng, Y., Wang, Y., Ma, T., Yang, H. and He, J., 2011. Arsenic associations in sediments from shallow aquifers of northwestern Hetao Basin, Inner Mongolia. *Environmental Earth Sciences*, 64(8), pp.2001-2011.

Denizli, A., Senel, S., Alsancak, G., Tüzmen, N. and Say, R., 2003. Mercury removal from synthetic solutions using poly (2-hydroxyethylmethacrylate) gel beads modified with poly (ethyleneimine). *Reactive and Functional Polymers*, 55(2), pp.121-130.

Devillers, D., Buzier, R., Grybos, M., Charriau, A. and Guibaud, G., 2017. Key role of the sorption process in alteration of metal and metalloid quantification by fouling development on DGT passive samplers. *Environmental Pollution*, 230, pp.523-529.

Dhillon, S.K. and Dhillon, K.S., 2000. Selenium adsorption in soils as influenced by different anions. *Journal of Plant Nutrition and Soil Science*, 163(6), pp.577-582.

Ding, M.B.H.W., De Jong, B.H.W.S., Roosendaal, S.J. and Vredenberg, A.X.P.S., 2000. XPS studies on the electronic structure of bonding between solid and solutes: adsorption of arsenate, chromate, phosphate, Pb2+, and Zn2+ ions on amorphous black ferric oxyhydroxide. *Geochimica et Cosmochimica Acta*, 64(7), pp.1209-1219.

Ding, S., Xu, D., Wang, Y., Wang, Y., Li, Y., Gong, M. and Zhang, C., 2016. Simultaneous measurements of eight oxyanions using high-capacity diffusive gradients in thin films (Zr-oxide DGT) with a high-efficiency elution procedure. *Environmental Science & Technology*, 50(14), pp.7572-7580.

Directive, C., 2000. 60/EC (2000) Directive of the European Parliament and of the Council establishing a framework for the Community action in the field of water policy. The European parliament and the Council of the European Union. Official Journal L, 327(22), p.12.

Dixit, S. and Hering, J.G., 2003. Comparison of arsenic (V) and arsenic (III) sorption onto iron oxide minerals: implications for arsenic mobility. *Environmental Science & Technology*, 37(18), pp.4182-4189.

Dixon, W., Smyth, G.K. and Chiswell, B., 1999. Optimized selection of river sampling sites. *Water Research*, 33(4), pp.971-978.

Dočekalová, H. and Diviš, P., 2005. Application of diffusive gradient in thin films technique (DGT) to measurement of mercury in aquatic systems. *Talanta*, *65*(5), pp.1174-1178.

Dold, B., 2010. Basic concepts in environmental geochemistry of sulfidic mine-waste management. In Waste management. InTech.

Dold, B., 2014. Evolution of acid mine drainage formation in sulphidic mine tailings. *Minerals*, 4(3), pp.621-641.

Drewniak, L. and Sklodowska, A., 2013. Arsenic-transforming microbes and their role in biomining processes. *Environmental Science and Pollution* Research, 20(11), pp.7728-7739.

Dunn, R.J.K., Teasdale, P.R., Warnken, J., Jordan, M.A. and Arthur, J.M., 2007. Evaluation of the in situ, time-integrated DGT technique by monitoring changes in heavy metal concentrations in estuarine waters. *Environmental Pollution*, 148(1), pp.213-220.

Dworak, T., Gonzalez, C., Laaser, C. and Interwies, E., 2005. The need for new monitoring tools to implement the WFD. *Environmental Science & Policy*, 8(3), pp.301-306.

Dyrssen, D. and Wedborg, M., 1991. The sulphur-mercury (II) system in natural waters. *Water Air & Soil Pollution*, *56*(1), pp.507-519.

Edmonds, J.S. and Francesconi, K.A., 1997. Arsenic and marine organisms. *Advanced Inorganic Chemistry*, *44*, pp.147-189.

Ellis, A.S., Johnson, T.M., Herbel, M.J. and Bullen, T.D., 2003. Stable isotope

fractionation of selenium by natural microbial consortia. *Chemical Geology*, 195(1-4), pp.119-129.

El-Ramady, H.R., Domokos-Szabolcsy, É., Abdalla, N.A., Alshaal, T.A., Shalaby, T.A., Sztrik, A., Prokisch, J. and Fári, M., 2014. Selenium and nano-selenium in agroecosystems. *Environmental Chemistry Letters*, 12(4), pp.495-510.

Ernstberger, H., Zhang, H., Tye, A., Young, S. and Davison, W., 2005. Desorption kinetics of Cd, Zn, and Ni measured in soils by DGT. *Environmental Science & Technology*, 39(6), pp.1591-1597.

Farooq, M.A., Islam, F., Ali, B., Najeeb, U., Mao, B., Gill, R.A., Yan, G., Siddique, K.H. and Zhou, W., 2016. Arsenic toxicity in plants: cellular and molecular mechanisms of its transport and metabolism. *Environmental and Experimental Botany*, 132, pp.42-52.

Fatin-Rouge, N., Milon, A., Buffle, J., Goulet, R.R. and Tessier, A., 2003. Diffusion and partitioning of solutes in agarose hydrogels: the relative influence of electrostatic and specific interactions. *The Journal of Physical Chemistry B*, *107*(44), pp.12126-12137.

Feng, X., Li, G. and Qiu, G., 2004. A preliminary study on mercury contamination to the environment from artisanal zinc smelting using indigenous methods in Hezhang county, Guizhou, China—Part 1: mercury emission from zinc smelting and its influences on the surface waters. *Atmospheric Environment*, 38(36), pp.6223-6230.

Feng, X., Li, P., Qiu, G., Wang, S., Li, G., Shang, L., Meng, B., Jiang, H., Bai, W., Li, Z. and Fu, X., 2007. Human exposure to methylmercury through rice intake in mercury mining areas, Guizhou Province, China. *Environmental Science & Technology*, 42(1), pp.326-332.

Feng, Z., Zhu, P., Fan, H., Piao, S., Xu, L. and Sun, T., 2016. Effect of biofilm on passive sampling of dissolved orthophosphate using the diffusive gradients in thin films technique. *Analytical Chemistry*, 88(13), pp.6836-6843.

Fernández-Gómez, C., Bayona, J.M. and Díez, S., 2012. Laboratory and field evaluation of diffusive gradient in thin films (DGT) for monitoring levels of dissolved mercury in natural river water. *International Journal of Environmental Analytical Chemistry*, 92(15), pp.1689-1698.

Fernández-Martínez, A. and Charlet, L., 2009. Selenium environmental cycling and bioavailability: a structural chemist point of view. *Reviews in Environmental Science and Bio/Technology*, 8(1), pp.81-110.

Ferrara, R., Mazzolai, B., Edner, H., Svanberg, S. and Wallinder, E., 1998. Atmospheric mercury sources in the Mt. Amiata area, Italy. *Science of the Total Environment*, 213(1-3), pp.13-23.

Ferrara, R., Mazzolai, B., Lanzillotta, E., Nucaro, E. and Pirrone, N., 2000. Volcanoes as emission sources of atmospheric mercury in the Mediterranean basin. *Science of the Total Environment*, 259(1-3), pp.115-121.

Finnegan, P. and Chen, W., 2012. Arsenic toxicity: the effects on plant metabolism. *Frontiers in Physiology*, 3, p.182.

Fitz, W.J., Wenzel, W.W., Zhang, H., Nurmi, J., Štipek, K., Fischerova, Z., Schweiger, P., Köllensperger, G., Ma, L.Q. and Stingeder, G., 2003. Rhizosphere characteristics of the arsenic hyperaccumulator Pteris vittata L. and monitoring of phytoremoval efficiency. *Environmental Science & Technology*, *37*(21), pp.5008-5014.

Fitzgerald, W.F., Engstrom, D.R., Mason, R.P. and Nater, E.A., 1998. The case for atmospheric mercury contamination in remote areas. *Environmental Science & Technology*, 32(1), pp.1-7.

Fleming, G.A., 1980. Essential micronutrients. II. Iodine and selenium. *Applied soil trace elements.* edited by Brian E. Davies.

Floor, G.H. and Román-Ross, G., 2012. Selenium in volcanic environments: a review. *Applied Geochemistry*, 27(3), pp.517-531.

Fordyce, F., 2007. Selenium geochemistry and health. AMBIO: *A Journal of the*

Human Environment, 36(1), pp.94-97.

Fordyce, F.M., 2013. Selenium deficiency and toxicity in the environment. *In Essentials of Medical Geology* (pp. 375-416). Springer, Dordrecht.

Fripp, J., Ziemkiewicz, P.F. and Charkavorki, H., 2000. Acid mine drainage treatment.

Frohne, T., Rinklebe, J., Langer, U., Laing, G.D., Mothes, S. and Wennrich, R., 2012. Biogeochemical factors affecting mercury methylation rate in two contaminated floodplain soils. *Biogeosciences*, 9(1), pp.493-507.

Fu, X., Feng, X., Zhang, G., Xu, W., Li, X., Yao, H., Liang, P., Li, J., Sommar, J., Yin, R. and Liu, N., 2010. Mercury in the marine boundary layer and seawater of the South China Sea: concentrations, sea/air flux, and implication for land outflow. *Journal of Geophysical Research: Atmospheres*, 115(D6).

Gabriel, M.C. and Williamson, D.G., 2004. Principal biogeochemical factors affecting the speciation and transport of mercury through the terrestrial environment. *Environmental Geochemistry and Health*, 26(3-4), pp.421-434.

Gailer, J., 2002. Reactive selenium metabolites as targets of toxic metals/metalloids in mammals: a molecular toxicological perspective. *Applied Organometallic Chemistry*, *16*(12), pp.701-707.

Gailer, J., 2007. Arsenic–selenium and mercury–selenium bonds in biology. *Coordination Chemistry Reviews*, *251*(1-2), pp.234-254.

Gao, Y., De Canck, E., Leermakers, M., Baeyens, W. and Van Der Voort, P., 2011. Synthesized mercaptopropyl nanoporous resins in DGT probes for determining dissolved mercury concentrations. *Talanta*, *87*, pp.262-267.

Garmo, Ø.A., Røyset, O., Steinnes, E. and Flaten, T.P., 2003. Performance study of diffusive gradients in thin films for 55 elements. *Analytical chemistry*, *75*(14), pp.3573-3580.

Garnier, J.M., Garnier, J., Jézéquel, D. and Angeletti, B., 2015. Using DET and

DGT probes (ferrihydrite and titanium dioxide) to investigate arsenic concentrations in soil porewater of an arsenic-contaminated paddy field in Bangladesh. *Science of the Total Environment*, *536*, pp.306-315.

Gimpel, J., Zhang, H., Hutchinson, W. and Davison, W., 2001. Effect of solution composition, flow and deployment time on the measurement of trace metals by the diffusive gradient in thin films technique. *Analytica Chimica Acta*, *448*(1-2), pp.93-103.

Goh, K.H. and Lim, T.T., 2004. Geochemistry of inorganic arsenic and selenium in a tropical soil: effect of reaction time, pH, and competitive anions on arsenic and selenium adsorption. *Chemosphere*, 55(6), pp.849-859.

Goh, K.H. and Lim, T.T., 2005. Arsenic fractionation in a fine soil fraction and influence of various anions on its mobility in the subsurface environment. *Applied Geochemistry*, 20(2), pp.229-239.

Goldhaber, S.B., 2003. Trace element risk assessment: essentiality vs. toxicity. *Regulatory Toxicology and Pharmacology*, 38(2), pp.232-242.

Golmohamadi, M., Davis, T.A. and Wilkinson, K.J., 2012. Diffusion and partitioning of cations in an agarose hydrogel. *The Journal of Physical Chemistry A*, *116*(25), pp.6505-6510.

Gopalan, R., 2009. *Inorganic chemistry for undergraduates*. Universities Press.

Górecki, T. and Namieśnik, J., 2002. Passive sampling. *TrAC Trends in Analytical Chemistry*, 21(4), pp.276-291.

Gray, N.F., 1998. Acid mine drainage composition and the implications for its impact on lotic systems. *Water Research*, *32*(7), pp.2122-2134.

Gray, W.B. and Shimshack, J.P., 2011. The effectiveness of environmental monitoring and enforcement: A review of the empirical evidence. Review of *Environmental Economics and Policy*, 5(1), pp.3-24.

Grotti, M., Soggia, F., Lagomarsino, C., Goessler, W. and Francesconi, K.A.,

2008. Arsenobetaine is a significant arsenical constituent of the red Antarctic alga Phyllophora antarctica. *Environmental Chemistry*, *5*(3), pp.171-175.

Guan, D.X., Sun, F.S., Yu, G.H., Polizzotto, M.L. and Liu, Y.G., 2018. Total and available metal concentrations in soils from six long-term fertilization sites across China. *Environmental Science and Pollution Research*, 25(31), pp.31666-31678.

Guo, C., Zhang, T., Hou, S., Lv, J., Zhang, Y., Wu, F., Hua, Z., Meng, W., Zhang, H. and Xu, J., 2017. Investigation and application of a new passive sampling technique for in situ monitoring of illicit drugs in waste waters and rivers. *Environmental Science & Technology*, 51(16), pp.9101-9108.

Hall, G.E., Pelchat, J.C. and Gauthier, G., 1999. Stability of inorganic arsenic (III) and arsenic (V) in water samples. *Journal of Analytical Atomic Spectrometry*, *14*(2), pp.205-213.

Hamilton, S.J., 2004. Review of selenium toxicity in the aquatic food chain. *Science of the Total Environment*, 326(1-3), pp.1-31.

Han, M.J., Hao, J., Christodoulatos, C., Korfiatis, G.P., Wan, L.J. and Meng, X., 2007. Direct evidence of arsenic (III)− carbonate complexes obtained using electrochemical scanning tunneling microscopy. *Analytical Chemistry*, *79*(10), pp.3615-3622.

Hansen, R.N., 2015. Contaminant leaching from gold mining tailings dams in the Witwatersrand Basin, South Africa: A new geochemical modelling approach. *Applied Geochemistry*, 61, pp.217-223.

Harada, M., 1995. Minamata disease: methylmercury poisoning in Japan caused by environmental pollution. *Critical Reviews in Toxicology*, 25(1), pp.1-24.

Harada, M., Nakanishi, J., Yasoda, E., Maria da Conceicâo, N.P., Oikawa, T., de Assis Guimarâes, G., da silva Cardoso, B., Kizaki, T. and Ohno, H., 2001. Mercury pollution in the Tapajos River basin, Amazon: mercury level of head hair and health effects. *Environment International*, 27(4), pp.285-290.

Harper, M.P., Davison, W., Zhang, H. and Tych, W., 1998. Kinetics of metal

exchange between solids and solutions in sediments and soils interpreted from DGT measured fluxes. *Geochimica et Cosmochimica Acta*, 62(16), pp.2757-2770.

Hassett-Sipple, B., Swartout, J. and Schoeny, R., 1997. Mercury study report to Congress. Volume 5. Health effects of mercury and mercury compounds (No. PB-98-124779/XAB; EPA-452/R-97/007). Environmental Protection Agency, Research Triangle Park, NC (United States). Office of Air Quality Planning and Standards.

Hawkesford, M.J. and Zhao, F.J., 2007. Strategies for increasing the selenium content of wheat. *Journal of Cereal Science*, 46(3), pp.282-292.

He, Z., Yang, X., Zhu, Z., Zhang, Q., Xia, W. and Tan, J., 1994. Effect of phosphate on the sorption, desorption and plant-availability of selenium in soil. *Fertilizer Research*, 39(3), pp.189-197.

Holmes, C.D., Jacob, D.J. and Yang, X., 2006. Global lifetime of elemental mercury against oxidation by atomic bromine in the free troposphere. *Geophysical Research Letters*, 33(20).

Hooda, P.S., Zhang, H., Davison, W. and Edwards, A.C., 1999. Measuring bioavailable trace metals by diffusive gradients in thin films (DGT): soil moisture effects on its performance in soils. *European Journal of Soil Science*, *50*(2), pp.285-294.

Horowitz, A.J., 1997. Some thoughts on problems associated with various sampling media used for environmental monitoring. *Analyst*, 122(11), pp.1193-1200.

Horvat, M., Tratnik, J.S. and Miklavčič, A., 2011. H: Mercury: Biomarkers of Exposure and Human Biomonitoring. In *Biomarkers and Human Biomonitoring* (pp. 381-417).

Hseu, Z.Y., Su, S.W., Lai, H.Y., Guo, H.Y., Chen, T.C. and Chen, Z.S., 2010. Remediation techniques and heavy metal uptake by different rice varieties in metal-contaminated soils of Taiwan: new aspects for food safety regulation and

sustainable agriculture. *Soil Science & Plant Nutrition*, 56(1), pp.31-52.

Huang, J., Bennett, W.W., Teasdale, P.R., Gardiner, S. and Welsh, D.T., 2016. Development and evaluation of the diffusive gradients in thin films technique for measuring nitrate in freshwaters. *Analytica Chimica Acta*, 923, pp.74-81.

Huckins, J.N., Petty, J.D. and Booij, K., 2006. Monitors of organic chemicals in the environment: semipermeable membrane devices. Springer Science & Business Media.

Hug, S.J., Canonica, L., Wegelin, M., Gechter, D. and Von Gunten, U., 2001. Solar oxidation and removal of arsenic at circumneutral pH in iron containing waters. *Environmental Science & Technology*, *35*(10), pp.2114-2121.

Huston, D.L., Sie, S.H., Suter, G.F., Cooke, D.R. and Both, R.A., 1995. Trace elements in sulfide minerals from eastern Australian volcanic-hosted massive sulfide deposits; Part I, Proton microprobe analyses of pyrite, chalcopyrite, and sphalerite, and Part II, Selenium levels in pyrite; comparison with delta 34 S values and implications for the source of sulfur in volcanogenic hydrothermal systems. *Economic Geology*, *90*(5), pp.1167-1196.

Hutchins, C.M., Panther, J.G., Teasdale, P.R., Wang, F., Stewart, R.R., Bennett, W.W. and Zhao, H., 2012. Evaluation of a titanium dioxide-based DGT technique for measuring inorganic uranium species in fresh and marine waters. *Talanta*, *97*, pp.550-556.

Huynh, T., Zhang, H. and Noller, B., 2012. Evaluation and application of the diffusive gradients in thin films technique using a mixed-binding gel layer for measuring inorganic arsenic and metals in mining impacted water and soil. *Analytical Chemistry*, 84(22), pp.9988-9995.

IARC Working Group on the Evaluation of Carcinogenic Risks to Humans, 2012. Arsenic, metals, fibres, and dusts. *IARC Monographs on the Evaluation of Carcinogenic Risks to Humans*, 100(PT C), p.11.

Israr, M. and Sahi, S.V., 2006. Antioxidative responses to mercury in the cell

cultures of Sesbania drummondii. *Plant Physiology and Biochemistry*, 44(10), pp.590-595.

Jacobs, L.W., 1990. Selenium in Agriculture and the Environment. *Soil Science, 149*(2), p.121.

Jennings, S.R., Blicker, P.S. and Neuman, D.R., 2008. *Acid mine drainage and effects on fish health and ecology: a review*. Reclamation Research Group.

Jewell, S.A.L.L.Y. and Kimball, S.M., 2015. Mineral commodity summaries 2015. *US Geological Survey*, 9, p.196.

Jia, J., Wu, A. and Luan, S., 2014. Synthesis and investigation of the imprinting efficiency of ion imprinted nanoparticles for recognizing copper. *Physical Chemistry Chemical Physics*, 16(30), pp.16158-16165.

Jin, Y., Zhao, F., Zhong, Y., Yu, X., Sun, D., Liao, Y., Lv, X., Li, G. and Sun, G., 2010. Effects of exogenous GSH and methionine on methylation of inorganic arsenic in mice exposed to arsenite through drinking water. *Environmental Toxicology*, *25*(4), pp.361-366.

Johnson, D.B. and Hallberg, K.B., 2005. Acid mine drainage remediation options: a review. *Science of the total environment*, *338*(1-2), pp.3-14.

Johnson, C.C., Fordyce, F.M. and Rayman, M.P., 2010. Symposium on Geographical and geological influences on nutrition'Factors controlling the distribution of selenium in the environment and their impact on health and nutrition: Conference on 'Over-and undernutrition: challenges and approaches'. *Proceedings of the Nutrition Society*, *69*(1), pp.119-132.

Jones, A.M., Griffin, P.J., Collins, R.N. and Waite, T.D., 2014. Ferrous iron oxidation under acidic conditions–The effect of ferric oxide surfaces. *Geochimica et Cosmochimica Acta*, 145, pp.1-12.

Kabata-Pendias, A. and Pendias, H., 1984. *Trace elements in soil and plants* (No. 631.41 K3).

Kabata-Pendias, A., 2010. Trace elements in soils and plants. CRC press.

Kessi, J., Ramuz, M., Wehrli, E., Spycher, M. and Bachofen, R., 1999. Reduction of selenite and detoxification of elemental selenium by the Phototrophic BacteriumRhodospirillum rubrum. *Applied and Environmental Microbiology*, 65(11), pp.4734-4740.

Khalil, B. and Ouarda, T.B.M.J., 2009. Statistical approaches used to assess and redesign surface water-quality-monitoring networks. *Journal of Environmental Monitoring*, 11(11), pp.1915-1929.

Khare, A.R. and Peppas, N.A., 1993. Investigation of hydrogel water in polyelectrolyte gels using differential scanning calorimetry. *Polymer*, 34(22), pp.4736-4739.

Khoei, N.S., Lampis, S., Zonaro, E., Yrjälä, K., Bernardi, P. and Vallini, G., 2017. Insights into selenite reduction and biogenesis of elemental selenium nanoparticles by two environmental isolates of Burkholderia fungorum. *New Biotechnology*, *34*, pp.1-11.

Kieliszek, M. and Błażejak, S., 2013. Selenium: significance, and outlook for supplementation. *Nutrition*, 29(5), pp.713-718.

Kim, M.J., Nriagu, J. and Haack, S., 2000. Carbonate ions and arsenic dissolution by groundwater. *Environmental Science & Technology*, *34*(15), pp.3094-3100.

Kingston, J.K., Greenwood, R., Mills, G.A., Morrison, G.M. and Persson, L.B., 2000. Development of a novel passive sampling system for the time-averaged measurement of a range of organic pollutants in aquatic environments. *Journal of Environmental Monitoring*, 2(5), pp.487-495.

Klapec, T., Mandić, M.L., Grgić, J., Primorac, L., Perl, A. and Krstanović, V., 2004. Selenium in selected foods grown or purchased in eastern Croatia. *Food Chemistry*, 85(3), pp.445-452.

Kojima, C., Ramirez, D.C., Tokar, E.J., Himeno, S., Drobná, Z., Stýblo, M., Mason, R.P. and Waalkes, M.P., 2009. Requirement of arsenic biomethylation for

oxidative DNA damage. *Journal of the National Cancer Institute*, *101*(24), pp.1670-1681.

Korthals, E.T. and Winfrey, M.R., 1987. Seasonal and spatial variations in mercury methylation and demethylation in an oligotrophic lake. *Applied and Environmental Microbiology*, 53(10), pp.2397-2404.

Kot, A., Zabiegała, B. and Namieśnik, J., 2000. Passive sampling for long-term monitoring of organic pollutants in water. *TrAC Trends in Analytical Chemistry*, 19(7), pp.446-459.

Kot-Wasik, A., Zabiegała, B., Urbanowicz, M., Dominiak, E., Wasik, A. and Namieśnik, J., 2007. Advances in passive sampling in environmental studies. *Analytica Chimica Acta*, 602(2), pp.141-163.

Kreuzeder, A., Santner, J., Prohaska, T. and Wenzel, W.W., 2013. Gel for simultaneous chemical imaging of anionic and cationic solutes using diffusive gradients in thin films. *Analytical Chemistry*, 85(24), pp.12028-12036.

Kudo, A., Nagase, H. and Ose, Y., 1982. Proportion of methylmercury to the total amount of mercury in river waters in Canada and Japan. *Water Research*, 16(6), pp.1011-1015.

Kumar, A.R. and Riyazuddin, P., 2010. Preservation of inorganic arsenic species in environmental water samples for reliable speciation analysis. *TrAC Trends in Analytical Chemistry*, *29*(10), pp.1212-1223.

Lapakko, K., 2002. Metal mine rock and waste characterization tools: an overview. *Mining, Minerals and Sustainable Development*, 67, pp.1-30.

Latorre, C.H., García, J.B., Martín, S.G. and Crecente, R.P., 2013. Solid phase extraction for the speciation and preconcentration of inorganic selenium in water samples: A review. *Analytica Chimica Acta*, *804*, pp.37-49.

Leermakers, M., Baeyens, W., Quevauviller, P. and Horvat, M., 2005. Mercury in environmental samples: speciation, artifacts and validation. *TrAC Trends in*

Analytical Chemistry, 24(5), pp.383-393.

Leermakers, M., Meuleman, C. and Baeyens, W., 1996. Mercury distribution and fluxes in Lake Baikal. In Global and regional mercury cycles: Sources, fluxes and mass balances (pp. 303-315). Springer, Dordrecht.

Lemly, A.D., 1993. Guidelines for evaluating selenium data from aquatic monitoring and assessment studies. *Environmental monitoring and assessment*, *28*(1), pp.83-100.

Lemly, A.D., 1999. Selenium transport and bioaccumulation in aquatic ecosystems: a proposal for water quality criteria based on hydrological units. *Ecotoxicology and Environmental Safety*, 42(2), pp.150-156.

Lemly, A.D., 2004. Aquatic selenium pollution is a global environmental safety issue. *Ecotoxicology and Environmental safety*, 59(1), pp.44-56.

Lemly, A.D., 2014. Teratogenic effects and monetary cost of selenium poisoning of fish in Lake Sutton, North Carolina. *Ecotoxicology and Environmental safety*, 104, pp.160-167.

Lenz, M., Gmerek, A. and Lens, P.N., 2006. Selenium speciation in anaerobic granular sludge. *International Journal of Environmental and Analytical Chemistry*, *86*(9), pp.615-627.

Li, B., Zhou, F., Huang, K., Wang, Y., Mei, S., Zhou, Y. and Jing, T., 2016. Highly efficient removal of lead and cadmium during wastewater irrigation using a polyethylenimine-grafted gelatin sponge. *Scientific Reports*, 6, p.33573.

Li, P., Feng, X., Shang, L., Qiu, G., Meng, B., Zhang, H., Guo, Y. and Liang, P., 2011. Human co-exposure to mercury vapor and methylmercury in artisanal mercury mining areas, Guizhou, China. *Ecotoxicology and Environmental Safety*, 74(3), pp.473-479.

Li, W., Zhao, H., Teasdale, P.R., John, R. and Zhang, S., 2002. Application of a cellulose phosphate ion exchange membrane as a binding phase in the diffusive gradients in thin films technique for measurement of trace metals. *Analytica*

Chimica Acta, 464(2), pp.331-339.

Yuan-Hui, L. and Gregory, S., 1974. Diffusion of ions in sea water and in deep-sea sediments. *Geochimica et cosmochimica acta*, *38*(5), pp.703-714.

Li, W.C. and Tse, H.F., 2015. Health risk and significance of mercury in the environment. *Environmental Science and Pollution Research*, 22(1), pp.192-201.

Lin, C.J., Pongprueksa, P., Lindberg, S.E., Pehkonen, S.O., Byun, D. and Jang, C., 2006. Scientific uncertainties in atmospheric mercury models I: Model science evaluation. *Atmospheric Environment*, 40(16), pp.2911-2928.

Lindqvist, O., Johansson, K., Bringmark, L., Timm, B., Aastrup, M., Andersson, A., Hovsenius, G., Håkanson, L., Iverfeldt, Å. and Meili, M., 1991. Mercury in the Swedish environment—recent research on causes, consequences and corrective methods. *Water, Air, and Soil Pollution*, 55(1-2), pp.xi-261.

Livesey, N.T. and Huang, P.M., 1981. Adsorption of arsenate by soils and its relation to selected chemical properties and anions. *Soil Science*, 131(2), pp.88-94.

Lovett, G.M., Burns, D.A., Driscoll, C.T., Jenkins, J.C., Mitchell, M.J., Rustad, L., Shanley, J.B., Likens, G.E. and Haeuber, R., 2007. Who needs environmental monitoring?. *Frontiers in Ecology and the Environment*, 5(5), pp.253-260.

Luo, J., Zhang, H., Santner, J. and Davison, W., 2010. Performance characteristics of diffusive gradients in thin films equipped with a binding gel layer containing precipitated ferrihydrite for measuring arsenic (V), selenium (VI), vanadium (V), and antimony (V). *Analytical chemistry*, *82*(21), pp.8903-8909.

Luoma, S.N. and Presser, T.S., 2009. Emerging opportunities in management of selenium contamination.

Luoma, S.N., Adams, W.J., Chapman, P.M., Brooks, M., Delos, C.G., Maher, W.A., Ohlendorf, H.M., Presser, T.S. and Shaw, P., 2010. *Ecological Assessment of Selenium in the Aquatic Environment*. CRC Press.

Luther III, G.W., 1987. Pyrite oxidation and reduction: molecular orbital theory considerations. *Geochimica et Cosmochimica Acta*, 51(12), pp.3193-3199.

Lyman, B.W., Reehl, W.F. and Rosenblatt, D.H., 1998. *Environmental Inorganic Chemistry: Properties, Processes and Estimation Methods*.

Lyons, W.B., Welch, K.A. and Bonzongo, J.C., 1999. Mercury in aquatic systems in Antarctica. *Geophysical Research Letters*, 26(15), pp.2235-2238.

Ma, Y., Liu, W.J., Zhang, N., Li, Y.S., Jiang, H. and Sheng, G.P., 2014. Polyethylenimine modified biochar adsorbent for hexavalent chromium removal from the aqueous solution. *Bioresource Technology*, 169, pp.403-408.

Ma, W.W., Zhu, M.X., Yang, G.P. and Li, T., 2017. In situ, high-resolution DGT measurements of dissolved sulfide, iron and phosphorus in sediments of the East China Sea: insights into phosphorus mobilization and microbial iron reduction. *Marine Pollution Bulletin*, *124*(1), pp.400-410.

Mackenzie, F.T., Lantzy, R.J. and Paterson, V., 1979. Global trace metal cycles and predictions. *Journal of the International Association for Mathematical Geology*, 11(2), pp.99-142.

Madrid, Y. and Zayas, Z.P., 2007. Water sampling: Traditional methods and new approaches in water sampling strategy. *TrAC Trends in Analytical Chemistry*, 26(4), pp.293-299.

Mady, M.M., Mohammed, W.A., El-Guendy, N.M. and Elsayed, A.A., 2011. Interaction of DNA and polyethylenimine: Fourier-transform infrared (FTIR) and differential scanning calorimetry (DSC) studies. *International Journal of Physical Sciences*, *6*(32), pp.7328-7334.

Magos, L. and Clarkson, T.W., 2006. Overview of the clinical toxicity of mercury. *Annals of Clinical Biochemistry*, 43(4), pp.257-268.

Maier, K.J., Foe, C.G. and Knight, A.W., 1993. Comparative toxicity of selenate, selenite, seleno-DL-methionine and seleno-DL-cystine to Daphnia magna.

Environmental Toxicology and Chemistry, *12*(4), pp.755-763.

Malaj, E., Peter, C., Grote, M., Kühne, R., Mondy, C.P., Usseglio-Polatera, P., Brack, W. and Schäfer, R.B., 2014. Organic chemicals jeopardize the health of freshwater ecosystems on the continental scale. *Proceedings of the National Academy of Sciences*, *111*(26), pp.9549-9554.

Mandal, B.K. and Suzuki, K.T., 2002. Arsenic round the world: a review. *Talanta*, 58(1), pp.201-235.

Mao, J., Kwak, I.S., Sathishkumar, M., Sneha, K. and Yun, Y.S., 2011. Preparation of PEI-coated bacterial biosorbent in water solution: optimization of manufacturing conditions using response surface methodology. *Bioresource Technology*, 102(2), pp.1462-1467.

Mason, R.A. and Sullivan, K.A., 1999. The distribution and speciation of mercury in the South and equatorial Atlantic. *Deep Sea Research Part II: Topical Studies in Oceanography*, 46(5), pp.937-956.

Mason, R.P., Choi, A.L., Fitzgerald, W.F., Hammerschmidt, C.R., Lamborg, C.H., Soerensen, A.L. and Sunderland, E.M., 2012. Mercury biogeochemical cycling in the ocean and policy implications. *Environmental Research*, 119, pp.101-117.

Mason, S., Hamon, R., Nolan, A., Zhang, H. and Davison, W., 2005. Performance of a mixed binding layer for measuring anions and cations in a single assay using the diffusive gradients in thin films technique. *Analytical Chemistry*, 77(19), pp.6339-6346.

Mass, M.J., Tennant, A., Roop, B.C., Cullen, W.R., Styblo, M., Thomas, D.J. and Kligerman, A.D., 2001. Methylated trivalent arsenic species are genotoxic. *Chemical research in toxicology*, *14*(4), pp.355-361.

Mathiesen, T., Ellingsen, D.G. and Kjuus, H., 1999. Neuropsychological effects associated with exposure to mercury vapor among former chloralkali workers.

Scandinavian Journal of Work, Environment & Health, pp.342-350.

Matin, A., Khan, Z., Zaidi, S.M.J. and Boyce, M.C., 2011. Biofouling in reverse osmosis membranes for seawater desalination: phenomena and prevention. *Desalination*, 281, pp.1-16.

Mayer, P., Tolls, J., Hermens, J.L.M. and Mackay, D., 2003. Equilibrium sampling devices (vol 37, pg 186, 2003). *Environmental Science & Technology*, 37(15), pp.270A-270A.

McCarthy, T.S., 2011. The impact of acid mine drainage in South Africa. *South African Journal of Science*, *107*(5-6), pp.01-07.

McKibben, M.A. and Barnes, H.L., 1986. Oxidation of pyrite in low temperature acidic solutions: Rate laws and surface textures. *Geochimica et Cosmochimica Acta*, 50(7), pp.1509-1520.

Meili, M., 1997. Mercury in lakes and rivers. *Metal ions in biological systems*, *34*, pp.21-52.

Meharg, A.A. and Hartley-Whitaker, J., 2002. Arsenic uptake and metabolism in arsenic resistant and nonresistant plant species. *New Phytologist*, *154*(1), pp.29-43.

Mengistu, H.A., 2009. *Application of DGT samplers in monitoring of mine waters of the Witwatersrand goldfields, RSA. International Mine Water Conference, Pretoria, South Africa*, pp. 314-320.

Mengistu, H., Roeyset, O., Tessema, A., Abiye, T.A. and Demlie, M.B., 2012. Diffusive gradient in thin-films (DGT) as risk assessment and management tools in the Central Witwatersrand Goldfield, South Africa. *Water SA*, 38(1), pp.15-22.

Mengistu, H.A., Tessema, A., Demlie, M.B., Abiye, T.A. and Roeyset, O., 2015. Surface-complexation modelling for describing adsorption of phosphate on hydrous ferric oxide surface. *Water SA*, *41*(1), pp.157-167.

Mirlean, N., Seus-Arrache, E.R. and Vlasova, O., 2018. Selenium deficiency in

subtropical littoral pampas: environmental and dietary aspects. *Environmental Geochemistry and Health*, 40(1), pp.543-556.

Mishra, B.K., Dubey, C.S., Shukla, D.P., Bhattacharya, P. and Usham, A.L., 2014. Concentration of arsenic by selected vegetables cultivated in the Yamuna flood plains (YFP) of Delhi, India. *Environmental Earth Sciences*, 72(9), pp.3281-3291.

Mitchell, K., Mason, P.R., Van Cappellen, P., Johnson, T.M., Gill, B.C., Owens, J.D., Diaz, J., Ingall, E.D., Reichart, G.J. and Lyons, T.W., 2012. Selenium as paleo-oceanographic proxy: A first assessment. *Geochimica et Cosmochimica Acta*, 89, pp.302-317.

Mohan, D. and Pittman Jr, C.U., 2007. Arsenic removal from water/wastewater using adsorbents—a critical review. *Journal of Hazardous Materials*, 142(1-2), pp.1-53.

Mongin, S., Uribe, R., Rey-Castro, C., Cecília, J., Galceran, J. and Puy, J., 2013. Limits of the linear accumulation regime of DGT sensors. *Environmental Science & Technology*, 47(18), pp.10438-10445.

Montero, N., Belzunce-Segarra, M.J., Gonzalez, J.L., Larreta, J. and Franco, J., 2012. Evaluation of diffusive gradients in thin-films (DGTs) as a monitoring tool for the assessment of the chemical status of transitional waters within the Water Framework Directive. *Marine Pollution Bulletin*, 64(1), pp.31-39.

Moore, J.N., Ficklin, W.H. and Johns, C., 1988. Partitioning of arsenic and metals in reducing sulfidic sediments. *Environmental Science & Technology*, *22*(4), pp.432-437.

Morcillo, M.A. and Santamaria, J., 1995. Whole-body retention, and urinary and fecal excretion of mercury after subchronic oral exposure to mercuric chloride in rats. *BioMetals*, *8*(4), pp.301-308.

Moreno-Jimenez, E., Six, L., Williams, P.N. and Smolders, E., 2013. Inorganic

species of arsenic in soil solution determined by microcartridges and ferrihydrite-based diffusive gradient in thin films (DGT). *Talanta*, 104, pp.83-89.

Moses, C.O., Nordstrom, D.K., Herman, J.S. and Mills, A.L., 1987. Aqueous pyrite oxidation by dissolved oxygen and by ferric iron. *Geochimica et Cosmochimica Acta*, 51(6), pp.1561-1571.

Motelica-Heino, M., Naylor, C., Zhang, H. and Davison, W., 2003. Simultaneous release of metals and sulfide in lacustrine sediment. *Environmental science & technology*, *37*(19), pp.4374-4381.

Movahedi, A., Lundin, A., Kann, N., Nydén, M. and Moth-Poulsen, K., 2015. Cu (I) stabilizing crosslinked polyethyleneimine. *Physical Chemistry Chemical Physics*, 17(28), pp.18327-18336.

Muscatello, J.R. and Janz, D.M., 2009. Selenium accumulation in aquatic biota downstream of a uranium mining and milling operation. *Science of the Total Environment*, 407(4), pp.1318-1325.

Muscatello, J.R., Belknap, A.M. and Janz, D.M., 2008. Accumulation of selenium in aquatic systems downstream of a uranium mining operation in northern Saskatchewan, Canada. *Environmental Pollution*, 156(2), pp.387-393.

Naftz, D.L. and Rice, J.A., 1989. Geochemical processes controlling selenium in ground water after mining, Powder River Basin, Wyoming, USA. *Applied Geochemistry*, 4(6), pp.565-575.

Naicker, K., Cukrowska, E. and McCarthy, T.S., 2003. Acid mine drainage arising from gold mining activity in Johannesburg, South Africa and environs. *Environmental Pollution*, 122(1), pp.29-40.

Nakamaru, Y., Tagami, K. and Uchida, S., 2006. Effect of phosphate addition on the sorption–desorption reaction of selenium in Japanese agricultural soils. *Chemosphere*, 63(1), pp.109-115.

Nakamaru, Y.M. and Sekine, K., 2008. Sorption behavior of selenium and antimony in soils as a function of phosphate ion concentration. *Soil Science &*

Plant Nutrition, 54(3), pp.332-341.

Namieśnik, J., Zabiegała, B., Kot-Wasik, A., Partyka, M. and Wasik, A., 2005. Passive sampling and/or extraction techniques in environmental analysis: a review. *Analytical and Bioanalytical Chemistry*, 381(2), pp.279-301.

Nancharaiah, Y.V. and Lens, P.N., 2015. Selenium biomineralization for biotechnological applications. *Trends in Biotechnology*, 33(6), pp.323-330.

Navarro, R.R., Sumi, K., Fujii, N. and Matsumura, M., 1996. Mercury removal from wastewater using porous cellulose carrier modified with polyethyleneimine. *Water Research*, 30(10), pp.2488-2494.

Navarro, R.R., Tatsumi, K., Sumi, K. and Matsumura, M., 2001. Role of anions on heavy metal sorption of a cellulose modified with poly (glycidyl methacrylate) and polyethyleneimine. *Water Research*, 35(11), pp.2724-2730.

Neal, R.H. and Alloway, B.J., 1995. Selenium, in Heavy metals in soils. *BJ Alloway*, pp.237-260.

Nearing, M.M., Koch, I. and Reimer, K.J., 2014. Complementary arsenic speciation methods: a review. *Spectrochimica Acta Part B: Atomic Spectroscopy*, 99, pp.150-162.

Ng, J.C., 2005. Environmental contamination of arsenic and its toxicological impact on humans. *Environmental Chemistry*, 2(3), pp.146-160.

Ng, J.C., Wang, J. and Shraim, A., 2003. A global health problem caused by arsenic from natural sources. *Chemosphere*, *52*(9), pp.1353-1359.

Nickel, A., Kottra, G., Schmidt, G., Danier, J., Hofmann, T. and Daniel, H., 2009. Characteristics of transport of selenoamino acids by epithelial amino acid transporters. *Chemico-biological interactions*, *177*(3), pp.234-241.

Nolan, B.T. and Hitt, K.J., 2006. Vulnerability of shallow groundwater and drinking-water wells to nitrate in the United States. *Environmental Science & Technology*, 40(24), pp.7834-7840.

Nriagu, J.O., 1989. Global cycling of selenium. *Occurrence and Distribution of Selenium*, pp.327-340.

O'Day, P.A., 2006. Chemistry and mineralogy of arsenic. *Elements*, *2*(2), pp.77-83.

Okkenhaug, G., Zhu, Y.G., He, J., Li, X., Luo, L. and Mulder, J., 2012. Antimony (Sb) and arsenic (As) in Sb mining impacted paddy soil from Xikuangshan, China: differences in mechanisms controlling soil sequestration and uptake in rice. *Environmental Science & Technology*, 46(6), pp.3155-3162.

Onishi, H. and Wedepohl, K.H., 1969. *Handbook of Geochemistry*. *Vol. II*, Edited by KH Wedepohl.

Onken, B.M. and Adriano, D.C., 1997. Arsenic availability in soil with time under saturated and subsaturated conditions. *Soil Science Society of America Journal*, *61*(3), pp.746-752.

Pang, Y., Zeng, G., Tang, L., Zhang, Y., Liu, Y., Lei, X., Li, Z., Zhang, J. and Xie, G., 2011a. PEI-grafted magnetic porous powder for highly effective adsorption of heavy metal ions. *Desalination*, *281*, pp.278-284.

Pang, Y., Zeng, G., Tang, L., Zhang, Y., Liu, Y., Lei, X., Li, Z., Zhang, J., Liu, Z. and Xiong, Y., 2011b. Preparation and application of stability enhanced magnetic nanoparticles for rapid removal of Cr (VI). *Chemical Engineering Journal*, 175, pp.222-227.

Panther, J.G., Bennett, W.W., Welsh, D.T. and Teasdale, P.R., 2013. Simultaneous measurement of trace metal and oxyanion concentrations in water using diffusive gradients in thin films with a Chelex–Metsorb mixed binding layer. *Analytical Chemistry*, 86(1), pp.427-434.

Panther, J.G., Stillwell, K.P., Powell, K.J. and Downard, A.J., 2008. Development and application of the diffusive gradients in thin films technique for the measurement of total dissolved inorganic arsenic in waters. *Analytica Chimica Acta*, 622(1-2), pp.133-142.

Panther, J.G., Teasdale, P.R., Bennett, W.W., Welsh, D.T. and Zhao, H., 2011. Comparing dissolved reactive phosphorus measured by DGT with ferrihydrite and titanium dioxide adsorbents: Anionic interferences, adsorbent capacity and deployment time. *Analytica chimica acta*, *698*(1-2), pp.20-26.

Parker, D.R., Page, A.L. and Bell, P.F., 1992. Contrasting selenate-sulfate interactions in selenium-accumulating and nonaccumulating plant species. *Soil Science Society of America Journal*, 56(6), pp.1818-1824.

Parkhurst, D.L. and Wissmeier, L., 2015. PhreeqcRM: A reaction module for transport simulators based on the geochemical model PHREEQC. *Advances in Water Resources*, *83*, pp.176-189.

Patra, M. and Sharma, A., 2000. Mercury toxicity in plants. *The Botanical Review*, 66(3), pp.379-422.

Patra, M., Bhowmik, N., Bandopadhyay, B. and Sharma, A., 2004. Comparison of mercury, lead and arsenic with respect to genotoxic effects on plant systems and the development of genetic tolerance. *Environmental and Experimental Botany*, 52(3), pp.199-223.

Pelcová, P., Dočekalová, H. and Kleckerová, A., 2014. Development of the diffusive gradient in thin films technique for the measurement of labile mercury species in waters. *Analytica chimica acta*, *819*, pp.42-48.

Peng, Q., Wang, M., Cui, Z., Huang, J., Chen, C., Guo, L. and Liang, D., 2017. Assessment of bioavailability of selenium in different plant-soil systems by diffusive gradients in thin-films (DGT). *Environmental Pollution*, 225, pp.637-643.

Penglase, S., Hamre, K. and Ellingsen, S., 2014. Selenium and mercury have a synergistic negative effect on fish reproduction. *Aquatic Toxicology*, *149*, pp.16-24.

Persico, J.L. and Brookins, D.G., 1988. Selenium geochemistry at Bosque Del

Apache National Wildlife Refuge. In *New Mex Geeological Soc Guidebook 39th F Conf. New Mexico: New Mexico Geological Society Guidebook* (pp. 211-216).

Persson, L.B., Morrison, G.M., Friemann, J.U., Kingston, J., Mills, G. and Greenwood, R., 2001. Diffusional behaviour of metals in a passive sampling system for monitoring aquatic pollution. *Journal of Environmental Monitoring*, 3(6), pp.639-645.

Petersen, J., Paschke, A., Gunold, R. and Schüürmann, G., 2015. Calibration of Chemcatcher® passive sampler for selected highly hydrophobic organic substances under fresh and sea water conditions. *Environmental Science: Water Research & Technology*, 1(2), pp.218-226.

Petrick, J.S., Ayala-Fierro, F., Cullen, W.R., Carter, D.E. and Aposhian, H.V., 2000. Monomethylarsonous acid (MMAIII) is more toxic than arsenite in Chang human hepatocytes. *Toxicology and applied pharmacology*, *163*(2), pp.203-207.

Petrick, J.S., Jagadish, B., Mash, E.A. and Aposhian, H.V., 2001. Monomethylarsonous acid (MMAIII) and arsenite: LD50 in hamsters and in vitro inhibition of pyruvate dehydrogenase. *Chemical research in toxicology*, *14*(6), pp.651-656.

Pham, A.L.T., Johnson, C., Manley, D. and Hsu-Kim, H., 2015. Influence of sulfide nanoparticles on dissolved mercury and zinc quantification by diffusive gradient in thin-film passive samplers. *Environmental Science & Technology*, 49(21), pp.12897-12903.

Pichette, C., Zhang, H. and Sauvé, S., 2009. Using diffusive gradients in thin-films for in situ monitoring of dissolved phosphate emissions from freshwater aquaculture. *Aquaculture*, 286(3-4), pp.198-202.

Piotrowski, J.K., Szymańska, J.A., Skrzypińska-Gawrysiak, M., Kotelo, J. and Sporny, S., 1992. Intestinal absorption of inorganic mercury in rat. *Pharmacology & toxicology*, *70*(1), pp.53-55.

Pirrone, N. and Mahaffey, K.R. eds., 2005. Dynamics of mercury pollution on

regional and global scales: atmospheric processes and human exposures around the world. Springer Science & Business Media.

Pirrone, N., Cinnirella, S., Feng, X., Finkelman, R.B., Friedli, H.R., Leaner, J., Mason, R., Mukherjee, A.B., Stracher, G.B., Streets, D.G. and Telmer, K., 2010. Global mercury emissions to the atmosphere from anthropogenic and natural sources. *Atmospheric Chemistry and Physics*, 10(13), pp.5951-5964.

Pirrone, N., Costa, P., Pacyna, J.M. and Ferrara, R., 2001. Mercury emissions to the atmosphere from natural and anthropogenic sources in the Mediterranean region. *Atmospheric Environment*, 35(17), pp.2997-3006.

Plant, J.A., Kinniburgh, D.G., Smedley, P.L., Fordyce, F.M. and Klinck, B.A., 2003. Arsenic and selenium. *Treatise on Geochemistry*, 9, p.612.

Price, H.L., Teasdale, P.R. and Jolley, D.F., 2013. An evaluation of ferrihydrite- and Metsorb™-DGT techniques for measuring oxyanion species (As, Se, V, P): Effective capacity, competition and diffusion coefficients. *Analytica Chimica Acta*, 803, pp.56-65.

Puschenreiter, M., 2009. Trace Elements as Contaminants and Nutrients: Consequences in Ecosystems and Human Health. Edited by MNV Prasad. *ChemSusChem: Chemistry & Sustainability Energy & Materials*, 2(7), pp.677-677.

Pyrzyńska, K., 2002. Determination of selenium species in environmental samples. *Microchimica Acta*, *140*(1-2), pp.55-62.

Qian, J., Zhang, L., Chen, H., Hou, M., Niu, Y., Xu, Z. and Liu, H., 2009. Distribution of mercury pollution and its source in the soils and vegetables in Guilin area, China. *Bulletin of Environmental Contamination and Toxicology*, 83(6), p.920.

Qin, W., Gu, Y., Wang, G., Wu, T., Zhang, H., Tang, X., Zhang, Y. and Zhao, H., 2018. Zirconium metal organic frameworks-based DGT technique for in situ measurement of dissolved reactive phosphorus in waters. *Water research*, *147*,

pp.223-232.

Qiu, G., Feng, X., Wang, S. and Shang, L., 2005. Mercury and methylmercury in riparian soil, sediments, mine-waste calcines, and moss from abandoned Hg mines in east Guizhou province, southwestern China. *Applied Geochemistry*, 20(3), pp.627-638.

Qu, X., Wirsen, A. and Albertsson, A.C., 2000. Novel pH-sensitive chitosan hydrogels: swelling behavior and states of water. *Polymer*, *41*(12), pp.4589-4598.

Quinn, F.X., Kampff, E., Smyth, G. and McBrierty, V.J., 1988. Water in hydrogels. 1. A study of water in poly (N-vinyl-2-pyrrolidone/methyl methacrylate) copolymer. *Macromolecules*, *21*(11), pp.3191-3198.

Rascio, N. and Navari-Izzo, F., 2011. Heavy metal hyperaccumulating plants: how and why do they do it? And what makes them so interesting? *Plant Science*, 180(2), pp.169-181.

Rayman, M.P., 2000. The importance of selenium to human health. *The Lancet*, 356(9225), pp.233-241.

Reddy, M.M. and Aiken, G.R., 2001. Fulvic acid-sulfide ion competition for mercury ion binding in the Florida Everglades. *Water, Air, and Soil Pollution*, 132(1-2), pp.89-104.

Reeder, R.J., Schoonen, M.A. and Lanzirotti, A., 2006. Metal speciation and its role in bioaccessibility and bioavailability. *Reviews in Mineralogy and Geochemistry*, 64(1), pp.59-113.

Reisinger, H.J., Burris, D.R. and Hering, J.G., 2005. Remediating subsurface arsenic contamination with monitored natural attenuation.

Rensing, C. and Rosen, B.P., 2009. Heavy metals cycles (arsenic, mercury, selenium, others) In: Schaechter M, editor. Encyclopedia of Microbiology.

Rinklebe, J., Kumpiene, J., Du Laing, G. and Ok, Y.S., 2017. Biogeochemistry of

trace elements in the environment–editorial to the special issue. *Journal of Environmental Management*, (186), pp.127-130.

Risher, J.F. and Tucker, P., 2016. Alkyl mercury-induced toxicity: Multiple mechanisms of action. In *Reviews of Environmental Contamination and Toxicology Volume 240* (pp. 105-149). Springer, Cham.

Ritchie, A.I.M., 1994. Sulfide oxidation mechanisms: controls and rates of oxygen transport. *The Environmental Geochemistry of Sulfide Mine Wastes*, pp.201-245.

Roll, I.B. and Halden, R.U., 2016. Critical review of factors governing data quality of integrative samplers employed in environmental water monitoring. *Water Research*, 94, pp.200-207.

Rosemond, A.D., Reice, S.R., Elwood, J.W. and Mulholland, P.J., 1992. The effects of stream acidity on benthic invertebrate communities in the south-eastern United States. *Freshwater Biology*, *27*(2), pp.193-209.

Ruello, M.L., Sileno, M., Sani, D. and Fava, G., 2008. DGT use in contaminated site characterization. The importance of heavy metal site specific behaviour. *Chemosphere*, 70(6), pp.1135-1140.

Rumpler, A., Edmonds, J.S., Katsu, M., Jensen, K.B., Goessler, W., Raber, G., Gunnlaugsdottir, H. and Francesconi, K.A., 2008. Arsenic-containing long-chain fatty acids in cod-liver oil: a result of biosynthetic infidelity?. *Angewandte Chemie*, *120*(14), pp.2705-2707.

Russo, K.E., 2017. Living Well, Within the Limits of Our Planet: Terms in EU Press Releases.

Saad, D.M., Cukrowska, E.M. and Tutu, H., 2011. Development and application of cross-linked polyethylenimine for trace metal and metalloid removal from mining and industrial wastewaters. *Toxicological & Environmental Chemistry*, 93(5), pp.914-924.

Saad, D.M., Cukrowska, E.M. and Tutu, H., 2012. Phosphonated cross-linked polyethylenimine for selective removal of uranium ions from aqueous solutions.

Water Science and Technology, 66(1), pp.122-129.

Saad, D.M., Cukrowska, E.M. and Tutu, H., 2012. Sulfonated cross-linked polyethylenimine for selective removal of mercury from aqueous solutions. *Toxicological & Environmental Chemistry*, 94(10), pp.1916-1929.

Saad, D.M., Cukrowska, E.M. and Tutu, H., 2013. Functionalisation of cross-linked polyethylenimine for the removal of As from mining wastewater. *Water SA*, 39(2), pp.257-264.

Saad, D.M., Cukrowska, E.M. and Tutu, H., 2013. Modified cross-linked polyethylenimine for the removal of selenite from mining wastewaters. *Toxicological & Environmental Chemistry*, 95(3), pp.409-421.

Saad, D.M., Cukrowska, E.M. and Tutu, H., 2013. Selective removal of mercury from aqueous solutions using thiolated cross-linked polyethylenimine. *Applied Water Science*, 3(2), pp.527-534.

Sadiq, M., 1997. Arsenic chemistry in soils: an overview of thermodynamic predictions and field observations. *Water, Air, and Soil Pollution*, 93(1-4), pp.117-136.

Santos, S., Ungureanu, G., Boaventura, R. and Botelho, C., 2015. Selenium contaminated waters: an overview of analytical methods, treatment options and recent advances in sorption methods. *Science of the Total Environment*, *521*, pp.246-260.

Say, R., Tuncel, A. and Denizli, A., 2002. Adsorption of Ni^{2+} from aqueous solutions by novel polyethyleneimine-attached poly (p-chloromethylstyrene) beads. *Journal of Applied Polymer Science*, 83(11), pp.2467-2473.

Scally, S., Davison, W. and Zhang, H., 2006. Diffusion coefficients of metals and metal complexes in hydrogels used in diffusive gradients in thin films. *Analytica Chimica Acta*, 558(1-2), pp.222-229.

Schaeffer, R., Fodor, P. and Soeroes, C., 2006. Development of a liquid chromatography/electrospray selected reaction monitoring method for the

determination of organoarsenic species in marine and freshwater samples. *Rapid Communications in Mass Spectrometry: An International Journal Devoted to the Rapid Dissemination of Up-to-the-Minute Research in Mass Spectrometry*, *20*(19), pp.2979-2989.

Séby, F., Potin-Gautier, M., Giffaut, E., Borge, G. and Donard, O.F.X., 2001. A critical review of thermodynamic data for selenium species at 25 C. *Chemical Geology*, 171(3-4), pp.173-194.

Seddique, A.A., Masuda, H., Mitamura, M., Shinoda, K., Yamanaka, T., Itai, T., Maruoka, T., Uesugi, K., Ahmed, K.M. and Biswas, D.K., 2008. Arsenic release from biotite into a Holocene groundwater aquifer in Bangladesh. *Applied Geochemistry*, 23(8), pp.2236-2248.

Seethapathy, S., Gorecki, T. and Li, X., 2008. Passive sampling in environmental analysis. *Journal of Chromatography A*, 1184(1-2), pp.234-253.

Selim, H.M. and Amacher, M.C., 2001. Sorption and release of heavy metals in soils: nonlinear kinetics. *Heavy Metals release in soils*, pp.1-29.

Semu, E., Singh, B.R. and Selmer-Olsen, A.R., 1987. Adsorption of mercury compounds by tropical soils II. Effect of soil: solution ratio, ionic strength, pH, and organic matter. *Water, Air, and Soil Pollution*, 32(1-2), pp.1-10.

Setyono, D. and Valiyaveettil, S., 2016. Functionalized paper—A readily accessible adsorbent for removal of dissolved heavy metal salts and nanoparticles from water. *Journal of Hazardous Materials*, 302, pp.120-128.

Shahid, M., Niazi, N.K., Khalid, S., Murtaza, B., Bibi, I. and Rashid, M.I., 2018. A critical review of selenium biogeochemical behavior in soil-plant system with an inference to human health. *Environmental Pollution*, 234, pp.915-934.

Sharma, A.K., 1990. Genetic architecture of chromosome. *Advances in Cell and Chromosome Research.*, pp.145-160.

Sharma, V.K. and Sohn, M., 2009. Aquatic arsenic: toxicity, speciation,

transformations, and remediation. *Environment international*, *35*(4), pp.743-759.

Sharma, V.K., McDonald, T.J., Sohn, M., Anquandah, G.A., Pettine, M. and Zboril, R., 2015. Biogeochemistry of selenium. A review. *Environmental Chemistry Letters*, 13(1), pp.49-58.

Shiva, A.H., Teasdale, P.R., Bennett, W.W. and Welsh, D.T., 2015. A systematic determination of diffusion coefficients of trace elements in open and restricted diffusive layers used by the diffusive gradients in a thin film technique. *Analytica Chimica Acta*, 888, pp.146-154.

Sigrist, M.E., Brusa, L., Beldomenico, H.R., Dosso, L., Tsendra, O.M., González, M.B., Pieck, C.L. and Vera, C.R., 2014. Influence of the iron content on the arsenic adsorption capacity of Fe/GAC adsorbents. *Journal of Environmental Chemical Engineering*, 2(2), pp.927-934.

Singer, P.C. and Stumm, W., 1970. Acidic mine drainage: the rate-determining step. *Science*, 167(3921), pp.1121-1123.

Skousen, J., Rose, A., Geidel, G., Foreman, J., Evans, R. and Hellier, W., 1998. Handbook of technologies for avoidance and remediation of acid mine drainage. National Mine Land Reclamation Center, Morgantown, 131.

Skyllberg, U., 2008. Competition among thiols and inorganic sulfides and polysulfides for Hg and MeHg in wetland soils and sediments under suboxic conditions: Illumination of controversies and implications for MeHg net production. *Journal of Geophysical Research: Biogeosciences*, 113(G2).

Smedley, P.L. and Kinniburgh, D.G., 2002. A review of the source, behaviour and distribution of arsenic in natural waters. *Applied Geochemistry*, 17(5), pp.517-568.

Smedley, P.L., Zhang, M., Zhang, G. and Luo, Z., 2003. Mobilisation of arsenic and other trace elements in fluviolacustrine aquifers of the Huhhot Basin, Inner Mongolia. *Applied Geochemistry*, 18(9), pp.1453-1477.

Smith, A.H., Lingas, E.O. and Rahman, M., 2000. Contamination of drinking-

water by arsenic in Bangladesh: a public health emergency. *Bulletin of the World Health Organization*, 78, pp.1093-1103.

Smith, E., Naidu, R. and Alston, A.M., 2002. Chemistry of inorganic arsenic in soils. *Journal of Environmental Quality*, 31(2), pp.557-563.

Smith, J.V.S., Jankowski, J. and Sammut, J., 2003. Vertical distribution of As (III) and As (V) in a coastal sandy aquifer: factors controlling the concentration and speciation of arsenic in the Stuarts Point groundwater system, northern New South Wales, Australia. *Applied Geochemistry*, 18(9), pp.1479-1496.

Sogn, T.A., Eich-Greatorex, S., Røyset, O., Falk Øgaard, A. and Almås, Å.R., 2008. Use of diffusive gradients in thin films to predict potentially bioavailable selenium in soil. *Communications in soil science and plant analysis*, *39*(3-4), pp.587-602.

Søndergaard, J., Bach, L. and Gustavson, K., 2014. Measuring bioavailable metals using diffusive gradients in thin films (DGT) and transplanted seaweed (Fucus vesiculosus), blue mussels (Mytilus edulis) and sea snails (Littorina saxatilis) suspended from monitoring buoys near a former lead–zinc mine in West Greenland. *Marine Pollution Bulletin*, 78(1-2), pp.102-109.

Spell, H.L., 1969. Determination of piperazine rings in ethyleneamines, poly (ethyleneamine), and polyethylenimine by infrared spectrometry. *Analytical Chemistry*, 41(7), pp.902-905.

Spyropoulou, A., Lazarou, Y.G. and Laspidou, C., 2018. Mercury Speciation in the Water Distribution System of Skiathos Island, Greece. *In Multidisciplinary Digital Publishing Institute Proceedings* (Vol. 2, No. 11, p. 668).

Stachowicz, M., Hiemstra, T. and Van Riemsdijk, W.H., 2007. Arsenic− bicarbonate interaction on goethite particles. *Environmental science & technology*, *41*(16), pp.5620-5625.

Staicu, L.C., Van Hullebusch, E.D., Oturan, M.A., Ackerson, C.J. and Lens, P.N., 2015. Removal of colloidal biogenic selenium from wastewater. *Chemosphere*,

125, pp.130-138.

Stewart, R., Grosell, M., Buchwalter, D.B., Fisher, N.S., Luoma, S.N., Mathews, T., Orr, P. and Wang, W., 2010. Bioaccumulation and trophic transfer of selenium. *In Ecological assessment of selenium in the aquatic environment*.

Stockdale, A., Davison, W. and Zhang, H., 2008. High-resolution two-dimensional quantitative analysis of phosphorus, vanadium and arsenic, and qualitative analysis of sulfide, in a freshwater sediment. *Environmental Chemistry*, *5*(2), pp.143-149.

Stroski, K.M., Challis, J.K. and Wong, C.S., 2018. The influence of pH on sampler uptake for an improved configuration of the organic-diffusive gradients in thin films passive sampler. *Analytica Chimica Acta*, 1018, pp.45-53.

Suda, I., Suda, M. and Hirayama, K., 1993. Degradation of methyl and ethyl mercury by singlet oxygen generated from sea water exposed to sunlight or ultraviolet light. *Archives of Toxicology*, 67(5), pp.365-368.

Sun, H.J., Rathinasabapathi, B., Wu, B., Luo, J., Pu, L.P. and Ma, L.Q., 2014. Arsenic and selenium toxicity and their interactive effects in humans. *Environment international*, *69*, pp.148-158.

Sun, Q., Chen, J., Zhang, H., Ding, S., Li, Z., Williams, P.N., Cheng, H., Han, C., Wu, L. and Zhang, C., 2014. Improved diffusive gradients in thin films (DGT) measurement of total dissolved inorganic arsenic in waters and soils using a hydrous zirconium oxide binding layer. *Analytical chemistry*, *86*(6), pp.3060-3067.

Sun, Q., Zhang, L., Ding, S., Li, C., Yang, J., Chen, J. and Wang, P., 2015. Evaluation of the diffusive gradients in thin films technique using a mixed binding gel for measuring iron, phosphorus and arsenic in the environment. *Environmental Science: Processes & Impacts*, 17(3), pp.570-577.

Sun, X.F., Ma, Y., Liu, X.W., Wang, S.G., Gao, B.Y. and Li, X.M., 2010. Sorption and detoxification of chromium (VI) by aerobic granules functionalized

with polyethylenimine. *Water Research*, 44(8), pp.2517-2524.

Sun, Z., Zhang, Y., Deng, X., Li, J. and Xiong, C., 2012. Fabrication and application of silicalite-1 and TS-1 hollow fibers with polyethylene imine (PEI) fibers as substrates. *Journal of Industrial and Engineering Chemistry*, 18(1), pp.92-97.

Sutcliffe, D.W. and Hildrew, A.G., 1989. Invertebrate communities in acid streams. *Acid toxicity and aquatic animals*, *34*, pp.13-28.

Suzuki, N., Naranmandura, H., Hirano, S. and Suzuki, K.T., 2008. Theoretical calculations and reaction analysis on the interaction of pentavalent thioarsenicals with biorelevant thiol compounds. *Chemical research in toxicology*, *21*(2), pp.550-553.

Swanson, H.K. and Kidd, K.A., 2010. Mercury concentrations in Arctic food fishes reflect the presence of anadromous Arctic charr (Salvelinus alpinus), species, and life history. *Environmental Science & Technology*, 44(9), pp.3286-3292.

Takamatsu, T., Kawashima, M. and Koyama, M., 1985. The role of Mn^{2+}-rich hydrous manganese oxide in the accumulation of arsenic in lake sediments. *Water Research*, *19*(8), pp.1029-1032.

Tan, L.C., Nancharaiah, Y.V., van Hullebusch, E.D. and Lens, P.N., 2016. Selenium: environmental significance, pollution, and biological treatment technologies. *Biotechnology Advances*, 34(5), pp.886-907.

Tan, L.C., Nancharaiah, Y.V., van Hullebusch, E.D. and Lens, P.N., 2018. Selenium: environmental significance, pollution, and biological treatment technologies. *In Anaerobic Treatment of Mine Wastewater for the Removal of Selenate and its Co-Contaminants* (pp. 9-71). CRC Press.

Tawfik, D.S. and Viola, R.E., 2011. Arsenate replacing phosphate: alternative life chemistries and ion promiscuity. *Biochemistry*, 50(7), pp.1128-1134.

Taylor, J.B., Reynolds, L.P., Redmer, D.A. and Caton, J.S., 2009. Maternal and fetal tissue selenium loads in nulliparous ewes fed supranutritional and excessive selenium during mid-to late pregnancy. *Journal of Animal Science*, 87(5), pp.1828-1834.

Terry, N., Zayed, A.M., De Souza, M.P. and Tarun, A.S., 2000. Selenium in higher plants. *Annual Review of Plant Biology*, 51(1), pp.401-432.

Thakur, A.K., Nisola, G.M., Limjuco, L.A., Parohinog, K.J., Torrejos, R.E.C., Shahi, V.K. and Chung, W.J., 2017. Polyethylenimine-modified mesoporous silica adsorbent for simultaneous removal of Cd (II) and Ni (II) from aqueous solution. *Journal of Industrial and Engineering Chemistry*, 49, pp.133-144.

Thiry, C., Ruttens, A., De Temmerman, L., Schneider, Y.J. and Pussemier, L., 2012. Current knowledge in species-related bioavailability of selenium in food. *Food Chemistry*, 130(4), pp.767-784.

Thorburn, P.J., Biggs, J.S., Weier, K.L. and Keating, B.A., 2003. Nitrate in groundwaters of intensive agricultural areas in coastal Northeastern Australia. *Agriculture, Ecosystems & Environment*, 94(1), pp.49-58.

Todo, K. and Sato, K., 2002. Directive 2000/60/EC of the European Parliament and of the Council of 23 October 2000 establishing a framework for Community action in the field of water policy. *ENVIRONMENTAL RESEARCH QUARTERLY*, pp.66-106.

Tokunaga, T.K., Pickering, I.J. and Brown, G.E., 1996. Selenium transformations in ponded sediments. *Soil Science Society of America Journal*, 60(3), pp.781-790.

Torres, J., Pintos, V., Gonzatto, L., Domínguez, S., Kremer, C. and Kremer, E., 2011. Selenium chemical speciation in natural waters: Protonation and complexation behavior of selenite and selenate in the presence of environmentally relevant cations. *Chemical Geology*, 288(1-2), pp.32-38.

Turner, G.S., Mills, G.A., Bowes, M.J., Burnett, J.L., Amos, S. and Fones, G.R., 2014. Evaluation of DGT as a long-term water quality monitoring tool in natural

waters; uranium as a case study. *Environmental Science: Processes & Impacts*, 16(3), pp.393-403.

Turnpenny, A.W.H., 1989. Field studies on fisheries in acid waters in the United Kingdom. *Acid toxicity and aquatic animals*, *34*, p.45.

Tutu, H., McCarthy, T.S. and Cukrowska, E., 2008. The chemical characteristics of acid mine drainage with particular reference to sources, distribution and remediation: The Witwatersrand Basin, South Africa as a case study. *Applied Geochemistry*, 23(12), pp.3666-3684.

Tutu, H., Camden-Smith, B., Cukrowska, E., Bakatula, E., Weiersbye, I. and Sutton, M., 2011. Mineral efflorescent crusts as sources of pollution in gold mining environments in the Witwatersrand Basin. *International Mine Water Association Proceedings:" Mine Water–Managing the Challenges", Aachen, Germany*, pp.623-626.

Tuzen, M. and Sarı, A., 2010. Biosorption of selenium from aqueous solution by green algae (Cladophora hutchinsiae) biomass: equilibrium, thermodynamic and kinetic studies. *Chemical Engineering Journal*, 158(2), pp.200-206.

Uher, E., Zhang, H., Santos, S., Tusseau-Vuillemin, M.H. and Gourlay-Francé, C., 2012. Impact of biofouling on diffusive gradient in thin film measurements in water. *Analytical Chemistry*, 84(7), pp.3111-3118.

Uher, E., Besse, J.P., Delaigue, O., Husson, F. and Lebrun, J.D., 2018. Comparison of the metal contamination in water measured by diffusive gradient in thin film (DGT), biomonitoring and total metal dissolved concentration at a national scale. *Applied Geochemistry*, *88*, pp.247-257.

Ullrich, S.M., Tanton, T.W. and Abdrashitova, S.A., 2001. Mercury in the aquatic environment: a review of factors affecting methylation. *Critical Reviews in Environmental Science and Technology*, 31(3), pp.241-293.

UNEP, G.M.A., 2002. United Nations Environment Programme. *Chemicals, Geneva, Switzerland*.

USGS, 2015. Mineral Commodity Summaries 2015. U.S. *Geological Survey*

Vandal, G.M., Mason, R.P., McKnight, D. and Fitzgerald, W., 1998. Mercury speciation and distribution in a polar desert lake (Lake Hoare, Antarctica) and two glacial meltwater streams. *Science of the Total Environment*, 213(1-3), pp.229-237.

Ventura, M.G., Stibilj, V., do Carmo Freitas, M. and Pacheco, A.M., 2009. Determination of ultratrace levels of selenium in fruit and vegetable samples grown and consumed in Portugal. *Food Chemistry*, 115(1), pp.200-206.

Vesper, D.J., Roy, M. and Rhoads, C.J., 2008. Selenium distribution and mode of occurrence in the Kanawha Formation, southern West Virginia, USA. *International Journal of Coal Geology*, *73*(3-4), pp.237-249.

von der Ohe, P.C., Dulio, V., Slobodnik, J., De Deckere, E., Kühne, R., Ebert, R.U., Ginebreda, A., De Cooman, W., Schüürmann, G. and Brack, W., 2011. A new risk assessment approach for the prioritization of 500 classical and emerging organic microcontaminants as potential river basin specific pollutants under the European Water Framework Directive. *Science of the Total Environment*, 409(11), pp.2064-2077.

Voulvoulis, N., Arpon, K.D. and Giakoumis, T., 2017. The EU Water Framework Directive: From great expectations to problems with implementation. *Science of the Total Environment*, *575*, pp.358-366.

Vrana, B., Allan, I.J., Greenwood, R., Mills, G.A., Dominiak, E., Svensson, K., Knutsson, J. and Morrison, G., 2005. Passive sampling techniques for monitoring pollutants in water. *TrAC Trends in Analytical Chemistry*, 24(10), pp.845-868.

Vrana, B., Mills, G.A., Dominiak, E. and Greenwood, R., 2006. Calibration of the Chemcatcher passive sampler for the monitoring of priority organic pollutants in water. *Environmental Pollution*, 142(2), pp.333-343.

Vrana, B., Mills, G.A., Kotterman, M., Leonards, P., Booij, K. and Greenwood, R., 2007. Modelling and field application of the Chemcatcher passive sampler

calibration data for the monitoring of hydrophobic organic pollutants in water. *Environmental Pollution*, 145(3), pp.895-904.

Wakim, R., Bashour, I., Nimah, M., Sidahmed, M. and Toufeili, I., 2010. Selenium levels in Lebanese environment. *Journal of Geochemical Exploration*, 107(2), pp.94-99.

Wang, C., Yao, Y., Wang, P., Hou, J., Qian, J., Yuan, Y. and Fan, X., 2016. In situ high-resolution evaluation of labile arsenic and mercury in sediment of a large shallow lake. *Science of the Total Environment*, 541, pp.83-91.

Wang, J. and Li, Z., 2015. Enhanced selective removal of Cu (II) from aqueous solution by novel polyethylenimine-functionalized ion imprinted hydrogel: behaviors and mechanisms. *Journal of Hazardous Materials*, 300, pp.18-28.

Wang, J., Feng, X., Anderson, C.W., Xing, Y. and Shang, L., 2012. Remediation of mercury contaminated sites–a review. *Journal of Hazardous Materials*, 221, pp.1-18.

Wang, S. and Mulligan, C.N., 2006. Occurrence of arsenic contamination in Canada: sources, behavior and distribution. *Science of the Total Environment*, 366(2-3), pp.701-721.

Wang, Y., Ding, S., Gong, M., Xu, S., Xu, W. and Zhang, C., 2016. Diffusion characteristics of agarose hydrogel used in diffusive gradients in thin films for measurements of cations and anions. *Analytica Chimica Acta*, 945, pp.47-56.

Wang, Y., Ding, S., Shi, L., Gong, M., Xu, S. and Zhang, C., 2017. Simultaneous measurements of cations and anions using diffusive gradients in thin films with a ZrO-Chelex mixed binding layer. *Analytica Chimica Acta*, 972, pp.1-11.

Wang, Y., Liang, S., Chen, B., Guo, F., Yu, S. and Tang, Y., 2013. Synergistic removal of Pb (II), Cd (II) and humic acid by Fe3O4@ mesoporous silica-graphene oxide composites. PLoS One, 8(6), p.65634.

Wang, Y., Wilson, J.M. and VanBriesen, J.M., 2015. The effect of sampling strategies on assessment of water quality criteria attainment. *Journal of*

Environmental Management, 154, pp.33-39.

Wang, Y., Wu, D., Wei, Q., Wei, D., Yan, T., Yan, L., Hu, L. and Du, B., 2017. Rapid removal of Pb (II) from aqueous solution using branched polyethylenimine enhanced magnetic carboxymethyl chitosan optimized with response surface methodology. *Scientific Reports*, 7(1), p.10264.

Warnken, K.W., Zhang, H. and Davison, W., 2005. Trace metal measurements in low ionic strength synthetic solutions by diffusive gradients in thin films. *Analytical Chemistry*, 77(17), pp.5440-5446.

Warnken, K.W., Zhang, H. and Davison, W., 2006. Accuracy of the diffusive gradients in thin-films technique: diffusive boundary layer and effective sampling area considerations. *Analytical Chemistry*, 78(11), pp.3780-3787.

Webb, J.A. and Keough, M.J., 2002. Measurement of environmental trace-metal levels with transplanted mussels and diffusive gradients in thin films (DGT): a comparison of techniques. *Marine Pollution Bulletin*, 44(3), pp.222-229.

Werdmüller, V.W. and Antrobus, E.S.A., 1986. The Central Rand, in Witwatersrand gold–100 years. Johannesburg: Geological Society of South Africa.

Mercury, W.I., 1991. Environmental Health Criteria 118. *Geneva: World Health Organization*, *107*.

White, P.J., Bowen, H.C., Parmaguru, P., Fritz, M., Spracklen, W.P., Spiby, R.E., Meacham, M.C., Mead, A., Harriman, M., Trueman, L.J. and Smith, B.M., 2004. Interactions between selenium and sulphur nutrition in Arabidopsis thaliana. *Journal of Experimental Botany*, 55(404), pp.1927-1937.

White, P.J., Broadley, M.R. and Gregory, P.J., 2012. Managing the nutrition of plants and people. *Applied and Environmental Soil Science*, 2012.

Wijnja, H. and Schulthess, C.P., 2000. Vibrational spectroscopy study of selenate and sulfate adsorption mechanisms on Fe and Al (hydr) oxide surfaces. *Journal of*

Colloid and Interface Science, 229(1), pp.286-297.

Williams, P.N., Lei, M., Sun, G., Huang, Q., Lu, Y., Deacon, C., Meharg, A.A. and Zhu, Y.G., 2009. Occurrence and partitioning of cadmium, arsenic and lead in mine impacted paddy rice: Hunan, China. *Environmental Science & Technology*, 43(3), pp.637-642.

Winkel, L., Vriens, B., Jones, G., Schneider, L., Pilon-Smits, E. and Bañuelos, G., 2015. Selenium cycling across soil-plant-atmosphere interfaces: a critical review. *Nutrients*, *7*(6), pp.4199-4239.

Winkel, L.H., Johnson, C.A., Lenz, M., Grundl, T., Leupin, O.X., Amini, M. and Charlet, L., 2011. Environmental selenium research: from microscopic processes to global understanding.

Wollast, R., Billen, G. and Mackenzie, F.T., 1975. Behavior of mercury in natural systems and its global cycle. *In Ecological Toxicology Research* (pp. 145-166). Springer, Boston, MA.

Won, S.W., Park, J., Mao, J. and Yun, Y.S., 2011. Utilization of PEI-modified Corynebacterium glutamicum biomass for the recovery of Pd (II) in hydrochloric solution. *Bioresource Technology*, 102(4), pp.3888-3893.

Wu, Y., Wang, S., Streets, D.G., Hao, J., Chan, M. and Jiang, J., 2006. Trends in anthropogenic mercury emissions in China from 1995 to 2003. *Environmental Science & Technology*, 40(17), pp.5312-5318.

Xie, H., Chen, J., Chen, Q., Chen, C.E.L., Du, J., Tan, F. and Zhou, C., 2018. Development and evaluation of diffusive gradients in thin films technique for measuring antibiotics in seawater. *Science of the Total Environment*, 618, pp.1605-1612.

Xu, D., Chen, Y., Ding, S., Sun, Q., Wang, Y. and Zhang, C., 2013. Diffusive gradients in thin films technique equipped with a mixed binding gel for simultaneous measurements of dissolved reactive phosphorus and dissolved iron. *Environmental Science & Technology*, 47(18), pp.10477-10484.

Xu, J., Kleja, D.B., Biester, H., Lagerkvist, A. and Kumpiene, J., 2014. Influence of particle size distribution, organic carbon, pH and chlorides on washing of mercury contaminated soil. *Chemosphere*, 109, pp.99-105.

Yamamoto, M., 1996. Stimulation of elemental mercury oxidation in the presence of chloride ion in aquatic environments. *Chemosphere,* 32(6), pp.1217-1224.

Yigit, N.O. and Tozum, S., 2012. Removal of Selenium Species from Waters Using Various Surface-Modified Natural Particles and Waste Materials. *CLEAN–Soil, Air, Water*, 40(7), pp.735-745.

Yin, Y., Allen, H.E., Li, Y., Huang, C.P. and Sanders, P.F., 1996. Adsorption of mercury (II) by soil: effects of pH, chloride, and organic matter. *Journal of Environmental Quality*, 25(4), pp.837-844.

Yin, Y., Allen, H.E., Huang, C.P., Sparks, D.L. and Sanders, P.F., 1997. Kinetics of mercury (II) adsorption and desorption on soil. *Environmental Science & Technology*, 31(2), pp.496-503.

Young, T.F., Finley, K., Adams, W.J., Besser, J., Hopkins, W.D., Jolley, D., McNaughton, E., Presser, T.S., Shaw, D.P. and Unrine, J., 2010. *What you need to know about selenium. Ecological Assessment of Selenium in the Aquatic Environment*, pp.7-45.

Younger, P.L., 2002. Coalfield closure and the water environment in Europe. *Mining Technology*, 111(3), pp.201-209.

Yu, T.R. ed., 1997. *Chemistry of variable charge soils*. Oxford University Press.

Zawislanski, P.T. and Zavarin, M., 1996. Nature and rates of selenium transformations: A laboratory study of Kesterson Reservoir soils. *Soil Science Society of America Journal*, 60(3), pp.791-800.

Zhang, H. and Davison, W., 1995. Performance characteristics of diffusion gradients in thin films for the in situ measurement of trace metals in aqueous solution. *Analytical Chemistry*, 67(19), pp.3391-3400.

Zhang, H. and Davison, W., 1999. Diffusional characteristics of hydrogels used in DGT and DET techniques. *Analytica Chimica Acta*, 398(2-3), pp.329-340.

Zhang, H., Davison, W., Gadi, R. and Kobayashi, T., 1998. In situ measurement of dissolved phosphorus in natural waters using DGT. *Analytica Chimica Acta*, *370*(1), pp.29-38.

Zhang, H., Davison, W., Gadi, R. and Kobayashi, T., 1998. In situ measurement of dissolved phosphorus in natural waters using DGT. *Analytica Chimica Acta*, 370(1), pp.29-38.

Zhang, H., Davison, W., Miller, S. and Tych, W., 1995. In situ high resolution measurements of fluxes of Ni, Cu, Fe, and Mn and concentrations of Zn and Cd in porewaters by DGT. *Geochimica et Cosmochimica Acta*, *59*(20), pp.4181-4192.

Zhang, H., Davison, W., Miller, S. and Tych, W., 1995. In situ high resolution measurements of fluxes of Ni, Cu, Fe, and Mn and concentrations of Zn and Cd in porewaters by DGT. *Geochimica et Cosmochimica Acta*, 59(20), pp.4181-4192.

Zhang, H., Feng, X., Chan, H.M. and Larssen, T., 2014. New insights into traditional health risk assessments of mercury exposure: implications of selenium. *Environmental Science & Technology*, 48(2), pp.1206-1212.

Zhang, H., Feng, X., Larssen, T., Qiu, G. and Vogt, R.D., 2010. In inland China, rice, rather than fish, is the major pathway for methylmercury exposure. *Environmental Health Perspectives*, 118(9), p.1183.

Zhang, L., Qin, X., Tang, J., Liu, W. and Yang, H., 2017. Review of arsenic geochemical characteristics and its significance on arsenic pollution studies in karst groundwater, Southwest China. *Applied geochemistry*, 77, pp.80-88.

Zhang, S., Williams, P.N., Zhou, C.Y., Ma, L.Q. and Luo, J., 2017. Extending the functionality of the slurry ferrihydrite-DGT method: Performance evaluation for the measurement of vanadate, arsenate, antimonate and molybdate in water. *Chemosphere*, 184, pp.812-819.

Zhang, Y., Amrhein, C. and Frankenberger Jr, W.T., 2005. Effect of arsenate and

molybdate on removal of selenate from an aqueous solution by zero-valent iron. *Science of the Total Environment*, 350(1-3), pp.1-11.

Zhao, F.J., McGrath, S.P. and Meharg, A.A., 2010. Arsenic as a food chain contaminant: mechanisms of plant uptake and metabolism and mitigation strategies. *Annual Review of Plant Biology*, 61, pp.535-559.

Zhou, C., van de Velde, S., Baeyens, W. and Gao, Y., 2018. Comparison of Chelex based resins in diffusive gradients in thin-film for high resolution assessment of metals. *Talanta*, *186*, pp.397-405.

Appendix

Table A.1: The mass accumulated in DGT devices deployed over 16 hours for a) arsenic and b) selenium

a)

Time (hrs)	As			C_e	SD	RSD (%)	V_g (L)	V_e (L)	$V_g + V_e$	f_e	M (mg)	M (µg)
4	0.09	0.10	0.10	0.096	0.005	5	0.002	0.02	0.022	0.96	0.002	2.20
6	0.16	0.16	0.15	0.155	0.006	4	0.002	0.02	0.022	0.96	0.004	3.56
8	0.22	0.22	0.22	0.216	0.001	0	0.002	0.02	0.022	0.96	0.005	4.96
10	0.24	0.28	0.23	0.249	0.027	11	0.002	0.02	0.022	0.96	0.006	5.71
14	0.41	0.39	0.47	0.422	0.043	10	0.002	0.02	0.022	0.96	0.010	9.68
16		0.55	0.62	0.582	0.047	8	0.002	0.02	0.022	0.96	0.013	13.34

b)

Time (hrs)	Se			C_e	SD	RSD (%)	V_g (L)	V_e (L)	$V_g + V_e$	f_e	M (mg)	M (µg)
4	0.16	0.17	0.15	**0.16**	0.009	5	0.002	0.02	0.022	0.91	0.004	3.84
6	0.30	0.27	0.25	**0.27**	0.024	9	0.002	0.02	0.022	0.91	0.007	6.61
8	0.39	0.40	0.39	**0.39**	0.003	1	0.002	0.02	0.022	0.91	0.009	9.47
10	0.46	0.52	0.43	**0.47**	0.044	9	0.002	0.02	0.022	0.91	0.011	11.39
14	0.83	0.78	0.95	**0.85**	0.083	10	0.002	0.02	0.022	0.91	0.021	20.64
16	0.79	1.12	1.23	**1.05**	0.230	22	0.002	0.02	0.022	0.91	0.025	25.30

Table A.2: The Flux as influenced by increasing diffusive gel thickness for a) arsenic and b) selenium

a)

Thickness (cm)	As (mg L^{-1})			C_e	SD	RSD (%)	V_g (L)	V_e (L)	$V_g + V_e$ (L)	mL	f_e	mol L^{-1}	nmol mL^{-1}	nmol cm^{-2}	nmol cm^{-2} s^{-1}
0.06	1.93	1.64	1.71	**1.76**	0.152	9	0.002	0.02	0.022	22.000	0.96	2.35×10^{-5}	23.49	171.45	6.61×10^{-4}
0.08	1.69	1.75	1.67	**1.70**	0.043	3	0.002	0.02	0.022	22.000	0.96	2.27×10^{-5}	22.73	165.86	6.40×10^{-4}
0.1	1.60	1.51	1.82	**1.65**	0.160	10	0.002	0.02	0.022	22.000	0.96	2.20×10^{-5}	21.98	160.41	6.19×10^{-4}
0.12	1.05	1.21	1.17	**1.14**	0.082	7	0.002	0.02	0.022	22.000	0.96	1.5×10^{-5}	15.24	111.25	4.30×10^{-4}

b)

Thickness (cm)	Se (mg L^{-1})			C_e	SD	RSD (%)	V_g (L)	V_e (L)	$V_g + V_e$ (L)	mL	f_e	mol L^{-1}	nmol mL^{-1}	nmol cm^{-2}	nmol cm^{-2} s^{-1}
0.06	4.83	4.01	4.11	**4.31**	0.446	10	0.002	0.02	0.022	22.000	0.91	5.46×10^{-5}	54.63	420.59	1.62×10^{-3}
0.08	4.70	3.66	4.47	**4.28**	0.043	13	0.002	0.02	0.022	22.000	0.91	5.41×10^{-5}	54.14	416.85	1.60×10^{-3}
0.1	4.05	4.21	4.35	**4.20**	0.148	4	0.002	0.02	0.022	22.000	0.91	5.32×10^{-5}	53.22	409.77	1.58×10^{-3}
0.12	1.76	2.09	1.98	**1.94**	0.167	9	0.002	0.02	0.022	22.000	0.91	2.46×10^{-5}	24.62	189.56	7.31×10^{-4}